Mechanical and genetics basis of cellularization and serosal window closure in Tribolium castaneum

Vazquez Faci, T.

Mechanical and genetics basis of cellularization and serosal window closure in *Tribolium castaneum*

Proefschrift

Ter verkrijging van
de graad van Doctor aan de Universiteit Leiden,
op gezag van Rector Magnificus prof.dr.ir. H. Bijl,
volgens besluit van het College voor Promoties
te verdedigen op dinsdag 9 maart 2021
klokke 11.15 uur

door

Tania Vazquez Faci
geboren te Ciudad de Mexico, Mexico
9 augustus, 1983

Promotor:

Prof. dr. H. P. Spaink (Universiteit Leiden)

Copromotor:

Dr. M. van der Zee (Universiteit Leiden)

Promotiecommissie:

Prof. dr. G. P. van Wezel (voorzitter)
Prof. dr. A. H. Meijer (secretaris)

Overige commissieleden:

Prof. dr. S. Roth (University of Cologne)
Dr. E. C. Verhulst (Wageningen Universiteit)
Prof. dr. M. K. Richardson (Universiteit Leiden)
Prof.dr.ir. S. J. T. van Noort (Universiteit Leiden)

This work was supported with a grant from CONACyT to Tania Vazquez Faci

To my grandparents

"It doesn't make any difference how smart you are, who made the guess, or what his name is. If it disagrees with experiment, it's wrong. That's all there is to it."

Richard Feynman

CONTENTS

CHAPTER 1

General introduction

Biological processes are complex and we need a multidisciplinary perspective to understand them. However, sometimes different fields take different perspectives to study the same process. One example is the development of organisms. In the 1930s it was studied by two separate fields: genetics and developmental embryology. Geneticists thought that it could be explained as result of a heritable function of the organism. On the other hand, embryologists thought that development was not necessarily related to a gene because it was not known yet that a gene was linked to the delicate timing of all events occurring during development (1).

The separation between developmental embryology and genetics lasted for more than 60 years until all the concepts of developmental embryology and genetics were understood. In 1942, Glueksohn discovered a mutation in the T-locus genes of mice that causes an aberration in the dorsal axis of the embryo. She traced the effects through the development and demonstrated that the defect in the embryo started during the induction of the dorsal axis in gastrulation (2). In 1953, the DNA structure was discovered by Watson and Crick (3). Later, in 1961, the gene concept was introduced by Jacob and Monod (4). The union between developmental embryology and genetics started in 1970 when Waddington found genes responsible for wing malformations in *Drosophila melanogaster*. Waddington showed that the malformations start in the early developmental stages of *D. melanogaster* (5). Another important step in understanding the connection between genes and development was made by Nüsslein-Volhard and Wieschaus which was awarded with the Nobel prize in 1995 for physiology or medicine. For instance in 1980, their groups published their work about 15 loci from *D. melanogaster*. When these luci mutate the segmental pattern of the larva is altered (6). Nowadays, we have a better understanding of the general principles of genetics and developmental embryology and we cannot study the development of an organism without combining the two fields.

In this thesis we combine the concepts and methods of genetics and developmental embryology to study the early development of *Tribolium castaneum*. For example, we use the RNA interference method to study the role of genes during the early development of *T. castaneum* (Figure 1). This method interferes in the translation of a specific gene by introducing a double-strand of RNA (dsRNA) into the cells (7). A dsRNA with the same

sequence as the target mRNA is injected into the cell. This dsRNA binds to a dicer protein, which is an endonuclease protein. Then, the dicer protein cuts the dsRNA into segments. After that, the argonaut protein attaches to the dicer protein and the dsRNA selecting one strain of the dsRNA. This complex of proteins and RNA is called RISC (RNA-induced silencing complex). Later, the full complex binds to a specific target of the mRNA by base paring. At the end, the Argonaut protein catalyzes the mRNA, which will be later degraded. If the mRNA is degraded, the translation of the protein does not occur and the gene is silenced (8). This method is commonly used for screening gene function (9, 10), to study the role of genes in a particular stage during development (11–13) and even for therapeutic applications (14).

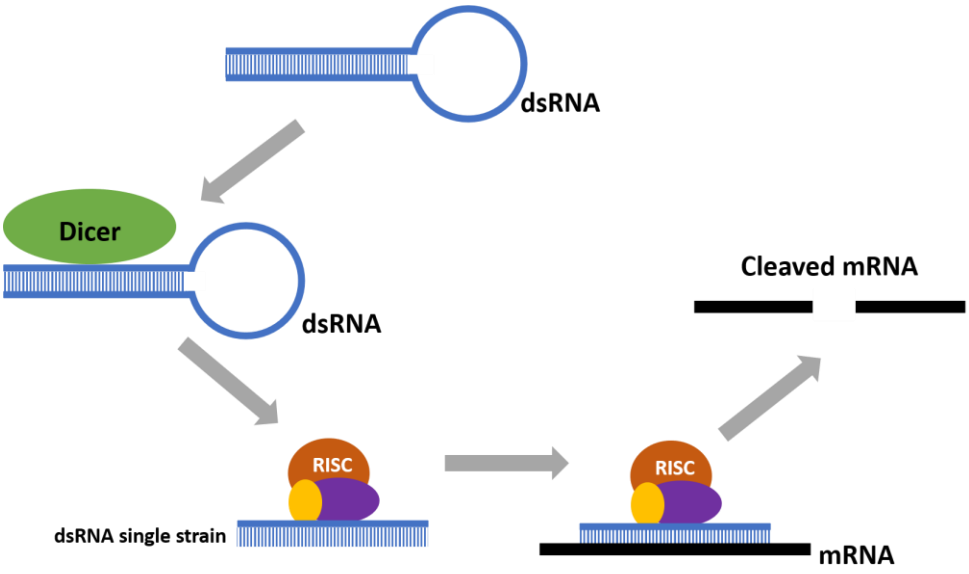

Figure 1. *The mechanism of RNAi interference. First the dsRNA binds to the dicer (endonuclease protein) cutting the dsRNA into segments. Then the dsRNA attaches to the RNA induced silence complex (RISC). At the end, the complex binds to the target mRNA producing its degradation.*

Early development of *Tribolium castaneum*

In this thesis we study the development of the red flour beetle, *Tribolium castaneum.* We follow processes from the early embryonic nuclear divisions until the formation of the larva and the extraembryonic

epithelium (serosal window closure) as explained below. Although *D. melanogaster* is the most used insect model in Biology, the utilization of *T. castaneum* to study insect development is becoming more common because the development of *T. castaneum* is closer to most of the insects (15).

Nuclear divisions and cellularization

In Biology, fertilization is the first step to start reproduction in diploids organisms. It is well-known that in humans the cellular division starts right after fertilization (1). In the case of insects and some vertebrates, in the first steps of embryogenesis, nuclei divide instead of cells (16–18). All the nuclei are enclosed in a single membrane, this arrangement is called syncytium (Figure 2). In *T. castaneum* the nuclei divide 12 times (14) (Figure 2). After the 12^{th} nuclear division the membrane starts to invaginate between the nuclei. In other words, the membrane starts to surrounds individual nuclei. This part of the membrane is called furrow canals. Cells are forming and connect through proteins called basal junctions, while the membrane grows to separate the nuclei. At this point the forming cells are called protocells. In the last step, the protein Innexin 7, that we describe further in this introduction, attaches to the sides of the furrow canals enclosing the nuclei (19). At this moment discrete cellular structures are formed. The process when the membrane starts to envelop the nuclei until the creation of cells is called cellularization.

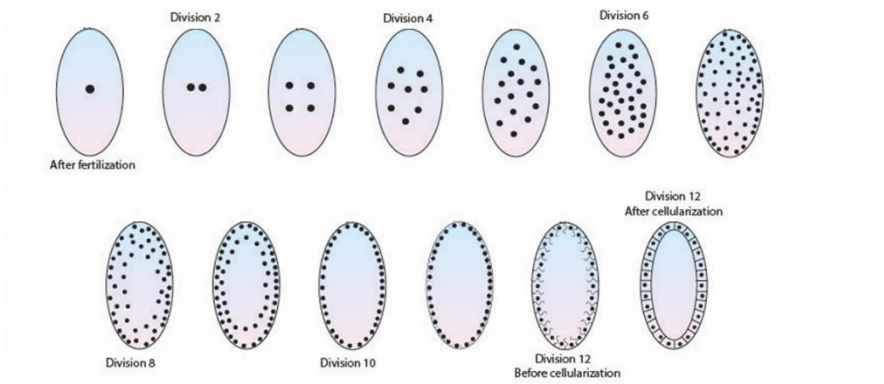

Figure 2 *Development of a T. castaneum embryo, from fertilization until cellularization. After fertilization, the nuclei divide surrounded by the same membrane, leading to a structure called syncytium. The cellularization starts after the 12th nuclear division, when all the nuclei are at the surface of the egg. At this stage, membrane material will separate each nucleus. At the end of cellularization the membrane closes around each nuclei leading to the formation of cells. Figure adapted from Gilbert et al, 2000 (1)*

Serosal window closure

After cellularization, the formation of a serosa starts. A serosa is an extraembryonic epithelium which surrounds the embryonic rudiment. *D. melanogaster*, has amnioserosa and it does not surrounds the entire embryo (Figure 3).

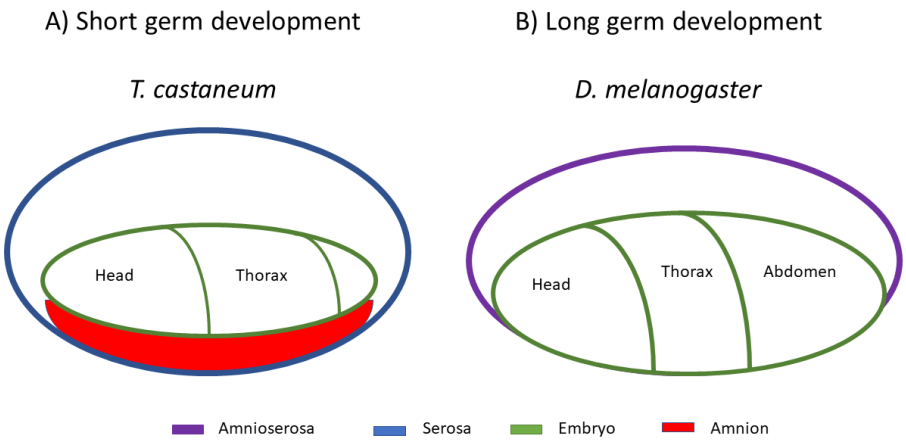

Figure 3. *The two types of development in insects. A) One example of the short germ development is shown for T. castaneum where the blastoderm only has the head and the thorax after gastrulation. Serosa and amnion are two different epithelia. B) D. melanogaster development is an example of the long germ development where all the segments are presents in the blastoderm after gastrulation. Serosa and amnion are combined in one epithelium called amnioserosa.*

The use of *T. castaneum* to study serosa has increased because the development of *T. castaneum* is more similar to the development of most of the insects than *D. melanogaster* (15). However, *D. melanogaster* is the most studied insect in Biology and therefore there is most information available.

D. melanogaster has a long germ development which means that after gastrulation all the segments develop at the same time. Additionally, the two extraembryonic epithelia have been strongly reduced to a single small amnioserosa that covers the yolk dorsally (Figure 3B) (19). In contrast, *T. castaneum* has a short germ development, as is the case for most of the insects. In this kind of development just the head and the thorax are present in the blastoderm . After gastrulation, the rest of the segments are developed. Additionally, *T. castaneum* has no amnioserosa, but two separate epithelia, amnion and serosa (Figure 3A). Most of the insects have these two epithelia during their embryonic stage. The serosa differentiates from the germ anlage at the blastoderm stage during development (21). In most hemimetabolous insects, the embryo invaginates into the yolk leaving the serosa to fully cover the yolk (katatrepsis) (Figure 4A) (22). Finally, the serosa retracts and the embryo emerges from the yolk (Figure 4B) (12).

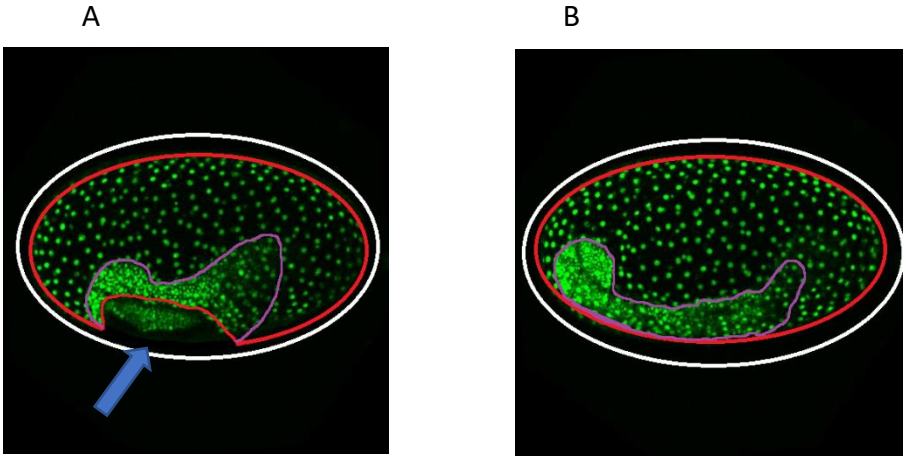

Figure 4 *T. castaneum embryo during the formation of serosa. In white is the chorion, in red the serosa and in purple the embryonic rudiment. The arrow points at the serosal window. : A) The serosa is folding over the germ rudiment and the serosal window (arrow) is still open. B) Germ band growing and the serosal window has closed*

Role of Innexins and Laminins during the early development

In this thesis we study the role of Laminin and Innexin in the development of *T. castaneum*. Laminin is an extracellular matrix protein and an essential component of the basal lamina. Innexin is an integral membrane protein. Integral membrane proteins are proteins which are attached to the cellular membrane. They are important because they are part of several cell functions and structures such as cell communication, channels, linkers, structural membrane-anchoring, cell adhesion, among others (23–26).

Gap junctions and Innexins

Gap junctions are channels that connect neighboring cells and enable cells to transport small molecules up to 1-2 kDa between cells. The gap junctions are important because they open and closed controlling various cell signals. For example, the transport of calcium during apoptosis (26).

There are three protein families that make gap-junction channels, Connexins, Pannexins and Innexins. Connexins and Pannexins are found

only in vertebrates while Innexins are in invertebrates (23, 28) (Figure 5). Until now 3 pannexins (29), 20 connexins (28) and 8 innexins (30) have been discovered. The first Innexins were identified in *D. melanogaster* and *C. elegans* (24, 31, 32). In particular, *D. melanogaster* has 8 different innexins in its genome. They play a role in the adult visual system, embryonic epithelia organization, morphogenesis, germ cell differentiation processes (33), and in neuronal connections (34).

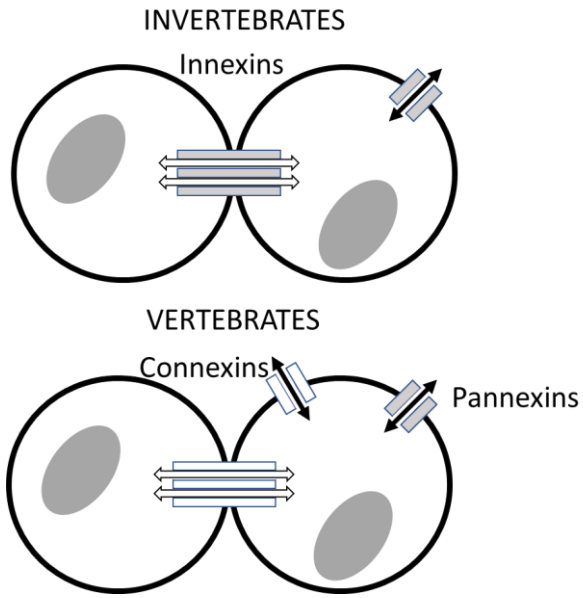

Figure 5. *The cell communication is mediated by gap junctions. In invertebrates are called innexins. In vertebrates there are two types of gap junctions pannexins and connexins. Figure adapted from Scemes et al 2008 (27)*

Innexins are important for cellular communication, which has an important role in several cellular functions. For example, in the immune system, cell communication is needed to react to external pathogens, and in the muscular system to stretch or retract the muscles. Blocking innexin function can lead to prevention of some parasitic diseases by blocking the communication between cells (23).

In this thesis we focus on Innexin 7 paralogs based on a small genetic knockdown screen that identified this gene group as important for development. These results showed that in *T. castaneum* Innexin 7

stabilizes the invagination of the furrow canals after the last nuclear division. Just before finishing the cellularization, Innexin 7 induces the cell closure by attaching the ends of the furrow canals. After the closure, neither the membrane or the nuclei elongate, leading to a thin layer of cells with cuboidal form (19). In comparison, Innexin 7 does not have any role in *D. melanogaster* cellularization. In this case, Actin protein plays a crucial role in the process of cellularization (16).

Laminins

Laminin is found in the basement membrane of animals and it plays a role in cell adhesion (35–38) (Figure 6). It is made by three subunits α, β and γ. The α subunit is the only subunit which is secreted independently of the other two. The secretion of β and γ subunits depends on the secretion of the α subunit (39).

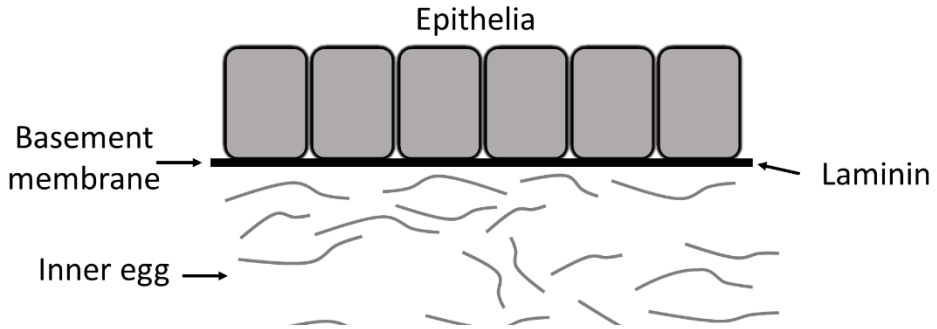

Figure 6. *The basement membrane is a thin, dense sheet matrix that surround most animal tissues. Laminin is a component of the basement membrane. Figure adapted from Jayadev et al, 2017 (39)*

There are different variants of Laminin subunits depending on the species. The mouse was the first animal where the variants were discovered, it has 15 variants of Laminin α (39). The genetics and biochemistry of Laminin in *T. castaneum* is similar to Laminin in *D. melanogaster*. Laminin in *T. castaneum* has four laminin chains: two α chains (α1,2 and α3,5), one β chain and one γ chain. In comparison, *D. melanogaster* has also four laminin chains: two α chains (α1,2 and α3,5), one β chain and one γ chain. They are arranged in two different trimers: the trimer formed by α3,5; β1; α1 is called laminin A and the trimer formed by α1,2; β1; γ1 is called laminin W. The Laminin α1,2 and α3,5 of *T.*

castaneum are orthologues of *D. melanogaster* Laminin α1,2 and α 3,5, respectively.

When Laminin is silenced this leads to different effects in animals. For example, in mammals, particularly in mice, it inhibits murine lung morphogenesis (41). Another example is seen in nematodes, specifically embryos of *C. elegans* suffer an arrest when they elongate and the organs are formed (19). Kao et al (42) observed a detachment of cells from tissues giving rise to cell disorganization. In the case of insects, the silencing of Laminin β produces blisters in the wings of adult silk worms (25); additionally Laminin has been found in the limb bud of grasshoppers where the tibial pioneer neurons grow (43). . In tissues of *D. melanogaster* there is an abnormal accumulation of major basement membrane components, such as Collagen IV and Perlecan. Additionally, silencing prevents the normal morphogenesis of most organs and tissues, including the gut, trachea, muscles and nervous system (45). In *D. melanogaster* adults when Laminin is silenced it produces wing blisters (46). In the case of *T. castaneum*, the knock down of Laminin induces a decrement of the circumference of the abdomen, generates problems with the development of muscles and results in bending of legs and antennas. Sometimes even the pupae do not hatch, hatching is delayed or their wings show blisters (https://ibeetle-base.uni-goettingen.de).

Outline

The main goal of this work is to understand the process of cellularization and serosal window closure in tribolium. This thesis is divided in five chapters. Chapter 1 describes in a broad sense cellularization and serosal window closure and gives an outline of the thesis.

In chapter 2, we study the cell shape during cellularization in *T. castaneum* and *D. melanogaster*. We created a new transgenic line of *T. castaneum*. We inserted the green fluorescent protein (GFP) gene of a jellyfish into the genome to create a gene fusion with the gene encoding the cytoskeletal actin protein of *T. castaneum* in order to visualize the membrane before and during cellularization (47). As a result the visualized membranes allowed us to make videos of the eggs to recognize the shape of the (proto)cells. In order to do this, we used a pattern recognition program. In this thesis we used the program of Aigouy et al., 2010. We

observed that the membranes of the cells are arranged in a pattern known as a Voronoi tessellation. To understand this natural pattern-forming process, we simulated the growth of the cells using a mechanical model comprising the nuclei, radial microtubules and actin cortex of the cells. The result of the simulation and the experiments are consistent.

In Chapter 3 we study the role of the gene Innexin 7a and its paralogs in *T. castaneum* development. We used parental RNA of interference (pRNAi) for a screen of junction proteins and to silence the gene Innexin 7a (8, 49, 50) . We found that knocking down innexin7a leads to failure of cellularization. We used RNA deep sequencing (RNAseq) to study the effect on transcriptome expression of signal transduction pathways when Innexin 7a is silenced (51). RNAseq analysis shows that the pRNAi targeting of Innexin 7a had a very strong effect on the transcription of a large group of genes including several genes of the innexin family during the early development.

In Chapter 4, we study the role of Laminin α1,2, β and γ (Laminin 1) in the serosal window closure of *T. castaneum* using pRNAi. We focused on the trimer Laminin 1 because the knock down of Laminin α1,2 induces wing blisters. This phenotype is indicative of cell adhesion defects which lead to morphogenetical mutations such as defects in serosal window closure. We observed that the trimer Laminin 1 is one of the key cell adhesion molecules during serosal window closure. To the best of our knowledge, Laminin 1 is the first discovered cellular component in the process of serosal window closure in *T. castaneum*.

In Chapter 5, we present the general conclusions and possibilities for future work and applications for the study of cellularization and serosal window closure.

References

1. Gilbert, S.F. 2000. Developmental Biology -- NCBI Bookshelf. Dev. Biol. .
2. Gluecksohn-Waelsch, S., and R.P. Erickson. 1970. The T-Locus of the Mouse: Implications for Mechanisms of Development. In: Current Topics in Developmental Biology. Elsevier. pp. 281–316.
3. Watson F, H.C.C. 1953. Molecular structure of nucleic acids. Camb. Dniv. Press.
4. Fran, B., D. Perrin, C. Sanchez, and J. Monod. 1960. The Operon : A Group of Genes Whose Expression is Coordinated by an Operator. J. Bacteriol. 1729: 1727–1729.
5. Waddington, C.H. 1942. Canalization of development and the inheritance of acquired characters. Nature. 287: 795–801.
6. Nüsslein-volhard, C., and E. Wieschaus. 1980. Mutations affecting segment number and polarity in drosophila. Nature. .
7. Bucher, G., J. Scholten, and M. Klingler. 2002. Parental RNAi in tribolium (coleoptera). Curr. Biol. 12: 85–86.
8. Carl D. Novina and Phillip A. Sharp. 2004. The RNAi revolution. Nature. 430: 161–164.
9. Schmitt-Engel, C., D. Schultheis, J. Schwirz, N. Ströhlein, N. Troelenberg, U. Majumdar, V.A. Dao, D. Grossmann, T. Richter, M. Tech, J. Dönitz, L. Gerischer, M. Theis, I. Schild, J. Trauner, N.D.B. Koniszewski, E. Küster, S. Kittelmann, Y. Hu, S. Lehmann, J. Siemanowski, J. Ulrich, K.A. Panfilio, R. Schröder, B. Morgenstern, M. Stanke, F. Buchhholz, M. Frasch, S. Roth, E.A. Wimmer, M. Schoppmeier, M. Klingler, and G. Bucher. 2015. The iBeetle large-scale RNAi screen reveals gene functions for insect development and physiology. Nat. Commun. 6.
10. Ulrich, J., V.A. Dao, U. Majumdar, C. Schmitt-Engel, J. Schwirz, D. Schultheis, N. Ströhlein, N. Troelenberg, D. Grossmann, T. Richter, J. Dönitz, L. Gerischer, G. Leboulle, A. Vilcinskas, M. Stanke, and G. Bucher. 2015. Large scale RNAi screen in Tribolium reveals novel target genes for pest control and the proteasome as prime target. BMC Genomics. 16: 1–9.
11. Rehwinkel, J., I. Behm-Ansmant, D. Gatfield, and E. Izaurralde. 2005. A crucial role for GW182 and the DCP1:DCP2 decapping complex in

miRNA-mediated gene silencing. Rna. 11: 1640–1647.
12. Ostrowski, K., R. Bauer, and M. Hoch. 2008. The Drosophila Innexin7 gap junction protein is required for development of the embryonic nervous system. Cell Commun. Adhes. 15: 155–167.
13. Panfilio, K.A. 2009. Late extraembryonic morphogenesis and its zenRNAi-induced failure in the milkweed bug Oncopeltus fasciatus. Dev. Biol. .
14. Lage, H. 2005. Potential applications of RNA interference technology in the treatment of cancer. Futur. Oncol. .
15. Handel, K., C.G. Grünfelder, S. Roth, and K. Sander. 2000. Tribolium embryogenesis: a SEM study of cell shapes and movements from blastoderm to serosal closure. Dev. Genes Evol. 210: 167–179.
16. Mazumdar, A., and M. Mazumdar. 2002. How one becomes many: blastoderm cellularization in Drosophila melanogaster. Bioessays. 24: 1012–22.
17. Schejter, E.D., and E. Wieschaus. 1993. Functional elements of the cytoskeleton in the early Drosophila embryo. Annu. Rev. Cell Biol. 9: 67–99.
18. Turner, F.R., and A.P. Mahowald. 1976. Scanning electron microscopy of Drosophila embryogenesis. Dev. Biol. 50: 95–108.
19. van der Zee, M., M.A. Benton, T. Vazquez-Faci, G.E.M. Lamers, C.G.C. Jacobs, and C. Rabouille. 2015. Innexin7a forms junctions that stabilize the basal membrane during cellularization of the blastoderm in Tribolium castaneum. Development. 142: 2173–2183.
20. Schmidt-Ott, U. 2000. The amnioserosa is an apomorphic character of cyclorrhaphan flies. Dev. Genes Evol. .
21. Roth, S. 2004. Gastrulation in other insects. In: Gastrulations: from cells to embryo. .
22. Panfilio, K.A. 2008. Extraembryonic development in insects and the acrobatics of blastokinesis. Dev. Biol. 313: 471–491.
23. Güiza, J., I. Barría, J.C. Sáez, and J.L. Vega. 2018. Innexins: Expression, regulation, and functions. Front. Physiol. 9: 1–9.
24. Phelan, P., and T.A. Starich. 2001. Innexins get into the gap. BioEssays. 23: 388–396.
25. Van Der Zee, M., M.A. Benton, T. Vazquez-Faci, G.E.M. Lamers, C.G.C. Jacobs, and C. Rabouille. 2015. Innexin7a forms junctions that stabilize the basal membrane during cellularization of the

blastoderm in Tribolium castaneum. Dev. 142: 2173–2183.
26. Tong, X., S. He, J. Chen, H. Hu, Z. Xiang, C. Lu, and F. Dai. 2015. A novel laminin β gene BmLanB1-w regulates wing-specific cell adhesion in silkworm, Bombyx mori. Sci. Rep. 5: 12562.
27. Pinton, P., C. Giorgi, R. Siviero, E. Zecchini, and R. Rizzuto. 2008. Calcium and apoptosis: ER-mitochondria Ca2+ transfer in the control of apoptosis. Oncogene. .
28. Scemes, E., D.C. Spray, and P. Meda. 2009. Connexins, pannexins, innexins: Novel roles of "hemi-channels." Pflugers Arch. Eur. J. Physiol. .
29. Ruan, Z., I.J. Orozco, J. Du, and W. Lü. 2020. Structures of human pannexin 1 reveal ion pathways and mechanism of gating. Nature. .
30. Hughes, A.L. 2014. Evolutionary Diversification of Insect Innexins. J. Insect Sci. 14: 1–5.
31. Phelan, P., J.P. Bacon, J.A. Davies, L.A. Stebbings, and M.G. Todman. 1998. Innexins: A family of invertebrate gap-junction proteins. Trends Genet. .
32. P, P. 2000. Gap junction communication in invertebrates: The innexin gene family. Curr. Trends Membr. .
33. Bauer, R., B. Löer, K. Ostrowski, J. Martini, A. Weimbs, H. Lechner, and M. Hoch. 2005. Intercellular communication: The Drosophila innexin multiprotein family of gap junction proteins. Chem. Biol. 12: 515–526.
34. Wu, C.L., M.F.M. Shih, J.S.Y. Lai, H.T. Yang, G.C. Turner, L. Chen, and A.S. Chiang. 2011. Heterotypic gap junctions between two neurons in the drosophila brain are critical for memory. Curr. Biol. 21: 848–854.
35. Kramer, J.M. 2005. Basement membranes. WormBook. 27: 1–15.
36. Engel, J., E. Odermatt, A. Engel, J.A. Madri, H. Furthmayr, H. Rohde, and R. Timpl. 1981. Shapes, domain organizations and flexibility of laminin and fibronectin, two multifunctional proteins of the extracellular matrix. J. Mol. Biol. 150: 97–120.
37. Kusche-Gullberg, M., K. Garrison, A.J. MacKrell, L.I. Fessler, and J.H. Fessler. 1992. Laminin A chain: expression during Drosophila development and genomic sequence. EMBO J. 11: 4519–27.
38. Fessler, J.H., and L.I. Fessler. 1989. DROSOPHILA EXTRACELLULAR MATRIX. Annu. Rev. Cell Biol. 5: 309–39.

39. Yurchenco, P.D., Y. Quan, H. Colognato, T. Mathus, D. Harrison, Y. Yamada, and J.J. O'Rear. 1997. The alpha chain of laminin-1 is independently secreted and drives secretion of its beta- and gamma-chain partners. Proc. Natl. Acad. Sci. U. S. A. 94: 10189–10194.
40. Jayadev, R., and D.R. Sherwood. 2017. Basement membranes. Curr. Biol. 27: R207–R211.
41. Schuger, L., A.P.N. Skubitz, K.S. O'Shea, J.F. Chang, and J. Varani. 1991. Identification of laminin domains involved in branching morphogenesis: Effects of anti-laminin monoclonal antibodies on mouse embryonic lung development. Dev. Biol. 146: 531–541.
42. Kao, G., C.C. Huang, E.M. Hedgecock, D.H. Hall, and W.G. Wadsworth. 2006. The role of the laminin β subunit in laminin heterotrimer assembly and basement membrane function and development in C. elegans. Dev. Biol. 290: 211–219.
43. Bonner, J., V. Auld, and T. O'Connor. 2002. Migrating mesoderm establish a uniform distribution of laminin in the developing grasshopper embryo. Dev Biol. 249: 57–73.
44. Wagner, N., D. Weber, S. Seitz, and G. Krohne. 2004. The lamin B receptor of Drosophila melanogaster. J. Cell Sci. 117: 2015–28.
45. Urbano, J.M., C.N. Torgler, C. Molnar, U. Tepass, A. Lopez-Varea, N.H. Brown, J.F. de Celis, and M.D. Martin-Bermudo. 2009. Drosophila laminins act as key regulators of basement membrane assembly and morphogenesis. Development. 136: 4165–4176.
46. Martin, D., S. Zusman, X. Li, E.L. Williams, N. Khare, S. DaRocha, R. Chiquet-Ehrismann, and S. Baumgartner. 1999. wing blister, A new Drosophila laminin chain required for cell adhesion and migration during embryonic and imaginal development. J. Cell Biol. 145: 191–201.
47. Drongelen, R. Van, T. Vazquez-Faci, M. Van Der Zee, and T. Idema. 2017. Mechanics of epithelial tissue formation. : 1–11.
48. Aigouy, B., R. Farhadifar, D.B. Staple, A. Sagner, J.-C.C. Röper, F. Jülicher, and S. Eaton. 2010. Cell Flow Reorients the Axis of Planar Polarity in the Wing Epithelium of Drosophila. Cell. 142: 773–786.
49. Tomoyasu, Y., and R.E. Denell. 2004. Larval RNAi in Tribolium (Coleoptera) for analyzing adult development. Dev. Genes Evol. 214: 575–578.
50. Tomoyasu, Y., S.C. Miller, S. Tomita, M. Schoppmeier, D. Grossmann,

and G. Bucher. 2008. Exploring systemic RNA interference in insects: a genome-wide survey for RNAi genes in Tribolium. Genome Biol. 9: R10.

51. Chu, Y., and D.R. Corey. 2012. RNA Sequencing : Platform Selection ,. 22: 10–13.

CHAPTER 2

Mechanics of blastodermal cell arrangement and cell shape in insect embryos

Tania Vazquez Faci*, Ruben van Drongelen*, Teun A.P.M. Huijben Maurijn van der Zee and Timon Idema

*These authors contributed equally

van Drongelen, R., Vazquez-Faci, T., Huijben, T. A. P. M., van der Zee, M., & Idema, T. (2018). Mechanics of epithelial tissue formation. *Journal of Theoretical Biology*, *454*, 182–189. https://doi.org/10.1016/j.jtbi.2018.06.002

Abstract

A key process in the life of any multicellular organism is its development from a single fertilized egg into a fully grown adult. Naturally, this process has been studied in great detail, with particular focus on its biochemical and genetic aspects. However, the mechanics of development have gained much less attention. Here we use two model organisms, the red flour beetle *Tribolium castaneum* and the fruit fly *Drosophila melanogaster*, to determine the role of mechanics in the formation of their first tissue layer. We find that the membranes of the cells in this tissue arrange in a specific mathematical pattern known as a Voronoi tessellation, with the nuclei of the cells in the centers. To understand this pattern-forming process, we simulate the growth of the cells using a mechanical model comprising the nuclei, radial microtubules and actin cortex of the cells. We find that cell-cell interactions in such a purely mechanical system indeed lead to the formation of a Voronoi tessellation. The geometric and topological properties of the tessellations we find in our experiments quantitatively match with our simulations. Moreover, comparison with recent jamming models suggests that the tissues spontaneously organize at the highest possible density that is still on the liquid side of the jamming transition.

Introduction

Multicellular organisms start life as a single fertilized cell. From this modest beginning, they undergo a developmental process that leads to the formation of complex tissues and organs with a wide range of different functions. Although it has long been appreciated that these various components of an organism have very different mechanical properties, the role of mechanical interactions in the developmental process has only become the focus of detailed studies relatively recently. One of the earliest milestones in this field is the seminal work by Discher et al. (1) and Engler et al. (2), who showed that identical stem cells, when placed on substrates of different stiffness, differentiate into cells of tissues with the corresponding stiffness. Cells in living multicellular organisms, however, do not exist on a substrate in isolation; instead, they are part of a tissue that consists of both cells and extracellular material and together form a mechanical system (3). These mechanical systems have unusual material properties, which moreover can change dynamically as cells are intrinsically out of equilibrium. Naturally, these changes are especially prominent during development and growth. Moreover, cells react strongly to both direct mechanical interactions with their neighbors (4–6) and indirect interactions via deformations of a shared substrate (7–9). Finally, the interior organization of the cell, in particular the position of the nucleus, is also mechanically coupled to its outside environment (10). To understand how epithelial tissues develop, we thus need a mechanical model coupling the inside to the outside of the cell.

A number of studies have come out in recent years specifically focusing on the role of mechanics in embryonic tissue development. Fickentscher et al. demonstrated that the cellular arrangements in early Caenorhabditis elegans embryos are also due to mechanics (11). Kanesaki et al. showed how the cytoskeletal networks in Drosophila melanogaster protocells are responsible for re-establishing an ordered pattern of the nuclei after a division (12). The nuclear divisions in *Drosophila melanogaster* embryos are wavefronts, which can be understood in a context where mechanical interactions between the nuclei are taken into account (13). More broadly, mechanical signals can also be translated into biochemical ones, giving a direct and highly conserved mechanism for

influencing developmental processes inside cells, as recently reviewed by Fernandez-Sanchez et al. (14).

In this Chapter, we study the formation of the first tissue, the epithelial blastoderm, in the embryos of two model organisms: the fruit fly *Drosophila melanogaster* and the flour beetle *Tribolium castaneum*. Like all insects in their early stage of development, these embryos form a syncytium: the nuclei are not separated by plasma membranes into cells. The nuclei are embedded in a full cellular apparatus. We refer to these compartments as protocells, which thus all share a single cytoplasm. During the first nuclear divisions the nuclei reside in the inside of the egg. After the eighth nuclear division, they migrate to the surface of the egg and form a single layer of nuclei, called the syncytial blastoderm. Once the nuclei are at the periphery of the egg, the plasma membrane surrounding the entire egg moves in between the nuclei (invagination) and separates them. Finally, after the 12th nuclear division in *T. castaneum* (15), or 13th nuclear division in *D. melanogaster* (16–18), the plasma membrane closes around the protocells, creating actual cells . This process, known as cellularization, turns the syncytial blastoderm into a proper epithelial tissue, known as the cellular blastoderm.

Remarkably, the process of cellularization happens in a different fashion in our two model embryos. In *D. melanogaster*, actin filaments cover the tips of the invaginating membrane and form a network that might actively be pulled inward by myosin motors (16–18). In addition, when the membrane furrows have reached the basal side of the protocells, an actin-myosin ring is constructed and contracts to complete cellularization in Drosophila (16–18). In contrast, no such actin-myosin ring is formed in T. castaneum. Instead, the closing protein Innexin7a forms junctions between the developing basal membrane at the bottom of the furrows and the yolk plasmalemma underneath the protocells. These junctions act as patch-clamps, allowing the basal membrane to spread until it closes off the protocell (19). The initial steps of the development of *T. castaneum* are illustrated in Figure 1 a.

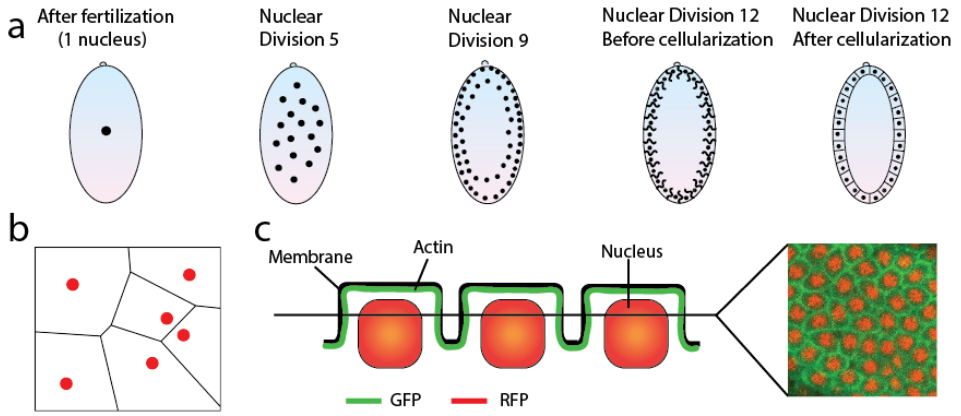

Figure 1. *Formation of the syncytial and cellular blastoderm in Tribolium castaneum. (a) Sketch of the syncytial stage of the development of T. castaneum. During the first eight nuclear divisions, the nuclei duplicate in the yolk of the egg. The eighth and ninth nuclear divisions, the nuclei migrate to the surface of the egg, forming the syncytial blastoderm. After the twelfth nuclear divisions, cellularization occurs, and the syncytium is converted into a cellular blastoderm tissue. (b) Example of a Voronoi tessellation of the plane, starting from random centers indicated by the red dots. The plane is divided in regions such that the points in each region are closest to a given center. The boundaries between two regions are equidistant from the corresponding centers, and perpendicular to the line connecting these centers. (c) Example of a summed z-stack (11 images) of the syncytial blastoderm of D. melanogaster (right), with histones labeled with Red Fluorescence Protein (RFP in red) and actin with Green Fluorescence Protein (GFP in green). As shown in the schematic on the left, although the two-dimensional cross section of the protocells shows no holes, at this stage (before cellularization) the plasma membrane does not yet separate these protocells into complete cells.*

In this Chapter, we study the geometrical patterns that the cells create when the first epithelial tissue is formed before and immediately after cellularization. We observe the patterns directly by labeling both the nuclei and the actin cortex of the (proto)cells. We find that, initially, the protocells do not form a confluent layer, but over time, as they divide, fill up the available space. The touching boundaries of the cells correspond closely to a Voronoi tessellation of their nuclei (see Figure b), an effect that becomes more pronounced after cellularization. Although Voronoi tessellations have occasionally been used to describe cellular patterns in epithelial tissues (20–25), to the best of our knowledge, the fact that the nuclei are located at the centers of the corresponding Voronoi cells has not been shown previously. To understand how this very specific pattern emerges, we develop a mechanical model of the cells and their

interactions. Our model faithfully reproduces the Voronoi tessellation, and matches the experimental data quantitatively on a number of geometric and topological measures. We conclude that the mechanical interactions between the (proto)cells in early embryonic epithelial tissues are directly responsible for the observed geometrical cellular patterns of those tissues.

Methods

Transgenic line with nuclei and life-actin labeled with gfp (lan-gfp)

To be able to concurrently observe the nuclei and the actin cortex of *D. melanogaster* and *T. castaneum*, we required lines in which both parts are fluorescently labeled.

For *D. melanogaster*, we used His2A-RFP/sGMCA flies (Bloomington Drosophila Stock Centre number 59023) that ubiquitously express Histone2A fused to Red Fluorescent Protein (RFP) and the Actin-binding domain of Moesin fused to Green Fluorescent Protein (GFP) (26).

Our objective was to create a transgenic line of Tribolium castaneum with in which both LifeActin and the nuclei were labeled with Green Fluorescent Protein (GFP). To create a LifeActin line, we amplified LifeActin (27) fused to EGFP from the pT7-LifeAct-EGFP vector (28) by high fidelity PCR, using a forward primer that introduced an FseI restriction site and a reverse primer that introduced an AscI site. We cloned this fragment FseI-AscI under the alpha Tubulin1 promoter (29) into the piggyBac vector (30) provided by Peter Kitzmann and Gregor Bucher (Georg August Universität, Göttingen). Sequences are available on request. The construct containing vermillion under the 3xP3 promoter as marker was injected into vermillion white Tribolium strain embryos (31). For obtaining stable transgenic lines we performed standard crosses (31). Two lines in which LifeAct-GFP is ubiquitously expressed all over oogenesis, embryogenesis and larval life were selected.

To obtain the transgenic line used in this Chapter, we crossed our stable LifeAct-GFP line to an existing line ubiquitously expressing GFP extended with a Nuclear Localisation Signal (NLS) (32) We named the combined line LAN-GFP.

Maintenance

T. casteneum was kept at 30°C with a humidity of 50% in a box with wheat flour and dry yeast (1:0.05) which was refreshed weekly (1). Flies were kept under standard conditions on standard medium (2).

Live imaging

We put *T. castaneum* on fine flour at 30°C for one hour. Subsequently, we removed the adults using a sieve with 600-850 µm meshes and collected the eggs using a sieve with a 250 µm mesh size. We then let the eggs develop for four hours at 30°C. After the four hours, we dechorionated the eggs in 5% bleach. We put *D. melanogaster* on egg laying at 25°C for one hour. We subsequently collected the eggs and immediately dechorionated them with 5% bleach. We lined the eggs of both insects on a microscope glass-bottomed Petri dish (Willco Wells BV). To avoid desiccation of the eggs we covered them with Voltalef 10S Halocarbon oil.

We imaged the embryos on an inverted Zeiss confocal microscope at 30°C for *T. castaneum* and 25°C for *D. melanogaster*. We observed the embryos at a cross-section of the syncytial blastoderm (Fig. 1c). We took *z*-stacks consisting of eleven focal planes with a 40×/1.5 N.A. water-immersion objective. The time interval between frames was 3 minutes for *T. castaneum* and 1 minute for *D. melanogaster*. The total observation time was six hours for *T. castaneum* and two hours for *D. melanogaster*.

We used imageJ 1.49t to process the images and to obtain the area of the cells in the experiments we use the program done by Benoit Aigouy (3). We summed all the planes in the *z*-stack at each timepoint to make a time-lapse video. To make the Voronoi tessellation, we made a program in Matlab using the pre-existing function of Voronoi tessellation from a list of coordinates.

Quantification of the match between the Voronoi tessellation and actual cells

We introduce a quality number Q to quantify the match between the Voronoi tessellation of the nuclei and the actual cells. To do so, we compare the actual area, A_r, of the cells to the area of their corresponding Voronoi cells, A_V. We define Q as:

$$Q = \frac{1}{N}\sum_{i=1}^{N}\left(\frac{A_{r,i} - A_{V,i}}{A_{r,i}}\right)^2,$$

where N is the total number of cells. When the Voronoi tessellation has a perfect match with the actual cells the value of Q is 0. For comparison, we calculated Q for a random close packing of identical discs, which gives a value of 0.05.

Simulations

The cells are in two dimensions, treating them as purely mechanical objects. The cells consist of a nucleus, a radial and stiff microtubule network, and a more excitable actin cortex at the cell perimeter [35]. The nucleus is a single large bead with radius Rn, and the cortex as a collection of M small beads with radius Rc that surround the nucleus (Figure 2). The cortical beads initially form a circle around the nuclei. We connect each bead to its two neighbors by a spring with spring constant kc and rest length $u_c = 2R_c$ to mimic the forces in the actin cortex. Cortical beads that are not connected through these springs interact via the repulsive part of the same potential. Microtubules are modeled as springs that connect the nuclear bead to individual beads in the membrane. To do so, we select at random a fraction f = 1/6 of the cortex beads and connect them to the nuclear bead with a spring of spring constant R_{MT} and rest length $u_{MT}=2R_n$.

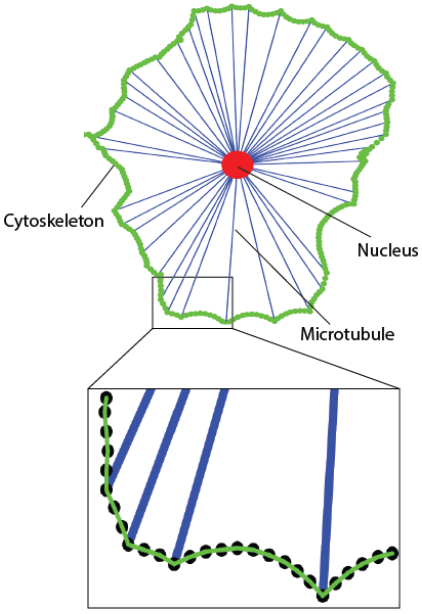

Figure 2. *Schematic showing the entire cell, including microtubules (blue), with an inset showing how the microtubules and the actin cortex (green) are connected with the beads (black).*

We initiate our system by placing N non-overlapping, circular cells at random positions in the plane. To let the cells grow, we allow the rest length of the microtubules and actin filaments to increase linearly over time. Because cells cannot interpenetrate, they exert forces on each other when they touch. These forces counteract the growth of the microtubules, which halts at a given stall force. A microtubule stops extending when the membrane bead it is connected to comes within 99% of the minimal equilibrium distance to a bead of another protocell. In this event we also lock the relative position of the beads. When half of the microtubules have stopped growing, the growth of the actin filaments also stops.

To let the cells divide, we first double the number of beads in the membrane and the number of microtubules connecting them to the nucleus. We then split the nucleus into two daughter nuclei of half the size. Of the cortical beads connected to a microtubule, we select the two beads forming the shortest axis across the cell. We then use this axis to divide the microtubules over the two nuclei (Figure 1 b). To help the nuclei separate, an extra spring is positioned between the nuclei, mimicking the interpolar microtubules. The rest length of the interpolar spring is gradually increased

from zero to the radius of the nucleus, while the rest length of the other microtubules is reduced with a factor $\sqrt{2}$, so that the total area of the cell remains the same. Once this process is completed, the two axis beads are contracted using a new spring, and when brought together, duplicated and re-connected to complete the division of the cells.

The dynamics of the cytoskeleton and the nuclei are overdamped because the inertia of these small cell components is negligible compared to their viscous drag. Therefore, our equation of motion follows from equating the net force to the drag force, as given by Stokes' law:

$$F_{i,net} = 6\pi\eta R_i v_i$$

Where $F_{i,net}$ is the total (net) force on object *i,* which can be either a nuclear or a cortical bead. The viscosity is denoted by η, R_i is the radius of object *i*, and v_i is its velocity.

In our simulations, we scale our measure of length by setting R_c= 1. For the repulsion between two cortical beads we can define$\tau \equiv 6\pi\eta/k_c$ a characteristic time . We non-dimensionalize the units of time and force by setting τ= k_c = 1.

Results

Observations

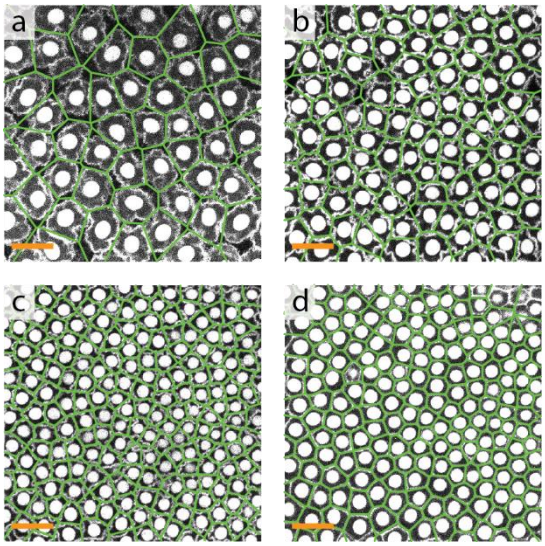

Figure 3. *Four snapshots from a video of a Tribolium castaneum embryo from our new LAN-GFP line, in which both the actin and the nuclei are labeled with GFP. Overlaid in green is the Voronoi tessellation of the centers of the nuclei. Figures a-c show snapshots from the 10th, 11th and 12th nuclear divisions before cellularization, and figure d shows a snapshot of the embryo after cellularization. Scale bar 25 µm.*

We used our new *Tribolium* line expressing LifeAct-EGFP and nuclearGFP (LAN-GFP) to concurrently visualize the cortical actin and the nuclei. Using the existing line His2A-RFP/sGMCA (Bloomington Drosophila Stock Centre number 59023), we similarly visualized the cytoskeleton and nuclei in *D. melanogaster*. For each of the images, we determined the position of the centers of all the nuclei. From these, we constructed the associated Voronoi tessellation (Figure 3 a-d), i.e., the division of space into cells such that each point is part of the cell corresponding to the closest center. We overlaid these Voronoi tessellations with the experimental images for the last three nuclear divisions in the syncytium, and after cellularization.

Although the protocells are basally connected by the plasma membrane of the entire egg, the lateral sides of the protocells are not tightly adjacent and leave space between the protocells in *T. castaneum* (Figure 3a and 3b) until the last division before cellularization (12^{th} nuclear division, Figure 3c). In the 10^{th} nuclear division, the protocells only cover about 70% of the available space, rising to 85% after the 11^{th} nuclear division and close to 100% after the 12^{th} and last nuclear division. Consequently, the Voronoi tessellation of the nuclei does not correspond closely with the position of the protocellular boundaries in 11 and 12 nuclear divisions (Figure 3a and 3b). Their quality numbers are Q=0.16 and

Q=0.12, respectively. However, we note that where two adjacent protocells touch, their boundary typically does follow the boundary between the corresponding Voronoi cells. After the 12th nuclear division but before cellularization, the match between the Voronoi tessellation and the protocellular boundaries is better (Figure 3c), although the quality number, *Q*=0.10 still indicates a low match. The reason for this poor match is that, unlike the tessellation boundaries, the cellular boundaries are not straight at this point, indicating that they are not under tension. After cellularization, when the membrane is straight, the match between the experimental data and overlaid tessellation becomes almost perfect (Figure 3d) with a Q number close to zero ($Q = 9 \cdot 10^{-4}$).

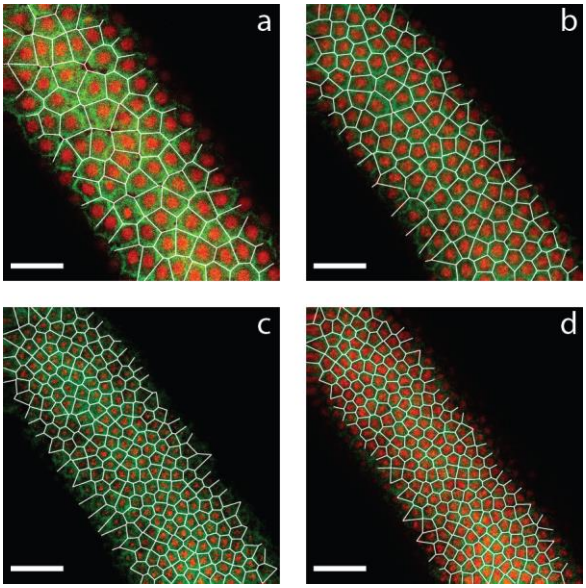

Figure 4 Four snapshots from a video of a *Drosophila melanogaster* embryo in which the nuclear histones are labeled with RFP (red) and the actin with GFP (green). Overlaid in white is the Voronoi tessellation of the centers of the nuclei. Figures a-c show snapshots after the 11th, 12th and 13th nuclear division before cellularization and figure d shows a snapshot of the embryo after cellularization. Scale bar 25 μm.

The picture for *D. melanogaster* is largely similar to that of *T. castaneum*, though different in the details. The nuclei of *D. melanogaster* divide once more before cellularization. After the 11th nuclear division, the cells cover about 75% of the available space, and the Voronoi tessellation has a poor match, with *Q*=0.15, like in *T. castaneum* (Figure 4a). The match with the Voronoi tessellation improves after the 12th nuclear division, with *Q*=0.04 (Figure 4b). After the 13th nuclear division, before and after cellularization, we obtain *Q*=0.07 and Q=0.01, respectively (Figure c and d). The pattern of the protocells in *D. melanogaster* thus already matches the Voronoi tessellation at an earlier stage than happens in *T. castaneum*.

The difference between the two species may be due to two effects. First, as the nuclei in *D. melanogaster* undergo an additional division before cellularization, they are more densely packed than those in *T. castaneum*, resulting in less unoccupied space and hence more mechanical contacts between the protocells. Our simulation results (detailed below) suggest that such mechanical contacts will inevitably lead to the formation of boundaries that correspond to the Voronoi tessellation of the nuclei. Second, as the mechanism of basal cell closure is quite different in both species (active constriction for *D. melanogaster* versus passive patch-clamp constriction for *T. castaneum*), the membrane after cellularization may be different as well.

Simulations

First, we observe what happens when we let our model cells grow without division, using random initial placement and double periodic boundary conditions. Because the cortical beads experience drag, the ones that are not connected to a growing microtubule lag behind those that are. When growing cells touch and connect, the forces from the growing microtubules also feedback on the nuclear bead, which shifts position. Figure 5c shows a snapshot of a simulation in which the cells have reached about 70% coverage of the plane. Where neighboring cells touch, their boundaries coincide with the Voronoi tessellation of the nuclei. The Q number for this case is high (Q = 0.22), representing the fact that there are still big gaps between the cells (Table 1). When we let the cells grow further, they eventually reach 100% coverage, and their geometrical pattern matches the Voronoi tessellation of their nuclei almost perfectly (Q = 2.1×10^{-3}, Figure 5d). If we let the cells divide during the developmental process, the general picture is much the same, with again an almost perfect match to the Voronoi tessellation (Q = 3×10^{-3}, Figure 5e). However, if we give one of the initial cells a larger growth rate (inherited by its daughters), we find that this pattern is broken (Figure 5f). The faster-growing cells cover a larger fraction of the available area than their corresponding Voronoi cells, whereas their slower-growing neighbors are left with a compressed shape.

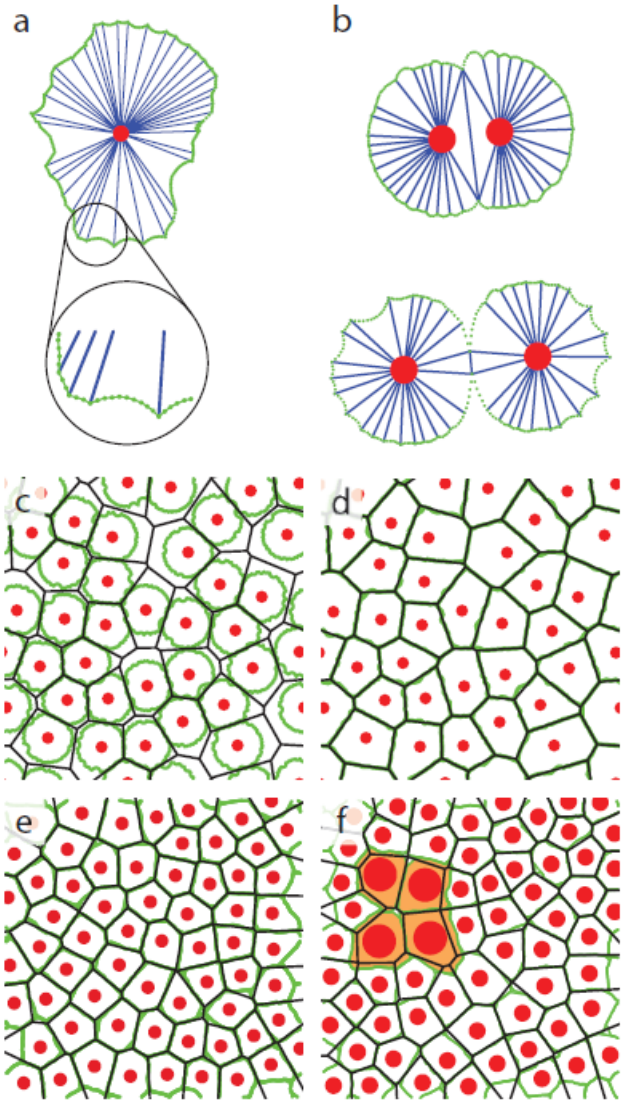

Figure 5. *Mechanical cell model and simulation results. (a) Cells consist of a sphere representing the nucleus (red), connected via microtubules modeled as stiff_ springs (blue) to the actin cortex, which is modeled as a number of beads connected by weaker springs (green). (b) Cell division. (c) Growing cells at 70% coverage. Where cell boundaries touch, they coincide with the Voronoi boundaries of their nuclei. (d) Growing cells at 100% coverage (no division). (e) Growing and dividing cells at 98% coverage after two divisions. (f) Growing and dividing cells at 98% coverage after two divisions, for the case in which one initial cell (with four daughters, indicated in orange) has a growth rate that is 2.5X larger than that of the others.*

Table 1. *Values of the two geometrical measures and quality number of the Voronoi tessellations of our experimental and simulated systems. The variance of the area is very small in the first four cases, indicating that in each case, all resulting cells have roughly the same size. In the case where a single cell grows 2.5 times faster than the others (last column), we immediately obtain a significant increase in this variance. The reduced area (area divided by the perimeter squared normalized such that a circle has a value of 1) is very similar in all cases. Notably, the reduced area is significantly less than that of a regular hexagon (0.91), consistent with the topological observation that only about half of the cells in our system have six vertices.*

	Experiments		Simulation		
	T. castaneum	D. melanogaster	No division	With division	Unequal grow
Area variance	0.02±0.02	0.05±0.005	0.02± 0.005	0.01± 0.002	0.04±0.004
Reduced area	0.85±0.02	0.83± 0.02	0.83± 0.01	0.83± 0.01	0.83± 0.01
Q number	0.0009	0.02	0.002	0.003	0.017

In both insect that we studied, the picture is very similar to the simulation results. (Proto)cells appear on the surface at random positions, and grow to confluency after two (*T. castaneum*) or three (*D. melanogaster*) divisions. When the cells cover 100% of the available area, their boundaries also closely match the Voronoi tessellation of their nuclei. Moreover, in both the experimental and simulation results, we find that the positions of the nuclei are close to (though not exactly on top of) the centroids of the Voronoi cells .

Geometric and topological comparison between experimental data and model

To quantify the match between the experimental and the numerical results, we determine the value of two geometrical and one topological property of the cells. First, we measure the variance of the area per Voronoi cell, which we find to be very low in both embryos and in the simulations (Table 1), indicating that all cells grow to roughly the same size. Second, we measure the reduced area A^* per Voronoi cell, defined as $A^* = 4\pi A/P^2$, where A is the area and P the perimeter of the cell (5). With this definition, circles have a reduced area of 1, and hexagons have reduced area of $\pi/2\sqrt{3} \approx 0.91$. We find that the average reduced area of the Voronoi cells in both our experimental systems and in our simulations is again a close match with a value of about 0.83 (Table 1).

In addition to the two geometrical measures given above, we also consider a topological measure: the relative occurrence of cells with a given number of vertices. For a perfectly regular pattern (a honeycomb lattice), all cells are hexagons, and thus all cells have six vertices. Deviations from this pattern occur in the form of cells with five and seven vertices (with the total number of vertices of all cells being conserved), or even four or eight vertices. Not surprisingly, hexagonal cells are most abundant in our Voronoi tessellations. However, we also find large numbers of pentagons and heptagons, which each account for about 25% of the cells (Figure 6). Again, the two experimental systems and the simulation all agree quantitatively.

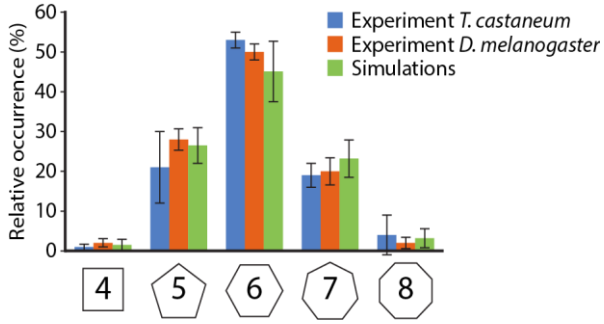

Figure 6 *Relative occurrence of cells with a given number of vertices in the Voronoi tessellation after cellularization for our experimental observations on T. castaneum (blue) and D. melanogaster (orange) and our simulations (green). Note that where a perfect honeycomb lattice would exist exclusively of hexagons, only about half of our cells have six vertices, in both experiments and in the simulations.*

Discussion

We observed that the spatial pattern produced by the cells in the first epithelial tissue in insects corresponds very closely to a Voronoi tessellation of their nuclei. While the match of the actual cells to those of the tessellation only becomes very high after cellularization for *T. castaneum*, we already obtain a good match in the penultimate cycle for *D. melanogaster*. The better match originates at least in part from a higher protocell density and possibly also from the mechanism of cellularization.

In both experimental systems and in the simulations, we measure a reduced area A^* of the cells at about 0.83, just below the order-disorder phase transition reported by Hočevar and Ziherl at A^*=0.865 (6). For higher values, epithelial tissues consist almost exclusively of hexagons and are ordered. For values of A^* below the critical value the tissues are disordered and contain considerable fractions of polygons which are not hexagons, as we observe in our systems. Interestingly, recent work by Bi et al. (7, 8) showed that at almost the same value of the reduced area (A^*=0.866) tissues exhibit a rigidity transition. They modeled an active tissue using self-propelled Voronoi cells and found that below the reported critical value, the tissues behave fluid-like, whereas for higher values they are solid-like. The tissues in our insect embryos have a reduced area A^* between 0.83 and 0.85, which classifies them as (just) liquid-like. This observation is consistent with the stage of development we observe. After cellularization, the embryos undergo a massive shape change, known as gastrulation, in which the mesoderm is formed. Another round of divisions before cellularization would probably push the system over the critical point into a jammed state, which would make gastrulation much more difficult. On the other hand, the cells must be confluent to form a fairly stable tissue. Our observation that the system exists just on the liquid side of the jamming transition may therefore well correspond to a necessary step in development. This might also underlie the different number of nuclear divisions before cellularization in different insects (9, 10).

Conclusion

We observe that the newly formed cells of the epithelial blastoderm in both *Drosophila melanogaster* and *Tribolium castaneum* arrange in a geometrical pattern that closely matches the Voronoi tessellation of their nuclei. We find that in the specific tessellation the cells form, they all have roughly the same area, and their arrangement is such that the resulting tissue is just on the liquid side of the jamming transition. We can understand the formation of this pattern from mechanical interactions between the cells. Growing cells eventually come into contact with their neighbors, resulting in mechanical feedback that causes them to stop growing towards that neighbor. These contacts moreover translate back to a mechanical force on the nuclei of the cells, which causes them to re-position and eventually form the observed Voronoi tessellation. Thus, mechanical interactions largely determine cell arrangement and shape in the blastodermal epithelium.

Acknowledgements

Peter Kitzmann and Gregor Bucher (Georg August Universität Göttingen, Germany) for help with generating the transgenic *Tribolium* line; Matthew Benton (University of Cologne, Germany) for providing the pT7-LifeAct-EGFP construct and for help with live imaging; Ron Habets (Leiden University Medical Centre, The Netherlands) for help with selecting *Drosophila* stocks.

Contributions

Tania Vazquez Faci: Initial concept, experimental design, creation of transgenic line (Lan-GFP), experiments, time-laps videos, data analysis and writing.

Ruben van Drongelen: Simulation, data analysis and writing.

Teun A.P.M. Huijben: Simulation and data analysis.

Maurijn van der Zee: Initial concepts, experimental design and creation of transgenic line (Lan-GFP).

Timon Idema: Initial concepts, experimental design and writing

References

1. Discher, D.E., P. Janmey, and Y.-L. Wang. 2005. Tissue cells feel and respond to the stiffness of their substrate. Science (80-.). 310: 1139–1143.
2. Engler, A.J., S. Sen, H.L. Sweeney, and D.E. Discher. 2006. Matrix elasticity directs stem cell lineage specification. Cell. 126: 677–689.
3. Kasza, K.E., A.C. Rowat, J. Liu, T.E. Angelini, C.P. Brangwynne, G.H. Koenderink, and D.A. Weitz. 2007. The cell as a material. Curr. Opin. Cell Biol. 19: 101–107.
4. Vogel, V., and M. Sheetz. 2006. Local force and geometry sensing regulate cell functions. Nat. Rev. Mol. Cell Biol. 7: 265–275.
5. Schwarz, U.S., and S.A. Safran. 2013. Physics of adherent cells. Rev. Mod. Phys. 85: 1327–1381.
6. Shawky, J.H., and L.A. Davidson. 2015. Tissue mechanics and adhesion during embryo development. Dev. Biol. 401: 152–164.
7. Tang, X., P. Bajaj, R. Bashir, and T. a. Saif. 2011. How far cardiac cells can see each other mechanically. Soft Matter. 7: 6151.
8. Nitsan, I., S. Drori, Y.E. Lewis, S. Cohen, and S. Tzlil. 2016. Mechanical communication in cardiac cell synchronized beating. Nat. Phys. 12: 472–477.
9. Majkut, S., T. Idema, J. Swift, C. Krieger, A.J. Liu, and D.E. Discher. 2013. Heart-specific stiffening in early embryos parallels matrix and myosin expression to optimize beating. Curr. Biol. 23: 2434–2439.
10. Zemel, A. 2015. Active mechanical coupling between the nucleus, cytoskeleton and the extracellular matrix, and the implications for perinuclear actomyosin organization. Soft Matter. 11: 2353–2363.
11. Fickentscher, R., P. Struntz, and M. Weiss. 2013. Mechanical cues in the early embryogenesis of Caenorhabditis elegans. Biophys. J. 105: 1805–1811.
12. Kanesaki, T., C.M. Edwards, U.S. Schwarz, and J. Grosshans. 2011. Dynamic ordering of nuclei in syncytial embryos: a quantitative analysis of the role of cytoskeletal networks. Integr. Biol. 3: 1112–1119.
13. Idema, T., J.O. Dubuis, L. Kang, M.L. Manning, P.C. Nelson, T.C. Lubensky, and A.J. Liu. 2013. The syncytial Drosophila embryo as a mechanically excitable medium. PLoS One. 8: e77216.

14. Fernandez-Sanchez, M.-E., T. Brunet, J.-C. Röper, and E. Farge. 2015. Mechanotransduction's impact on animal development, evolution, and tumorigenesis. Annu. Rev. Cell Dev. Biol. 31: 373–397.
15. Handel, K., C.G. Grünfelder, S. Roth, and K. Sander. 2000. Tribolium embryogenesis: a SEM study of cell shapes and movements from blastoderm to serosal closure. Dev. Genes Evol. 210: 167–179.
16. Mazumdar, A., and M. Mazumdar. 2002. How one becomes many: blastoderm cellularization in Drosophila melanogaster. BioEssays. 24: 1012–1022.
17. Lecuit, T. 2004. Junctions and vesicular trafficking during Drosophila cellularization. J. Cell Sci. 117: 3427–3433.
18. Harris, T.J.C., J.K. Sawyer, and M. Peifer. 2009. How the cytoskeleton helps build the embryonic body plan: Models of morphogenesis from Drosophila. Curr. Top. Dev. Biol. 89: 55–85.
19. van der Zee, M., M.A. Benton, T. Vazquez-Faci, G.E.M. Lamers, C.G.C. Jacobs, and C. Rabouille. 2015. Innexin7a forms junctions that stabilize the basal membrane during cellularization of the blastoderm in Tribolium castaneum. Development. 142: 2173–2183.
20. Honda, H. 1978. Description of cellular patterns by Dirichlet domains: the two-dimensional case. J. Theor. Biol. 72: 523–543.
21. Sulsky, D., S. Childress, and J.K. Percus. 1984. A model of cell sorting. J. Theor. Biol. 106: 275–301.
22. Weliky, M., and G. Oster. 1990. The mechanical basis of cell rearrangement. I. Epithelial morphogenesis during Fundulus epiboly. Development. 109: 373–386.
23. Sharma, V., M. Crne, J.O. Park, and M. Srinivasarao. 2009. Structural origin of circularly polarized iridescence in jeweled beetles. Science (80-.). 325: 449–451.
24. Bock, M., A.K. Tyagi, J.-U. Kreft, and W. Alt. 2010. Generalized Voronoi tessellation as a model of two-dimensional cell tissue dynamics. Bull. Math. Biol. 72: 1696–1731.
25. Yu, W., H.K. Lee, S. Hariharan, W. Bu, and S. Ahmed. 2010. Evolving generalized voronoi diagrams for accurate cellular image segmentation. Cytom. Part A. 77: 379–386.
26. Kiehart, D.P., C.G. Galbraith, K.A. Edwards, W.L. Rickoll, and R.A. Montague. 2000. Multiple forces contribute to cell sheet morphogenesis for dorsal closure in Drosophila. J. Cell Biol. 149:

471–490.
27. Riedl, J., A.H. Crevenna, K. Kessenbrock, J.H. Yu, D. Neukirchen, M. Bista, F. Bradke, D. Jenne, T.A. Holak, Z. Werb, M. Sixt, and R. Wedlich-Soldner. 2008. Lifeact: a versatile marker to visualize F-actin. Nat. Methods. 5: 605–607.
28. Benton, M.A., M. Akam, and A. Pavlopoulos. 2013. Cell and tissue dynamics during Tribolium embryogenesis revealed by versatile fluorescence labeling approaches. Development. 140: 3210–3220.
29. Siebert, K.S., M.D. Lorenzen, S.J. Brown, Y. Park, and R.W. Beeman. 2008. Tubulin superfamily genes in Tribolium castaneum and the use of a Tubulin promoter to drive transgene expression. Insect Biochem. Mol. Biol. 38: 749–755.
30. Horn, C., and E. a. Wimmer. 2000. A versatile vector set for animal transgenesis. Dev. Genes Evol. 210: 630–637.
31. Berghammer, A.J., M. Weber, J. Trauner, and M. Klingler. 2009. Red flour beetle (Tribolium) germline transformation and insertional mutagenesis. Cold Spring Harb. Protoc. 4: 1–18.
32. Sarrazin, A.F., A.D. Peel, and M. Averof. 2012. A segmentation clock with two-segment periodicity in insects. Science (80-.). 336: 338–341.
33. Greenspan, R.J. 1997. Fly pushing: The theory and practice of Drosophila genetics. Cold Spring Harb. Lab. Press. : 418.
34. Farhadifar, R., J.-C.C. Röper, B. Aigouy, S. Eaton, and F. Jülicher. 2007. The Influence of Cell Mechanics, Cell-Cell Interactions, and Proliferation on Epithelial Packing. Curr. Biol. 17: 2095–2104.
35. Hočevar, a., and P. Ziherl. 2009. Degenerate polygonal tilings in simple animal tissues. Phys. Rev. E - Stat. Nonlinear, Soft Matter Phys. 80: 1–7.
36. Discher, D.E., P. Janmey, and Y.-L. Wang. 2005. Tissue cells feel and respond to the stiffness of their substrate. Science. 310: 1139–43.
37. Hočevar, A., and P. Ziherl. 2009. Degenerate polygonal tilings in simple animal tissues. Phys. Rev. E. 80: 011904.
38. Bi, D., J.H. Lopez, J.M. Schwarz, and M.L. Manning. 2015. A density-independent rigidity transition in biological tissues. Nat. Phys. 11: 1074–1079.
39. Bi, D., X. Yang, M.C. Marchetti, and M.L. Manning. 2016. Motility-driven glass and jamming transitions in biological tissues. Phys. Rev.

X. 6: 021011.
40. Anderson, D.T. 1972. The development of holometabolous insects. In: Counce SJ, CH Waddington, editors. Developmental Systems: Insects. London: Academic Press. pp. 1531–1545.

CHAPTER 3

Innexin7 forms junctions stabilizing the basal membrane during cellularization of the *Tribolium castaneum* blastoderm

Tania Vazquez-Faci, Matthew A. Benton, Gerda E.M. Lamers, Chris G.C. Jacobs and Catherine Rabouille, Herman P. Spaink, Maurijn van der Zee*

*An older version of this chapter has been published as:

Van Der Zee, M., Benton, M. A., Vazquez-Faci, T., Lamers, G. E. M., Jacobs, C. G. C., & Rabouille, C. (2015). Innexin7a forms junctions that stabilize the basal membrane during cellularization of the blastoderm in Tribolium castaneum. *Development (Cambridge)*, *142*(12), 2173–2183. https://doi.org/10.1242/dev.097113

Abstract

In insects, the fertilized egg undergoes a series of rapid nuclear divisions before the syncytial blastoderm starts to cellularize. Cellularization has been extensively studied in *Drosophila*, but its thick columnar blastoderm is unusual among insects. We therefore set out to describe cellularization in the beetle *Tribolium castaneum*, the embryos of which exhibit a thin blastoderm of cuboidal cells, like most insects. Using immunohistochemistry, live imaging and transmission electron microscopy, we describe several striking differences to cellularization in *Drosophila*, including the formation of junctions between the forming basal membrane and the yolk plasmalemma. To identify the nature of this novel junction, we used the parental RNAi technique (pRNAi) for a small-scale screen of junction proteins. We find that maternal knock-down of innexin7a (inx7a), an ortholog of the *Drosophila* gap junction gene innexin7, leads to failure of cellularization. RNAseq analysis shows that the pRNAi targeting of innexin 7a had a very strong effect on the transcription of a large group of genes at the egg stage. The results also show feedback on the transcription of various other innexin genes making it impossible to show specificity of the pRNAi approach on innexin 7a. Based on the close homology of the three identified innexin 7 paralogs, we assume that the effects of the pRNAi approach could be the result of silencing of all three paralogs and therefore mention them as the innexin 7 gene cluster. In Inx7 depleted eggs, the invaginated plasma membrane retracts when basal cell closure normally begins. Furthermore, transiently expressed tagged Inx7 localizes to the nascent basal membrane of the forming cells in wild type eggs. We propose that Inx7 proteins forms the newly identified junctions that stabilize the forming basal membrane and enable basal cell closure. We put forward *Tribolium* as a model for studying a more ancestral mode of cellularization in insects.

Introduction

In most insects, the nuclei of the fertilized egg divide multiple times and move to the cortex before cellularization starts. During cellularization, plasma membrane ingresses between the nuclei and encloses them in individual cells (1–3). In *Drosophila*, cellularization comprises different phases: a preliminary phase of membrane ingression, during which the so-called furrow canals are established (see below); a phase of slow membrane extension accompanied by elongation of the nuclei; a rapid phase of membrane extension required for the formation of tall columnar epidermal cells; and final basal closure of the cells by means of actin rings (4). The cells that are formed are tall and narrow.

The formation of the furrow canals during the preliminary phase is a conspicuous start of cellularization in *Drosophila*. The furrow canals are the dilated leading edges of the ingressing membrane to which actin is recruited so that an apical inter-connected hexagonal actin network is formed around each nucleus (5). This network ingresses during membrane extension. The furrow canals are separated from the rest of the ingressing membrane by basal adherens junctions (BAJs). Main components of the BAJs are β-catenin (Armadillo) and E-cadherin (DEcad) (2).

Polarized membrane insertion appears to be the main force driving membrane extension (6). Genes required for cellularization include key regulators of membrane trafficking, such as rab11 and nuf (7–9), and zygotic genes such as *slam* (Acharya et al., 2014) and *nullo*. The latter is involved in the regulation of F-actin at the furrow canals, which is required for stabilization of the cleavage furrow (10). In nullo mutants, some furrows regress during the phase of membrane extension (10).

Whereas cellularization is well studied in *Drosophila*, it is unclear to what extent the molecular mechanisms underlying cellularization are conserved in other insects. *Tribolium* castaneum is a beetle that exhibits traits more ancestral for insects than *Drosophila*, for instance short germ development (11). Also, the thin blastoderm of cuboidal cells seen in *Tribolium* is more typical for insects than the columnar cells of the *Drosophila* blastoderm (12). Hence, we set out to describe cellularization in this beetle using live imaging techniques with transient expression of the membrane marker GAP43-YFP and the filamentous-actin marker LifeAct-GFP (13), immunohistochemistry and Transmission Electron Microscopy

(TEM). We describe several key differences to *Drosophila* cellularization, the main one being the formation of junctions along the forming basal membrane.

To identify the nature of these junctions, we performed a small parental RNAi screen targeting junction proteins, and found that a *Tribolium* ortholog of the *Drosophila* gap junction protein Innexin7 has an essential role in cellularization. Innexin7 function has been studied and appears to have no role in cellularization in *Drosophila* (14–16). Innexins are a family of proteins related to the vertebrate Pannexins (17–20) and functionally similar to the vertebrate Connexins (21–25). Innexins contain four transmembrane (TM) domains, two extracellular loops and an intracellular N- and C-terminus. Groups of 6 protein units assemble into homomeric or heteromeric hemichannels. Interaction in trans of two hemichannels in adjacent membranes is mediated by the conserved cysteine residues in the extracellular protein loops and leads to the formation of a functional gap junction. The first innexins studied were in *Caenorhabditis elegans* (26) and in *D. melanogaster* (27). Later, the Innexins have been found in almost all metazoa (27). Genomic studies have revealed multiple innexin family genes in insect species. In *D. melanogaster*, there are seven genes and in *Tribolium* are 8 innexins (28). The role of innexins has been studied broadly in *D. melanogaster*. For example in the adult visual system, embryonic epithelia organization, morphogenesis, in germ cell differentiation processes, (14) and connection between neurons (29). It is also known that the interactions between the innnexins perform these functions. In comparison, the role of innexins in *Tribolium* has just started to be studied. The only role studied before is from innexin 7 but the role of the other innexins of the best of our knowledge has been not studied.

We performed RNA deep sequencing (RNAseq) to investigate the effect of RNAi knockdown of innexin 7a on the transcriptome. These results show a strong effect on the transcription of genes involved in many fundamental processes such as DNA replication and broad signaling pathways such as the notch pathway. The result could not confirm specificity of the RNAi approach for one particular innexin 7 genes and therefore can only be linked to the entire group of paralogues genes that are highly similar in sequence. Surprisingly RNAi also showed a strong effect on transcription of other innexin genes, including two innexin 7a paralogs. These results indicate a complex feedback mechanism controlled by innexin 7 gene

cluster. At the developmental level we show that RNAi targeting the innexin 7 genes leads to the retraction of the invaginated membrane when basal cell closure normally starts. We propose that Tc-Inx7 proteins forms junctions between the nascent basal membrane and the forming yolk plasmalemma, thus stabilizing the invaginated membrane and enabling basal cell closure.

Materials and Methods

Time-lapse movies

1-2 hours old eggs were dechorionated in 0.5% hypochlorite solution, mounted and injected with 3 µg/µl GAP43-YFP or LifeAct-GFP mRNA as described in Benton et al. 2013 (13). They were then left to develop for 3-4 hours under Voltalef 10S hydrocarbon oil at 32°C, and imaged with a Leica SP5 inverted confocal laser microscope in a heated chamber at 32°C (13). In total we analyzed movies of 22 wild type and 8 Tc-inx7a pRNAi eggs. Six to nine cells per movie were followed and measured in detail for Figure 1M.

Transmission Electron Microscopy

The eggs were incubated in 10% BSA (as a cryo-protectant) and high pressure freezing was performed with a LEICA-EM-PACT2, followed by freeze substitution. Specimens were embedded in Agar 100 resin, sectioned, and examined with a JEOL 1010 Transmission Electron Microscope.

Egg fixation and Immunohistochemistry

Eggs were fixed in a 1:1 4% formaldehyde/heptane mix, devittelinized with a methanol shock, and stored in methanol. Anti-β-catenin/Armadillo (30), anti-Actin (Sigma) or V5 (Invitrogen) antibodies were used 1:1000, 1:50 or 1:1000 respectively in PBS supplemented with 1% BSA overnight at 4°C. After washing, eggs were incubated with anti-rabbit Alexafluor488 at 1:250 in PBS-BSA 1%. For actin staining using

phalloidin, eggs were fixed in 4% paraformaldehyde for 15 minutes and devittelinized using forceps and needle before incubation with phalloidin 1:5000 for 20 min at room temperature. Eggs were mounted in vectashield with DAPI and imaged under a Leica DM6000 epifluorescent, SP5 or SPE confocal microscope.

Parental RNAi for images and videos

dsRNA was synthesized using SP6 and T7 polymerases (Ambion) and injected into pupae according to Bucher et al., 2002 (31). For parental RNAi see Supplementary Table S1 for details. Injection of dsRNA into eggs was performed as previously described for mRNA injection (13).

Phylogenetic analysis

Putative orthologs were identified by BLAST (32). Alignment was made using Praline (http://www.ibi.vu.nl/programs/pralinewww). Parts of the alignment where most sequences had gaps were not taken into account for phylogenetic analysis by creating a mask in Seaview (33). WAG+I+G was the most informative amino acid substitution model according to ProtTest (34). The maximum likelihood phylogeny was generated using PhyML (35) and was edited in MEGA3.1 (36). Accession numbers (NCBI, National Centre for Biotechnology Information) of the used sequences are: XP_002405917=IsInx1; XP_002415523=IsInx2; XP_002405920=IsInx8a; XP_002433826=IsInx8b, XP_002434835=Inx8c; EFX65318.1=DpInx1; EFX65316.1=DpInx2a; EFX77054.1=DpInx2b; EFX74755.1=DpInx3a; EFX74754.1=DpInx3b; EFX65317.1=DpInx7; EFX84089.1=DpInx8; XP_001946431=ApInx1; XP_001944681=ApInx2a; XP_003241809=ApInx2b; XP_001947982=ApInx2c; XP_001949382=ApInx3; XP_003247903.1=ApInx7; XP_001944798=ApInx8; XM_001121323=AmInx1; XM_003251623= AmInx2; XM_623560=AmInx3; XM_624661=AmInx7; XM_396916=AmInx8; XP_001603984=NvInx1; XP_001604034=NvInx2; XM_003427685=NvInx3; XM_001603958=NvInx7; XP_001599753=NvInx8; AGAP001476-PA=AgInx1; AGAP001488-PA=AgInx2; AGAP004510-PA=AgInx3; AGAP006241-PA=AgInx456; AGAP001477-PA=AgInx7; AGAP001487-PB=AgInx8.

Tc-Inx7a-V5 transient expression

The full coding sequence of Inx7a was cloned using the primers 5'-AGA ATT CAC ATG TTG AAA ACT TTC GAA GCG-3' and 5'AAC TCG AGG TCA AAT TTC GCC GGC TTT TTC-3'; digested with EcoRI and XhoI, and ligated into pMT/V5 (Invitrogen) that had been digested by the same enzymes. The fusion construct was excised with PciI and NotI, cloned into the modified expression vector pT7-DsRed (13), linearized with NotI, and in vitro transcribed using the T7 mMESSAGE mMACHINE kit (Ambion). 3µg/µl capped mRNA was injected in 0-2 hours old eggs. Eggs were allowed to develop for 8 hours at 32°C and fixed for staining with the anti-V5 antibody (Invitrogen).

Parental RNAi for RNA deep sequencing

We injected two different parental RNA of interference (RNAi) into adults *of Tribolium castaneum.* The first parental RNAi is the control. It is a *Tribolium* Non-targeting sequence of dsRNA synthesized from the vector pCRII (Invitrogen) using the forward primer 5'-TGCCGGATCAAGAGCTACCAA-3' and the reverse primer 5'-TGTGAGCAAAAGGCCAGCAA-3' (37). The second parental RNA of interference is a sequence to knock down the gene Innexin 7a (TC011061). These dsRNA were made by the company Eupheria . For injection of parental dsRNA. first, 268 females were selected at the pupa stage. Once the females became adults, they were fixed on a microscope slides with a tape at their abdomen. Later, one elytrum was raised to be injected dorsally with parental RNAi (38). We injected 134 adult females with control parental RNAi and 134 adult females with parental RNAi to silence the Innexin 7 gene. The amount of parental RNAi injected per female was about 2 µl of a 0.5 µg/µl. After two days of the injection, adult males were added.

Sample collection for transcriptional analysis

The beetles were on egg laying for 12 hours in fine flour. After, we isolated the eggs from the adults and flour. To separate the adults we used a grid of 800 µm. To remove the eggs from the flour we used a grid of 350 µm. Approximately 300 eggs were obtained. We extracted the RNA from

the eggs using Trizol extraction (Invitrogen). Later, we purified the RNA extracted and digested the DNA on column with the RNeasy kit (Mini Elute). We collected 3 biological samples for each parental RNAi injection. We sent the RNA purified from the eggs to Genomescan company for sequencing.

RNAseq data analysis and bioinformatics

RNA sequencing from the eggs injected with Innexins 7a RNAi and the eggs injected with the control were performed by the company Genomescan, Leiden and passed their internal quality control for RNA (using an Agilent fragment analyzer) and sequence cluster yield. A total of at least 20 million paired end sequencing reads was obtained for each sample. Mapping of the reads was performed using the program Genetiles (39) using the genome assembly version Tcas 5.2. The mapping statistics shows that for each sample at least 70 % of the reads could be mapped and at least 40% of the reads could be mapped with a paired end read. We coupled the Ensembl gene IDs for mapping the reads to those of orthologs of *D. melanogaster* because the *D. melanogaster* database is better annotated than the database of *T. castenum*. As a caveat, it should be mentioned that with this method we could not find orthologs for approximately 30% of the *Tribolium* genes.

To identify the enrichment pathways of the differential expressed genes in the knock downs of Innexin 7 we used the bioinformatics software Database for Annotation, Visualization and Integrated Discovery (DAVID) (40, 41). We upload RNAseq list into DAVID to find the main pathways where these genes play a role. To select the pathways, we used a household of p-value<0.05. DAVID is developed by the Frederick National Laboratory for Cancer Research, United States of America.

We obtained the most enriched pathways of the differentially expressed using PathVisio software (42). PathVisio is developed by Maastricht University, the Netherlands. We used a p-value<0.05.We used PathVisio to discover genes that are expressed differently when we knock down innexin 7. We compared the two pathways list from DAVID and PathVisio and we analyzed the pathways found in both lists. We obtained the pathways from WikiPathways. We used for identifier mapping database the Dr_Derby_Ensembl_91.bridge database that is available at the Pathvisio website. Some pathways have been converted manually using the

Basic Local Alignment Search Tool (BLAST) at NCBI73 and Ensembl to find or confirm the *D. melanogaster* orthologues of the *Tribolium* genes.

Results

To investigate cellularization in *Tribolium*, we followed development using live imaging of embryos in which the cell cortex was labeled with the YFP-fused, GPI-anchored plasma membrane protein GAP43 (43). This fusion protein was transiently expressed by mRNA injection into eggs from wild type beetles or from a transgenic line expressing nuclear-localized GFP (13, 44).

We found that membrane invaginates between the nuclei after the 10th nuclear division (i.e. about 6 hours after egg laying) (Figure 1 A-D'. The 11th division occurs 30 minutes later (Figure 1 A). In contrast to *Drosophila*, the invaginated membrane does not retract and then invaginate anew at each nuclear division. Instead, already invaginated membrane remains at its original depth, just below the nuclei, and a new cleavage furrow invaginates between the daughter nuclei to form two protocells (Figure 1 E-J). One hour after the 11th division, the 12th and last synchronous division takes place (Figure 1 B).

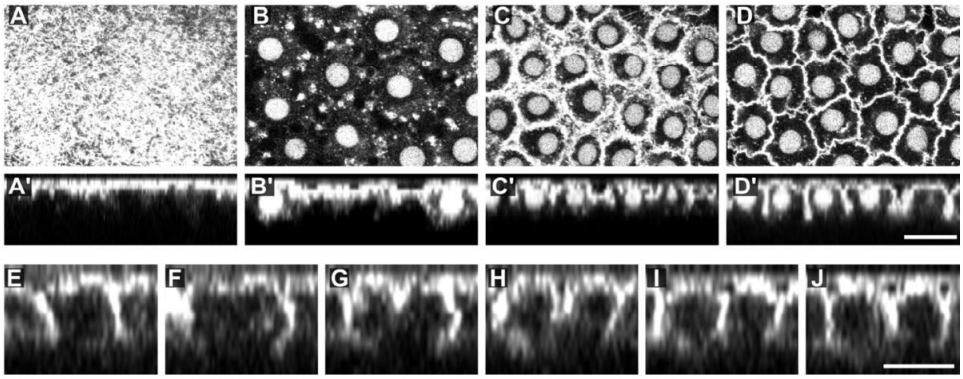

Figure 1. ***Membrane ingression during cellularization. (A-D')*** *Time series of membrane ingression during cellularization in a nuclear-GFP transgenic egg transiently expressing GAP43-YFP as membrane marker, timed from just before the moment that nuclei reach the surface of the egg (shown in A), i.e. after the 10th nuclear division. (A-D) optical sections either at the level of the membrane in (A), or at the level of the nuclei in (B-D). (A'-D') Orthogonal views from same time points. When nuclei are not visible in the orthogonal views it is because the cross section did not bisect them.* ***(E-J)*** *Time series of orthogonal views of membrane ingression during the 12th division in a GAP43-YFP transiently labelled embryo, timed from just before division begins as shown in (D). (E) prior to division a single protocell is visible. (F) when the nucleus divides (not visible) the membrane moves further apart. (G) Following separation of the chromosomes (not visible), membrane begins to invaginate between the new nuclei. (H-I) membrane continues to invaginate between new nuclei. (J) Two new protocells are visible. Scale bars: 20 µM*

About 90 minutes after this last synchronous division (at t≈2h30 after the 11th division), the protocells become refined into a regular array of pentagons and hexagons, with rare tetragons and heptagons (45). This suggests an increase in cortical tension. Concomitantly, a basal membrane starts to form (Figure 2 P, R1-4). Thus, a phase of rapid membrane extension is absent. Thirty minutes later, at t ≈3h, the cuboidal cells have completely closed at the basal side. Finally, at t≈3h30, the closed cuboidal cells of the germ rudiment start to divide asynchronously for the first time, giving rise to the differentiated blastoderm stage (Figure 2). Thus, cell closure in *Tribolium* appears to take place one cell cycle earlier than in *Drosophila*, i.e. after the 12th instead of the 13th division (1–3, 12).

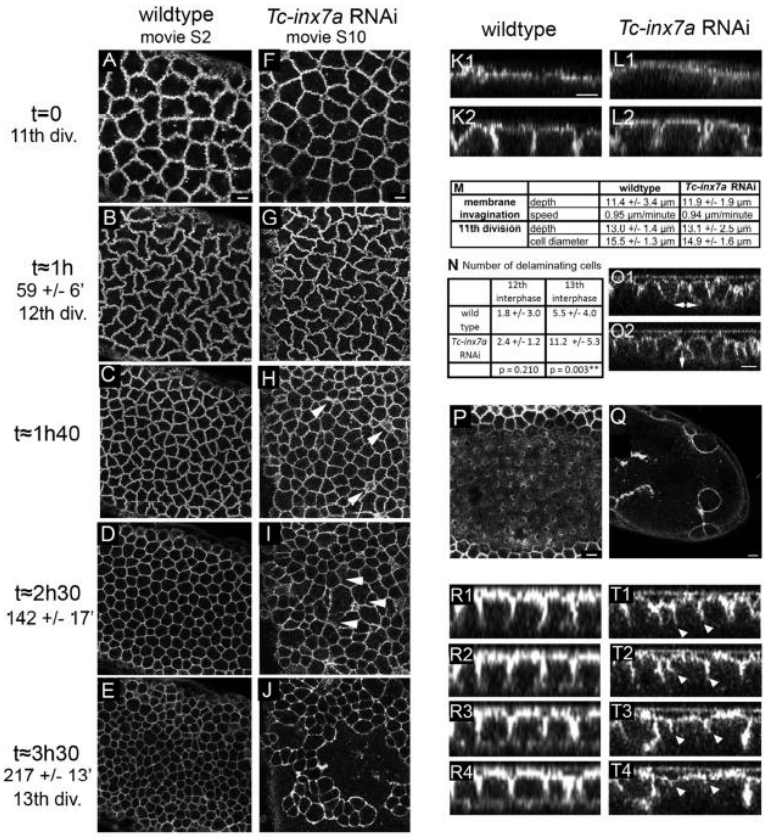

Figure 2. Cellularization in wild type and Inx7a depleted eggs. *(**A-E**) Stills from a time-lapse movie of a developing wild type egg transiently expressing GAP43-YFP as a plasma membrane marker In this movie, t=0 is set at the onset of the 11th division. The 12th division (t=1h) is the last synchronous division and the 13th (t=3h30) is the first asynchronous division of the germ rudiment. **(F-J)** Stills from a GAP43-YFP time-lapse movie of a developing Tc-inx7a pRNAi egg at approximately the same time points as (A-E). Arrowheads in H point at delaminating protocells. Arrowheads in I indicate retracting membrane. **(K,L)** Stills from GAP43-YFP time lapse movies showing the beginning (1) and the end (2) of the plasma membrane ingression after 10th division in wild type (K) and Tc-inx7a pRNAi eggs (L). (**M**) Quantitative measurements of the depth and speed of membrane invagination after the 10th nuclear division, as well as size of the protocells after the 11th division in wild type and Tc-inx7a RNAi eggs (see Materials and Methods). **(N)** Quantification of delaminating protocells in a 145µm x 145µm area before and after the 12th division in 8 wild type and 8 Tc-inx7a pRNAi eggs. **(O)** Lateral views of the process of protocell delamination. During delamination, membrane of a protocell is biased towards neighboring nuclei (O1 double-headed arrow). This protocell is extruded from the epithelium (arrow in O2). (**P**) Still from a GAP43-YFP time lapse movie of a wild type egg (at a basal focal plane at the time of basal closure. **(Q)** Still from a GAP43-YFP time lapse movie of a Tc-inx7a pRNAi egg (). Note the large uncellularized area. **(R, T)** Stills from GAP43-YFP time-lapse movies showing orthogonal views of basal membrane formation in a wild type egg (R) and Tc-inx7a pRNAi egg (T). Arrowheads in T indicate retracting membrane. Note that one cell on the left manages to close in T4. Scale bars: 10 µm. Scale bar in K1 applies to all orthogonal views.*

In Tribolium, furrow canals are not enriched with actin

In *Drosophila*, the leading edges of the ingressing membrane are dilated and form interconnected furrow canals that are enriched with actin and are separated from the rest of the membrane by an Armadillo-rich basal adherens junction (BAJ, see introduction). The described live imaging with the plasma membrane marker GAP43 was not carried out at sufficient resolution to determine whether furrow canals are present in *Tribolium*. To resolve this, we inspected the tips of the ingressing membrane by TEM, and observed dilated bases (Figure 3 A-D, asterisks). Furthermore, as in *Drosophila*, those dilations are separated from the rest of the membrane by junctions (Figure 3 A-D, green arrowheads). To establish if these junctions are BAJs, we used an antibody to localize Armadillo. Indeed, after the 12th division, Armadillo localization is consistent with BAJs above the furrow canal (Figure 3 E). We conclude that furrow canals are also present in *Tribolium*.

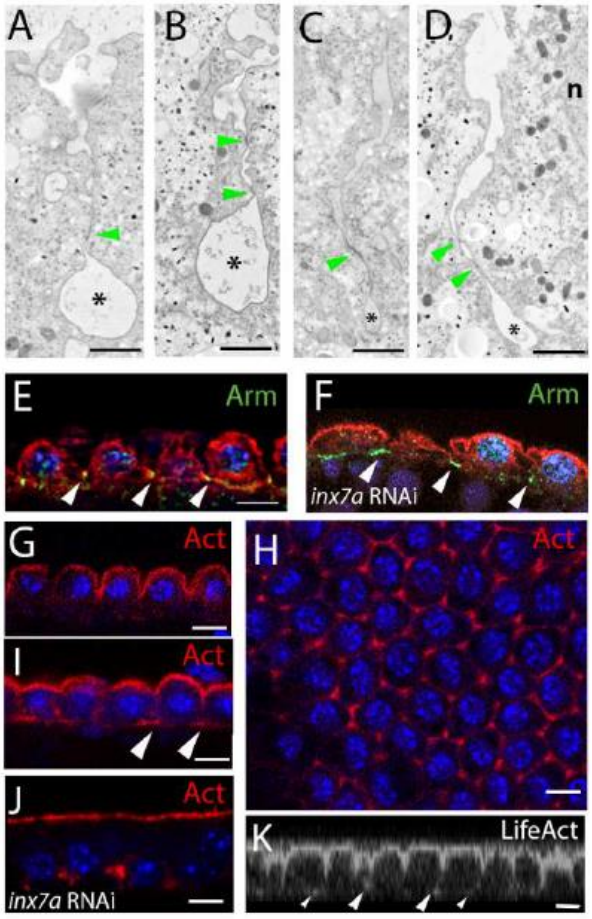

Figure 3. Analysis of the furrow canals in Tribolium. ***(A-D)*** *Transmission Electron Micrographs of ingressing membrane in wild type eggs. Furrow canals are indicated with asterisks. Junctions are indicated with green arrowheads. "n" denotes nucleus in (D).* ***(E, F)*** *Immunofluorescence (IF) visualisation of Armadillo (green) and tubulin (red) and nuclein with DAPI (blue) in wild type (E) and Tc-inx7a pRNAi (F) blastoderm. Note that in F, Armadillo is still detected on some retracting membranes (arrowheads).* ***(G-J)*** *IF visualisation of actin (red), nuclei with DAPI (blue), in wild type (G, I, H) and Tc-inx7a pRNAi (J) blastoderm. No enrichment of actin is observed at the base of the ingressing membrane (G), except for the corners where three cells meet (H, arrowheads in I). A few dots of actin remain basally after Tc-inx7a RNAi (J).* ***(K)*** *Orthogonal view of a LifeAct time-lapse movie revealing minor accumulations of Actin at the bases of some of the ingressed furrows (arrowheads). Scale bars:1µm (A-D); 10 µm (all other panels).*

However, in contrast to *Drosophila*, the furrow canals are not heavily enriched with actin. Neither phalloidin, nor an actin antibody could detect conspicuous actin enrichment at the bases of the ingressing membrane (Figure 3 G). We did detect some basal enrichments of actin when basal cell closure starts (Figure 3 I), but these enrichments correspond only to corners where three cells meet (Figure 3 H). As more membrane is present at these points, this apparent actin accumulation likely reflects normal levels of cortical actin. In order to exclude penetration problems of the actin antibody, we also injected mRNA coding for LifeAct-GFP that specifically labels F-actin (13, 46). Similar to the actin antibody, this revealed minor actin accumulation at the base of some of the ingressed

furrows (Figure 3 K), but incomparable to the well described and consistent localization of actin to all furrow canals in *Drosophila* (5).

Taken together, these results suggest that furrow canals are formed during *Tribolium* cellularization, but they are less enriched with actin than those in *Drosophila*.

Novel junctions form along the nascent basal membrane

After the 12th division, the dilated edges of the ingressed membrane start to enlarge (Figure 4 A-D). Subsequently, the ingressed membrane splits at the basal side as the furrow canals flatten (Figure 4 E, F). Surprisingly, we found that new junctions form between the nascent basal membrane and forming yolk plasmalemma (Figure 4 E, F, red arrow heads). As the basal membrane extends laterally, additional junctions are continuously added, until junctions are present along the whole basal membrane (Figure 4 G, see also supplementary Fig. S1). Such junctions have not been described in *Drosophila*.

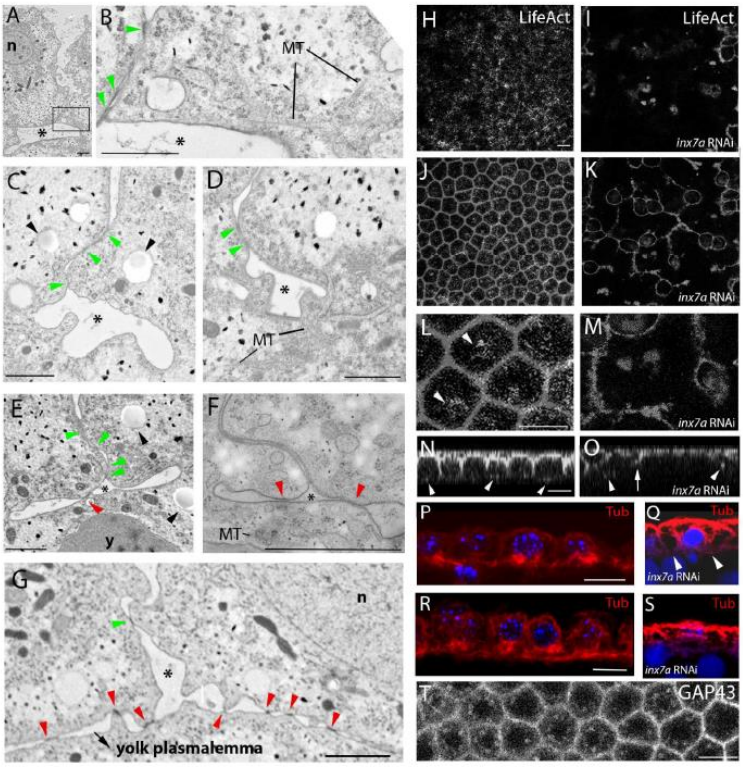

Figure 4. Basal cell closure in Tribolium. (A-D) *Transmission Electron Micrographs showing the enlarging and splitting furrow canals (asterisks). (B) is a magnification of the area boxed in (A).**(E-G)** TEM visualization of both the lateral BAJ (green arrowheads) as well as novel junctions between the nascent basal cell membrane and the forming yolk plasmalemma (red arrowheads, see also Supplementary Fig. S1.) Asterisks indicate the split furrow. n denotes nucleus in (A) and (G). MT denotes microtubuli in (B, D and F). y indicates yolk in (E). **(H, I)** Still from LifeAct-GFP time lapse movies in wild type (H) and after Tc-inx7a RNAi (I) at a basal focal plane. Note the extensive basal network of actin in (H) and its absence in (I). **(J, K)** Overlay of a more apical plane on the stills shown in (H) and (I). **(L, M)** Magnification of (J) and (K). Arrowheads in (L) point at accumulations of actin where the cells constrict. **(N, O)** Orthogonal views of (J) and (K), respectively. Arrowheads in (N) point at presence of actin where the cells constrict. Arrow in (O) indicates retracting membrane; arrowheads indicate remaining dots of actin. **(P-S)** IF visualization of Tubulin around nuclei in wild type (P, R) and Tc-inx7a pRNAi blastoderms (Q, S) presented as overlay of several confocal planes. DAPI (blue) stains the nuclei. Note that in wild type eggs, microtubules appear enriched and condensed during basal cell closure, whereas they retract in Tc-inx7a pRNAi (S).**(T)** Still from GAP43-YFP live imaging showing numerous moving compartments at the basal side of the forming cell.Scale bars: 1µm (A-G); 10 µm (all other panels).*

In *Drosophila*, cell closure is mediated by actin ring constriction (1). Although we could detect these rings using immunofluorescence in *Drosophila* (Supplementary Figure 1 F), we could not detect such rings in *Tribolium*. To exclude penetration difficulties of the antibody, we also analyzed basal cell closure by live imaging of embryos transiently expressing LifeAct-GFP (Figure 4 H, J, L, N). During basal membrane formation, a fine network of actin becomes visible at the base of the forming cells (Figure 4 H). An overlay of a more apical view revealed enrichments of actin at the constrictions of the basal membrane in some protocells (Figure 4 J, L, see Figure 4N for lateral view). However, these enrichments are incomparable to the obvious actin rings in *Drosophila* (Supplementary Figure S1F) and closely reflect the pattern observed with the membrane marker GAP43-YFP (Figure 4 P). This suggests that these actin enrichments represent normal levels of cortical actin, and that the role of the actin cytoskeleton in basal cell closure may not be as prominent as in *Drosophila*.

We did, however, detect enrichment of microtubules at the basal side of the closing cells (Figure 4 P, R). Microtubules are also evident in TEM micrographs (Figure 4 B, D, F). Thus, it is possible that polarized membrane insertion along microtubules plays a role in basal cell closure, like during the phase of rapid membrane extension in *Drosophila*. Consistent with this, we observed numerous highly mobile, GAP43-YFP positive compartments, suggesting extensive membrane activity (Figure 4 T). Furthermore, at the basal sides of the forming cells, TEM revealed conspicuous vesicles with a thin membrane and remnants of homogenous filling (Figure 4 C, E). These are probably lipid droplets and could supply lipids for membrane synthesis. However, we did not functionally test a possible role for membrane insertion in basal cell closure.

Taken together, basal cell closure in *Tribolium* relies on different mechanisms than *Drosophila*. First, the actin pattern found in *Tribolium* is incomparable to the conspicuous actin rings detected in *Drosophila* during basal constriction. Second, junctions form between the nascent basal membrane and the forming yolk plasmalemma. As we do not detect Armadillo at the basal membrane (Supplementary Figure S1E), these junctions are likely not adherents junctions.

TC011061 is an innexin7 ortholog and its maternal knockdown leads to a strong defect in cellularization

In an attempt to identify the nature of the basal junction during cellularization in *Tribolium*, we performed a small parental RNAi screen targeting candidate junction proteins (31). Knockdown of most genes encoding these proteins generated either sterile mothers (such as the E-cadherin knockdown) or mild non-penetrant egg phenotypes (47). In contrast, injection of dsRNA targeting TC011061, a gene with clear similarities to innexins, leads to a consistent and 100% penetrant phenotype in the early development of all eggs. In these eggs, late blastoderm stage nuclei are irregularly spaced when compared to wild type eggs (Figure 5 A-D). Phalloidin staining marking the cell cortex indicates the absence of membrane between many nuclei (Figure 5 E-H), giving the impression of multinucleated cells. Furthermore, some nuclei detach from the apical surface (Figure 5 F). These phenotypes are characteristic of cellularization mutants in *Drosophila* (3).

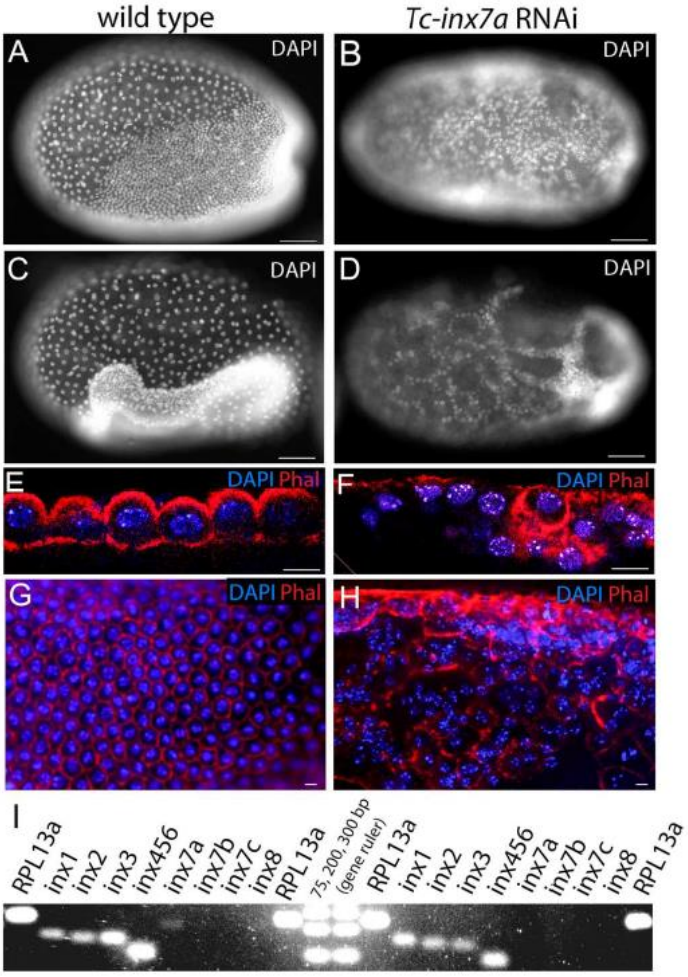

***Figure 5*. *Knockdown of Tc-inx7a leads to a strong cellularization phenotype*(*A-D*)** *Visualisation of nuclei with DAPI of wild type (B, D) and Tc-inx7a pRNAi (C, E) differentiated blastoderms (B, C) and at early gastrulation (D, E). Note in C and E that the nuclei are irregularly spaced. (**E-H**) Visualisation of nuclei (DAPI, blue) and actin marking the cell cortex (phalloidin, red) in wild type (F, H) and Tc-inx7a pRNAi eggs (G, I) by confocal (F, G) and epi (H, I) fluorescence microscopy. Note that cortical actin is absent between most nuclei in G. Note the apparent multinucleated cells in I. In I, the epifluorescent image has been deconvoluted. (**I**) RT PCR on cDNA from 0-6 hours old eggs from wild type and Tc-inx7a dsRNA injected mothers. Tc-inx7a is weakly expressed in wild type eggs, and this expression is absent in Tc-inx7a pRNAi eggs. Ribosomal Protein 13a (RPL13a) was used as reference gene (Lord et at, 2010). See Supplementary Table S2. Scale bars: 50µm (A-D); 10 µm (E-H).*

In total we found eight innexin genes in the *Tribolium* genome, all encoding proteins with the conserved four TM topology, a characteristic YYQW motif in the second TM domain, and the two conserved C residues (Supplementary Fig. S2) (14, 16). To establish the correct orthology of TC011061 and the other innexins, we first generated a Maximum Likelihood phylogeny including arthropod Innexins from available full genome sequences (Figure 6). Although the bootstrap values at the base of tree are low, the crustacean and insect innexins strongly cluster together in clear orthology groups, allowing unambiguous classification of the *Tribolium* Innexins. As in *Drosophila*, single orthologs of innexin1 (*ogre*), innexin2 (*kropf*) and innexin3 are present in *Tribolium*. Whereas the *Drosophila* genome contains the paralogs innexin4 (*zpg*), innexin5 and innexin6, *Tribolium* possesses a single ortholog that we named *Tc-inx456*. In the 3.0 version of the *Tribolium* genome, two *innexin8*-like genes are predicted (TC011065 and TC011066), but upon closer inspection these belong to a single gene that produces two isoforms with different first exons, similar to the *Drosophila* innexin8 shak-B locus (Phelan and Starich, 2001). Finally, our phylogenetic analysis clearly identified TC011061 as an innexin7 ortholog (bootstrap value=93), that we arbitrarily named *Tc-inx7a*, as the *Tribolium* genome contains two other innexin7 paralogs (named *Tc-inx7b* and *Tc-inx7c*). These three genes are close together in a head-to-tail orientation on the chromosome, and their phylogeny suggests that they are innexin7 duplications specific to the *Tribolium* lineage. Since these three paralogues are highly similar in sequence we are not sure that the pRNAi targeting of *inx7a* will lead to specific knockdown.

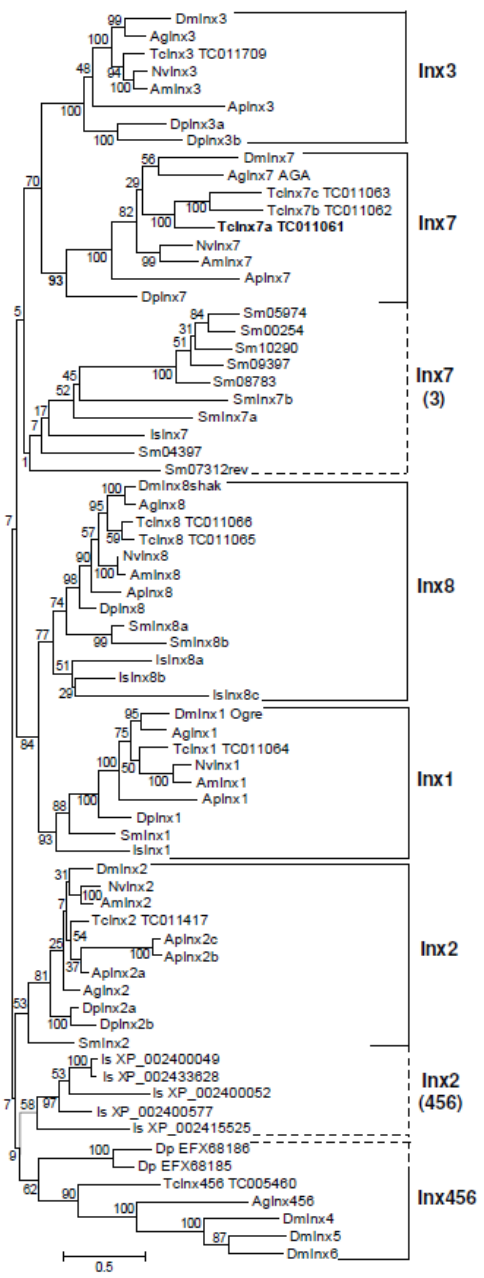

Figure 6. Maximum Likelyhood Phylogeny of the Arthropod Innexins. *Amino-acid substitution model: WAG+I+G, see Materials and Methods. Root was placed arbitrarily. Bootstrap values of 1000 replicates are indicated in percentage. The duplications of the pea aphid inx2 genes confuse the Inx2 branch somewhat. Abbreviations: Sm = the centipede Strigamia maritima; Is = the mite Ixodes scapularis; Dp = the water flea Daphnia pulex; Ap = the pea aphid Acyrthosiphon pisum; Am = the bee Apis mellifera; Nv = the wasp Nasonia vitripennis; Tc = the beetle Tribolium castaneum; Ag = the mosquito Anopheles gambiae; Dm = the fly Drosophila melanogaster. Strigamia maritima numbers are predictions from the preliminary genome sequence. SmInx7a and SmInx7b are named based on synteny in a gene cluster that is incorrectly predicted as one fused gene Sm07312 but consists of SmInx2, SmInx7a, SmInx7b, Inx1 and Inx8a. This synteny is also found in other Arthropods, like Nasonia and seems to be ancestral. Inx3-like sequences would then have arisen in the Pancrustacea. Sm08783, Sm09397, Sm10290, Sm00254, Sm05974 and possibly Sm04397 might be duplications of Inx7, but low bootstrap values do not allow unambiguous identification. Sm07312rev is an Inx7-like gene that has an inverted orientation in the Sm07312 cluster. Sm10724 is a duplication of Inx8a and is named SmInx8b. The mite sequences XP_002415525, XP_002400577, XP_002400052, IsXP002433628 and 002400049 cluster together with Inx456, but could as well belong to the Inx2-group. The latter would be more likely given the presence of Inx2 in the ancestral cluster. The Daphnia sequences EFX_18186 and EFX_68185 cluster together with Inx456. Since this could be due to long branch attraction, these sequences have not been named. Inx456 could thus have arisen in the higher holometabolous insects.*

RNAseq analysis of eggs after pRNAi targeting of innexin 7a

We performed RNAseq of RNA isolated from eggs of which the parents were injected with dsRNA targeting inx7a. The results from the differential expression of genes after pRNAi as compared to the control show a large set of genes that are differentially expressed (Figure 7). Using a P-value threshold of 0.05, a gene set of 1811 genes was identified that was different expressed after knockdown. We coupled the Ensembl gene IDs of these *Tribolium* genes to those of orthologs of *D. melanogaster* because the *D. melanogaster* database is better annotated than the database of *Tribolium* resulting in a list of 2414 *Drosophila* orthologs that were present in DAVID data base.

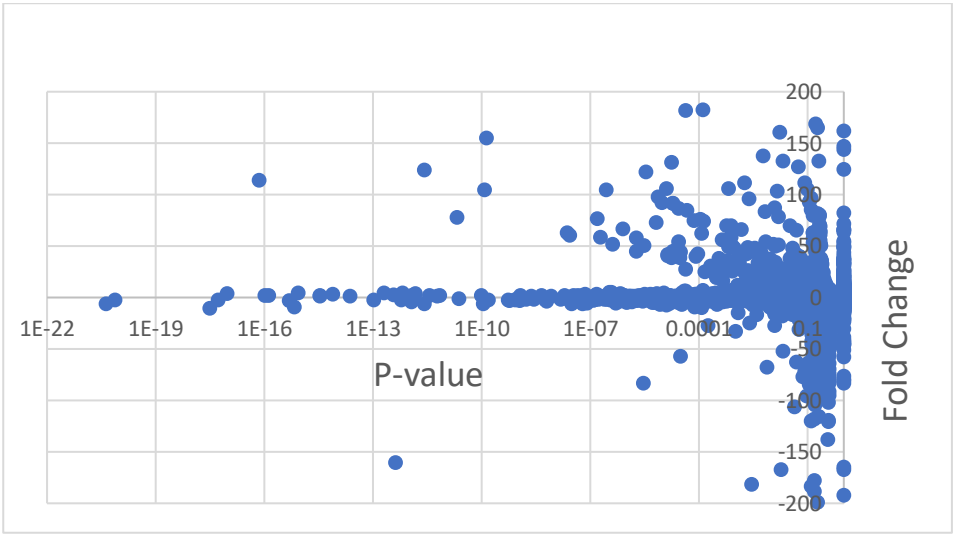

Figure 7. *Volcano plot showing the genes that are up or down regulated.*

We performed gene enrichment analysis of the *Drosophila* ortholog gene set to describe the effects of the pRNAi on the transcriptome. Functional annotation charts obtained from DAVID showed a strong enrichment with very low P values of many genes that are linked to development, particularly linked to insect cuticle development (see Gene Ontology in Table 2). We used two software programs for pathway enrichment analysis: DAVID and PathVisio. For PathVisio analysis we had to annotate manually many genes because they are poorly annotated in the

pathways available from Wikipathways (https://www.wikipathways.org/index.php/WikiPathways). We obtained two very different lists of enriched pathways from each software program (Table 2). The difference can be explained because the software programs uses different databases and algorithms to find the most enriched pathways (40–42). Therefore, as the two lists are different, we present them as complementary data. We focused on two pathways that were present in both lists: Notch signaling and DNA replication pathways.

Table 2. Comparison between the tables from PathVisio and David (KEEG and BP)

DAVID			
KEGG			
pathway	**Counts**	**%**	**p- value (PERMUTED)**
DNA Replication	40	25.7	0.072
Notch Signaling Pathway	16	28.6	0.127
Glycolysis and Gluconeogenesis	41	0.3	0.2
TGF Beta Signaling Pathway	15	0.3	0.125
mRNA processing	87	0.2	0.36
Non-homologous End joining	5	0.3	0.189
GO term			
Biological process	**Counts**	**%**	**p- value (PERMUTED)**
Chitin-based cuticle insect development	86	3.3	1.32E-20
Heterophilic cell-cell adhesion via plasma membrane cell adhesion molecules	25	1.0	9.66E-13
Transmembrane transport	110	4.2	5.90E-12
Flavonoid biosynthetic process	26	1.0	3.63E-11
Flavonoid glucuronidation	26	1.0	3.63E-11
Insecticide catabolic process	20	0.8	2.66E-10
PATHVISIO			
Pathway	**Counts**	**%**	**P-Value**
Endocytosis	105	1.3	4.10E-04
RNA degradation	51	0.6	1.10E-03
Fanconi anemia pathway	26	0.3	6.30E-03
Valine, leucine and isoleucine degradation	30	0.4	9.80E-03
N-Glycan biosynthesis	34	0.4	1.30E-02
DNA replication	33	0.4	1.60E-02
FoxO signaling pathway	47	0.6	1.60E-02
Notch signaling pathway	22	0.3	1.70E-02
Terpenoid backbone biosynthesis	20	0.3	2.70E-02
Pyrimidine metabolism	68	0.9	3.10E-02
beta-Alanine metabolism	18	0.2	4.30E-02
RNA polymerase	27	0.3	5.10E-02
Spliceosome	103	1.3	6.30E-02
Protein export	21	0.3	6.70E-02
Hippo signaling pathway - fly	50	0.6	7.00E-02
Ubiquitin mediated proteolysis	81	1	9.30E-02

We show visualization in PathVisio for the DNA replication pathway (Figure 8). In eukaryotes, DNA synthesis is complex, involving around 60 different proteins, depending on the organism, and therefore only part of it is shown: assembly of the pre-replicative complex (48).

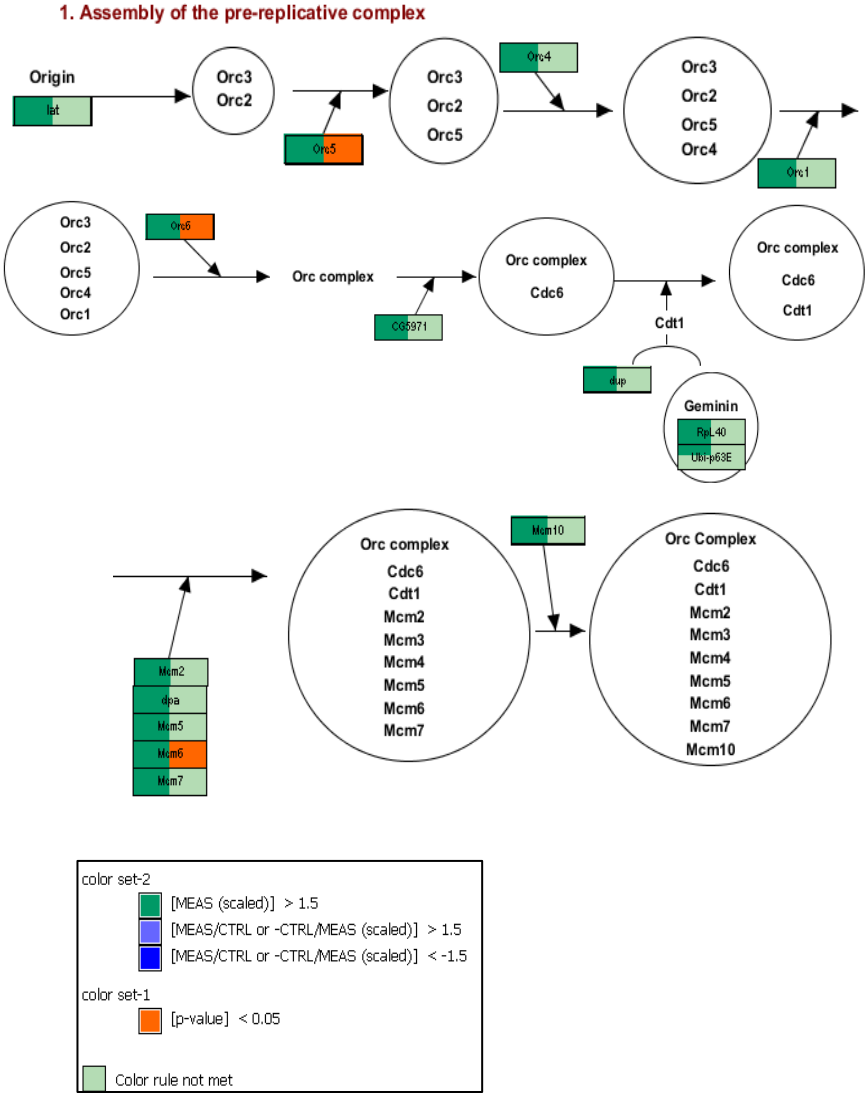

Figure 8. First step of DNA replication pathway using PathVisio for visualization. We did not show the rest of the pathways since there is no difference between the targeted RNAi and the control experiments. In eukaryotes, DNA synthesis is complex because the replication machinery has to deal with many difficulties, for example, specialized DNA structures, chromatin and even damaged DNA. This process involves around 60 different proteins, depending on the organism. DNA replication is related to the cell cycle and only happens once in each cell cycle (48).

We also used PathVisio to visualize the Notch signaling pathway (Figure 9). Notch signals are important in many process of the cell. For example, during development and maintenance of tissues, the Notch signal promote or suppress cell proliferation, cell death, acquisition of specific cell fates or activation of differentiation programs (49).

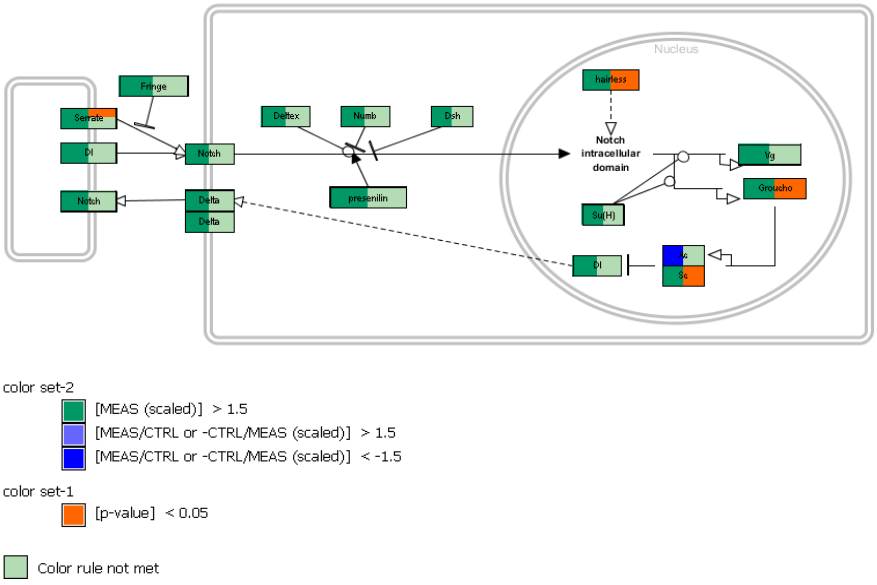

Figure 9. *Notch signaling pathway using PathVisio for visualization. In general, the Notch signaling pathway depends on the ability of a ligand to trigger receptor proteolysis, resulting in delivery of an active Notch fragment. The proteolysis is required for the receptor activation. After the Notch intracellular domain (NICD) is released by proteolysis, it travels to the nucleus. There, the NICD attaches to a DNA binding protein to gather a transcription complex that activates downstream target genes (49).*

In summary, the effect of knocking down inx7a has a strong effect on many pathways. This effect is expected since the knock down resulted in disturbance of cellularization which is a major transformation during embryonic development.

Changes in transcription of all innexin genes after pRNAi targeting of innexin 7a

Unexpectedly, the results show that inx7a is upregulated after pRNAi that targets this gene (Figure 10). This means that there is no evidence for the penetrance of the silencing on the RNA level of the targeted gene itself (Table 3). To analyze if there is a connection between targeting inx7a and the transcription of the rest of the innexins, we compared the level of expression of all the innexins after inx7a targeting (called treatment in the figures) with the control. In Figure 10, we plotted the level expression of the innexins comparing the control (orange) and the treatment (blue). We observed that innexin 7c and 8 (form 1) have very low coverage (in the order of 10 reads) and innexins 1, 2 and 3 have high coverage (in the order of 10000 reads). We performed a t-Test to analyze if there are significant differences in expression between the treatment and control. We observed that innexins 1, 2, 3, 456 and 8 have significantly different expression after treatment. The Innexins 1, 2, 456 and 8 have higher levels of expression than the control. On the contrary, inx3 has a lower level of expression in the treatment than in the control. In conclusion, the innexins 1, 2, 3, 456 and 8 are affected by targeting inx7a and therefore we assume that they have a connection with the silencing of inx7a. Based on the close homology of the three identified innexin 7 paralogs we assume that the effects of the pRNAi approach could be the result of silencing of all three paralogs and therefore we use the generic name innexin 7 (inx7) to indicate the entire gene cluster.

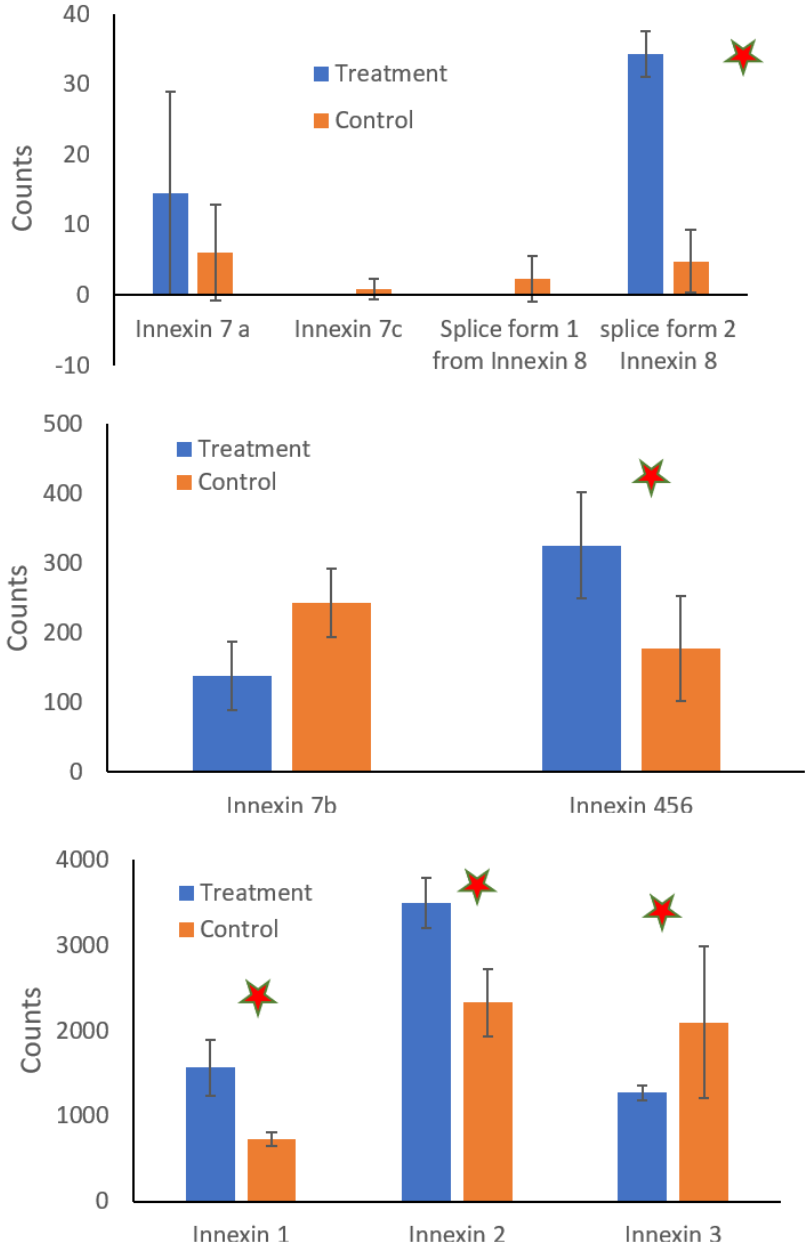

Figure 10. *Level of expression of innexins genes. The star means that the treatment and control are significantly different using a t- test with P-value<0.05. In blue is the treatment (Innexin 7 knocked down) and in orange is the control. Innexin 7c and 8 (splice form 1) have no detectable expression in the three repetitions of the experiment after treatment and also the controls have very low expression making it not possible to measure the effect of the knock down of inx7a.*

Table 3. Regulation of the genes after innexin 7 was silenced.

Name	TC Number	Fold Change	Regulation
Innexin 7 a	TC011061	2.337392808	upregulated
Innexin 7 b	TC011062	-1.648009698	down regulated
Innexin 7c	TC031404	-0.714082731	down regulated
Innexin 1	TC011064	2.197547938	upregulated
Splice form 1 Innexin 8	TC011065	-2.786227456	down regulated
Splice from 2 Innexin 8	TC011066	6.549326031	upregulated
Innexin 456	TC005460	1.936111705	upregulated
Innexin 3	TC011709	-1.502989278	down regulated
Innexin 2	TC011417	1.590002054	down regulated

Inx7 is required to maintain the invaginated membrane after the 12th division

To investigate how maternal knock-down of *innexin7a* leads to failure of cellularization, we compared cellularization of Tc-inx7a knockdown eggs to the wild type using GAP43-YFP live imaging movies. In Tc-inx7a pRNAi eggs, both the depth and speed of membrane invagination at the 10th division are unaltered (Figure 2 K-M,). Similarly, at the 11th division, no differences in depth of the cleavage furrows or diameter of the protocells are observed between wild type and Tc-inx7a pRNAi eggs (Figure 2 F, L, M).

The dramatic phenotype upon Tc-inx7a pRNAi starts to develop after the 12th division. First, directly after this last synchronous division, some protocells delaminate from the epithelium (arrowheads in Fig. 2H;). This also happens to a small extent before the 12th division, but not significantly more often than in wild type (Figure 4 N). After the 12th division, however, Inx7a depleted eggs show a highly significant increase in the number of delaminating protocells, suggesting a general instability of the blastoderm. During delamination, membrane of a protocell becomes skewed towards neighboring nuclei, ending in extrusion of that protocell (Figure 4). Second, ingressed membrane between the protocells strikingly disappears by the time basal cell closure starts in wild type eggs (Figure 4 T). Orthogonal views reveal that this disappearance is in fact a retraction of invaginated membrane to the apical surface (Figure 4 T). This leads to a

complete reversal of the cellularization process and gives rise to large cell-free areas (Figure 4 J). In the strongest cases, close to 100% of the invaginated membrane retracts (Figure 4 Q), and only a few cells have closed basally (Figure 4 Q, T,). In conclusion, in the absence of Inx7, plasma membrane invaginates normally, but retracts when basal cell closure starts.

No evidence for a direct role of Inx7 in BAJ, tubulin or actin localization

As Innexin2 in *Drosophila* colocalizes and interacts with Armadillo (50), we hypothesized that BAJ formation might be affected upon loss of Inx7a, causing destabilization of the ingressed membrane. However, Armadillo localizes normally in Tc-inx7a RNAi knock down eggs and even persists on retracting membrane (Figure 4F). This suggests that Inx7 is not required for BAJ formation and maintenance. Microtubules also appear in the basal part of the cell in Inx7a depleted eggs (Figure 4Q), suggesting that Inx7 does not affect initial formation of the basal microtubules. However, these microtubules never become as prominent as in wild type, and later retract with the retracting membrane (Figure 4S). Given the normal initial formation of microtubules, it is possible that this tubulin retraction is a consequence of the retraction of the membrane rather than its cause. Thus, we could not find evidence that incorrect localization of BAJs or microtubules causes the retraction of the ingresses plasma membrane.

In *Drosophila* cellularization mutants like Discontinuous Actin Hexagons (DAH) or *nullo*, membrane retraction is precipitated by reduced levels of F-actin at the furrow canals (10, 51). As interactions between the actin cytoskeleton and gap junction proteins have been shown for Connexin43 (Crespin et al., 2010; Wall et al., 2007) and the Pannexins (Bhalla-Gehi et al., 2010), we hypothesized that actin might be incorrectly localized upon Tc-inx7a RNAi. Indeed, a basal network of actin does not appear to form in Inx7a depleted eggs (Figure 4 I, K, M, O). In Inx7 depleted eggs, actin is visible at the cortex of the few cells that manage to close (Figure 4 K, M, O), at retracted membrane (Figure 4 O) and in a few basal dots (Figure 4J; Figure 4 K, M, O). However, no differences in actin localization are observed between Inx7a depleted eggs and wild type eggs until basal cell closure should start. This leaves the possibility that the

absence of the basal actin network is a mere consequence of the missing basal membrane, rather than its cause.

Overall, Inx7 is required for the stabilization of the ingressed membrane once basal membrane formation begins. We could find no evidence, however, that Inx7 exerts its function by directly localizing BAJs, microtubules, or actin.

Inx7a-V5 localizes to the basal membrane

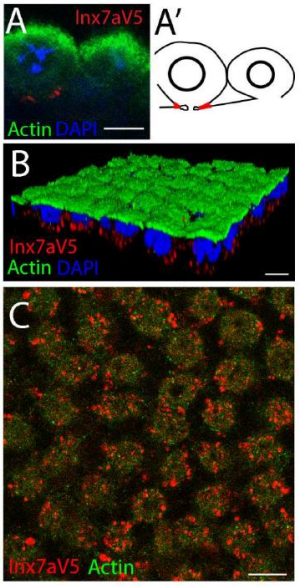

Figure 11. Localization of the transiently expressed Inx7a-V5 fusion protein (A-C) IF localization of transiently expressed Inx7a-V5 (using an anti-V5 antibody; red), actin (anti-actin antibody; green) and nuclei (DAPI, blue). (A) Orthogonal confocal section, showing that Inx7a-V5 localizes to the base of the invagination, where the membrane of the nascent cell and the yolk plasmalemma meet. (A') Schematic drawing of A. (B) 3D opaque reconstruction showing the basal localization of Inx7a-V5. Fixation was optimized for V5 antibody staining, resulting in poor actin antibody penetration that was insufficient to visualize the basal membrane in an opaque 3D reconstruction (C) Confocal section through the base of the forming cells where Inx7-V5 is detected in plaques, mostly overlapping with the basal cortical actin. Scale bars: 10 µm.

Next, we hypothesized that Inx7 is a component of the junctions identified by TEM between the forming basal membrane and the yolk plasmalemma. These junctions could flatten and split the enlarged furrow canal, thus stabilizing the ingressed membrane. In order to test this hypothesis, we aimed to visualize the localization of the Innexin7 protein. As the antibody against *Drosophila* Innexin7 recognizes a peptide stretch that is not present in the *Tribolium* Inx7a (Supplementary Fig. S2), we designed a Tc-Inx7a-V5 fusion protein, injected its mRNA into early wild type eggs and performed immunohistochemistry using an antibody against the V5 tag. The transiently expressed protein was detected in 15 out of 45 injected eggs and is indeed localized at the base of the invaginated membrane (Figure 11 A). This localization is observed when the tip of the invaginated membrane started to enlarge and split between the cells (Figure 11 A). This stage coincides with the delaminating protocells following Tc-inx7a pRNAi. Finally, during actual basal cell closure, Inx7a-V5 localizes all over the forming basal membrane in plaques typical for gap junctions (Figure 11 B, C) (52). This stage coincides with the retraction of the membranes following Tc-inx7a RNAi. We propose that Innexin7a forms gap junctions between the nascent basal cell membrane and the yolk plasmalemma, stabilizing the forming basal membrane.

Discussion and conclusions

We have described cellularization in the beetle *Tribolium castaneum* and identified junctions joining together the laterally extending basal membrane and the forming yolk plasmalemma. In a functional screen for junction proteins, we found a critical role for Inx7 in cellularization. When Tc-inx7a is depleted maternally, the basal cell membranes do not form and the ingressed plasma membrane retracts to the apical surface at the time basal cell closure starts. We propose that Inx7a is a component of the newly identified junctions that stabilize the ingressed membrane.

Differences in Tribolium and Drosophila cellularization

Cellularization in *Tribolium* exhibits six remarkable differences to *Drosophila*. First, the plasma membrane does not retract during divisions as in *Drosophila*. Second, cell closure in *Tribolium* appears to take place one cell cycle earlier than in *Drosophila*, i.e. after the 12th instead of the 13th division (1, 2, 53, 54). This difference is not surprising, as variation in the number and rate of nuclear divisions is common among insect groups (55). Third, the furrow canals are not enriched with actin.

Fourth, in *Drosophila*, the phase of slow membrane extension is accompanied by elongation of the nuclei and is followed by a phase of rapid membrane extension allowing deep ingression before final closure of the cell (4). In *Tribolium*, the nuclei remain spherical, and the rapid phase is absent. After the last synchronous division, the membrane does not extend any further (Figure 12 A), and cell closure directly follows (Figure 12 B, C) leading to a much thinner blastoderm with cuboidal cells. Cells of the embryonic ectoderm then elongate and form a pseudostratified columnar epithelium (13, 56). This is similar to most insect lineages studied, including basally branching insects, and is therefore likely to be ancestral (55, 57). In contrast, a thickened layer of cytoplasm with apically positioned nuclei has evolved in *Drosophila* and other Cyclorrhapha (higher Diptera) (58). Thus, the membrane has to ingress much further, requiring a long phase of rapid extension. As a result, cellularization in *Drosophila* directly yields columnar cells. This may facilitate more rapid development, as it has been suggested

that cuboidal cells first have to elongate before gastrulation, whereas columnar cells can directly enter gastrulation (58).

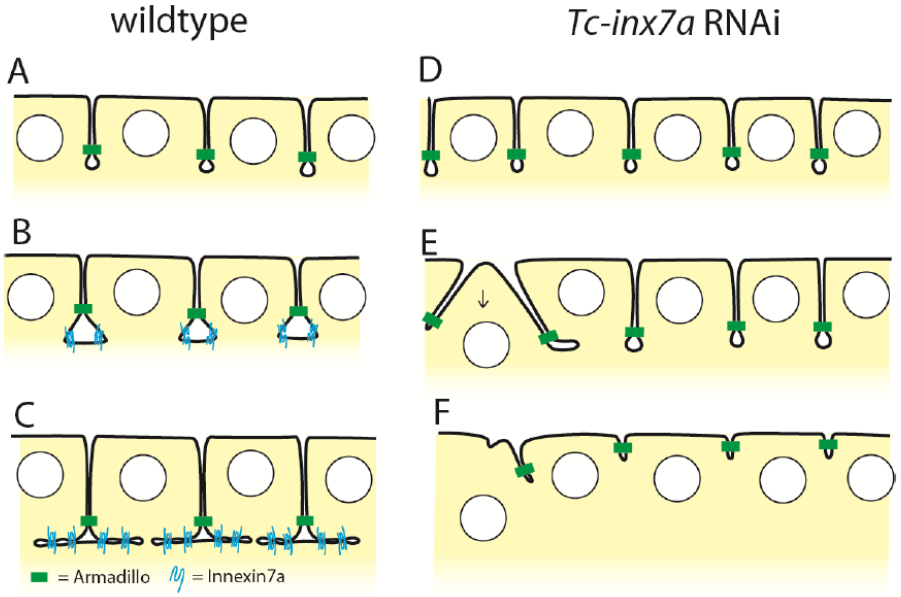

Figure 12. Model for a role of Inx7a in cellularization in Tribolium *(**A-C**) wild type cellularization. **(A)** Membrane invaginates between the nuclei after the 10th nuclear division and remains at this depth. Furrow canals and basal adherens junctions (green) form. **(B, C)** Inx7a forms junctions in the enlarging furrow canal mediating the splitting of the tip of the ingressed membrane (C). Inx7a forms gap junctions joining together the nascent basal cell membrane and the forming yolk plasmalemma stabilizing the ingressed membrane and enabling basal cell closure. (**D-F**) Tc-inx7a pRNAi severely affects cellularization. **(D)** Membrane invaginates normally in Tc-inx7a pRNAi embryos and basal adherens junctions form (green). **(E)** In absence of Inx7a, the tip of the ingressed membrane does not split properly. Ingressed membrane of a protocell can be inclined toward neighboring nuclei, this particular protocell will be extruded from the epithelium. **(F)** Finally, ingressed membrane retracts to the apical surface, as the membrane is not stabilized.*

Fifth, basal cell closure appears to take place through different mechanisms in *Drosophila* and *Tribolium*. Interestingly, in *Drosophila*, basal cell closure is mediated by contractile actin rings (1). We could not visualize such rings in *Tribolium* using either LifeAct-GFP live imaging or immunohistochemistry with an anti-actin antibody, whereas the latter method did reveal these rings in *Drosophila* (supplementary Fig. 1F). The microtubules visible in TEM micrographs and tubulin antibody stains, and the moving GAP43-positive vesicles, suggest the possibility that polarized membrane insertion may be a driving force involved in basal cell closure in *Tribolium*, similar to the fast phase of membrane extension in *Drosophila*.

However, the exact forces involved in basal cell closure in *Tribolium* remain to be elucidated.

Sixth, we found junctions that keep together the forming basal membrane and the forming yolk membrane. Such junctions have not been described in *Drosophila*. It seems that these junctions are instrumental in basal cell closure in *Tribolium*.

RNA deep sequencing

The method called parental RNAi (pRNAi) is used standardly in *Tribolium* and a few other insects to silence genes (59). It is systemic, highly penetrant and it can phenocopy genetic null phenotypes (31, 60). In contrast, in other organism other techniques are used to silence genes instead of pRNAi, such as canonical RNAi, mutagenesis or morpholino injections (61). These methods have been shown to trigger complex feedback mechanisms especially when paralogues genes are present. Recently, it has been shown that Non-sense Mediated Decay (NMD) caused by various mutations has a complex effect on the expression of many other genes in various organism (62). The mechanism of NMD is not yet understood, but it has not been reported yet for morpholino gene knockdown approaches. Hashimoto, et al found that there is a machinery to clear mRNA 5'-fragments produced by both RNAi and NMD in *D. melanogaster* cells (63). In yeast it was shown that this machinery, called nonstop mRNA decay (NSD), triggers nonstop mRNA degradation by removing stalled ribosomes (62). In *Tribolium* NMD after gene silencing using pRNAi has not been studied yet. Rehwinkel et al (63) studied the role of the argonaut proteins during NMD in *D. melanogaster*, but concluded that the mechanism is still not well understood. When a gene is knocked down using pRNAi, the mRNA is degraded by the RISC complex (65). It is possible that NMD works via the RISC complex, or the RISC complex might leave bits of RNA which triggers NMD. To further investigate complex feedback processes, including the effects of NSD, at the transcriptome level after pRNAi we performed RNAseq experiments after knockdown of inx7a. Especially since inx7a has two highly similar paralogs, complex feedback mechanisms could be expected.

The effects of pRNAi knockdown of inx7a on the transcriptome of eggs is very strong on a large set of genes (Figure 10). In line with the strong

developmental effects of the knock down. Unexpectedly, the results show that inx7a is upregulated after knock down, this means that there is no evidence of the penetrance of the silencing or NMD based on the RNA level of the targeted gene itself (Table 3). We also see a strong up regulation effect of the pRNAi of inx7a on several other innexin genes. We found that 5 out of the 8 studied innexins where upregulated by silencing inx7 (innexins 1, 2, 456 and splice form 2 of innexin 8). The only gene of which the RNA level is significantly down regulated is inx3. The down regulation of innexin 7b, although not statistically significant, could be explained by a direct effect of the silencing since it has a similar sequence to innexin inx7a. The results show a complex feedback mechanism. It would be interesting to further investigate whether this is the result of NMD mechanisms or indirect feedback loops at the gene transcription regulation machinery level.

By performing gene enrichment analysis using DAVID or PathVisio software, we found many enriched pathways with a P-value adjusted value of p-value < 0.05. We show six pathways with the most significant values in the shown parameters. Considering that the RNAi targeting of inx7a resulted in severe developmental differences, it is very likely that many effects at the RNA level are indirectly caused by in difference in developmental timing. Comparing the two lists resulting from using the two software programs, the enriched pathways are different and their parameters have different values. We took the two pathways, DNA replication and notch that are present in both the DAVID and PathVisio list with significant parameter values for more detailed analysis (Figure 8 and Figure 9). Interestingly, a paper by Lechner, et al (66) showed a connection between inx2, wingless, Delta/Notch and hedgehog signaling. They found that hedgehog signaling is essential for the expression of wingless and Delta/Notch. Hedgehog and wingless regulate gap junction communication by transcriptionally activating the inx2 gene. In a feedback loop, inx2 is needed for the transcriptional activation of hedgehog, wingless and Delta/Notch (66). In summary, we used RNAseq to perform enrichment analysis of pathways after innexin 7a pRNAi targeting showing a very strong effect in many pathways. There are no published connections of innexins with signaling pathways described in any species. Therefore, our results could be the basis for future endeavors resulting in such a pathway.

The function of Innexin 7

The phenotype upon Tc-inx7a knock down demonstrates a role for the Inx7 group in stabilization of the ingressed plasma membrane after the 12th nuclear division. Furthermore, the localization of Inx7a-V5 suggests that Inx7a forms newly identified junctions between the forming basal membrane and the yolk membrane. We propose that these Inx7a-based junctions convey stability to the ingressed plasma membrane in two ways. First, these junctions split the leading edges (furrow canals) of the ingressed membrane immediately after the 12th division (Figure 12 B). In the absence of proper splitting, membrane of a protocell can become skewed towards neighboring nuclei, as happens during protocell delamination (Figure 12 E). Second, these junctions stabilize the forming basal membrane during the phase of actual basal cell closure (Figure 12C). Absence of this stabilization leads to the retraction of the ingresses membrane to the apical surface (Figure 12 F), causing a complete reversal of the cellularization process.

As Inx7 proteins are gap junction proteins, we suggest that the newly identified junctions are gap junctions, and that Inx7a is a key component of them. However, this remains to be proven, as Innexins can also function in a hemichannel (67). It is also possible that the newly identified junctions are of completely different nature, and that Inx7a is merely involved in their initial assembly or stabilization. Our RNAseq results showing the effect of our pRNAi approach indicate a possible connection of inx7 with DNA replication. In this context, the publication of Doble et al (2004) that shows that phosphorylation of serine 262 in the gap junction protein connexin-43 regulates DNA synthesis in human cardiomyocytes supports our findings. It is therefore interesting to further investigate the role of gap junction regulation in the DNA replication process.

It might seem surprising that the sole depletion of Inx7a shows this strong cellularization phenotype, while Tc-inx1, inx2, inx3, inx456 are also expressed during cellularization. However, specific protein properties might distinguish the Innexin7 paralogs from the other expressed Innexins. For instance, Inx7a, b and c display a distinctive Trp196 at the beginning of TM3 (Supplementary Fig. S2), a position involved in the oligomerization compatibility of the vertebrate Connexin43 (68). This Trp residue is also conserved in *Nasonia, Apis* and *Anopheles* Inx7. It is also possible that the Inx7a primes and stabilizes formation of heteromeric gap junctions with

other Innexins. This has been proposed for *Drosophila* Inx3 in a Inx1/2/3 complex in the amnioserosa, as the sole loss of Inx3 leads to a strong dorsal closure phenotype, in contrast to individual loss of Inx1 or Inx2 (69). Since in other organisms, paralogs often develop to have a specialized function in heteromeric complexes (e.g. reference Toll-like receptors heterodimers) it wouldn't be surprising if the paralogs of the innexin 7 group are forming heteromeric gap junctions and therefore have an equally important function.

The proposed mechanism of basal cell closure involving Inx7 could be unique to *Tribolium*. However, since the *Drosophila* mode of cellularization involving columnar cells is evolutionary derived, it seems more likely that the Inx7-mediated process is ancestral.

Contribution

Tania Vazquez-Faci: Writing, pRNAi experiments, sample collection and quality control, for transcriptional analysis, RNAseq and subsequent bioinformatic analysis.
Mathew A. Benton: time laps movies, injection of the inx7a-V5 fusion construct and subsequent egg fixation, writing of the manuscript.
Gerda E.M. Lamers: Transmission electron images.
Catherine Rabouille: writing and experimental analysis, initial concepts.
Herman Spaink: writing, RNAseq and subsequent bioinformatic analysis
Maurijn van der Zee: writing, immuno-histochemistry, egg fixation, phylogenetic analysis, pRNAi (RNAi screen and innexin experiments) experimental analysis, final supervision, initial concepts.

References

1. Harris, T.J.C., J.K. Sawyer, and M. Peifer. 2009. How the cytoskeleton helps build the embryonic body plan: Models of morphogenesis from Drosophila. Curr. Top. Dev. Biol. 89: 55–85.
2. Lecuit, T. 2004. Junctions and vesicular trafficking during Drosophila cellularization. J. Cell Sci. 117: 3427–3433.
3. Mazumdar, A., and M. Mazumdar. 2002. How one becomes many: blastoderm cellularization in Drosophila melanogaster. Bioessays. 24: 1012–22.
4. Schejter, E.D., and E. Wieschaus. 1993. Functional elements of the cytoskeleton in the early Drosophila embryo. Annu. Rev. Cell Biol. 9: 67–99.
5. Warn, R.M., and R. Magrath. 1983. Experimental Cell Research 143 (1983) 103-114 Distribution during the cellulari2ation with fl-phalloidin of the drosophila embryo visualized Exp. Cell Res. 143.
6. Lecuit, T., and E. Wieschaus. 2000. Polarized insertion of new membrane from a cytoplasmic reservoir during cleavage of the Drosophila embryo. J. Cell Biol.150 (4): 849-860.
7. Pelissier, A., J.P. Chauvin, and T. Lecuit. 2003. Trafficking through Rab11 Endosomes Is Required for Cellularization during Drosophila Embryogenesis. Curr. Biol. 13 (21): 1848-1857.
8. Riggs, B., W. Rothwell, S. Mische, G.R.X. Hickson, J. Matheson, T.S. Hays, G.W. Gould, and W. Sullivan. 2003. Actin cytoskeleton remodeling during early Drosophila furrow formation requires recycling endosomal components Nuclear-fallout and Rab11. J. Cell Biol. 163: 143–154.
9. Rothwell, W.F., P. Fogarty, C.M. Field, and W. Sullivan. 1998. Nuclear-fallout, a Drosophila protein that cycles from the cytoplasm to the centrosomes, regulates cortical microfilament organization. Development. 125(7):1295-303.
10. Sokac, A.M., and E. Wieschaus. 2008. Local Actin-Dependent Endocytosis Is Zygotically Controlled to Initiate Drosophila Cellularization. Dev. Cell. 14(5):775-786.
11. Schröder, R., A. Beermann, N. Wittkopp, and R. Lutz. 2008. From development to biodiversity - Tribolium castaneum, an insect model organism for short germband development. Dev. Genes Evol. 218:

119–126.
12. Handel, K., C.G. Grünfelder, S. Roth, and K. Sander. 2000. Tribolium embryogenesis: a SEM study of cell shapes and movements from blastoderm to serosal closure. Dev. Genes Evol. 210: 167–179.
13. Benton, M. a, M. Akam, and A. Pavlopoulos. 2013. Cell and tissue dynamics during Tribolium embryogenesis revealed by versatile fluorescence labeling approaches. Development. 140: 3210–20.
14. Bauer, R., B. Löer, K. Ostrowski, J. Martini, A. Weimbs, H. Lechner, and M. Hoch. 2005. Intercellular communication: The Drosophila innexin multiprotein family of gap junction proteins. Chem. Biol. 12: 515–526.
15. Ostrowski, K., R. Bauer, and M. Hoch. 2008. The Drosophila Innexin7 gap junction protein is required for development of the embryonic nervous system. Cell Commun. Adhes. 15: 155–167.
16. Phelan, P. 2005. Innexins: Members of an evolutionarily conserved family of gap-junction proteins. Biochim. Biophys. Acta - Biomembr. 1711: 225–245.
17. Abascal, F., and R. Zardoya. 2013. Evolutionary analyses of gap junction protein families. Biochim. Biophys. Acta - Biomembr.
18. Baranova, A., D. Ivanov, N. Petrash, A. Pestova, M. Skoblov, I. Kelmanson, D. Shagin, S. Nazarenko, E. Geraymovych, O. Litvin, A. Tiunova, T.L. Born, N. Usman, D. Staroverov, S. Lukyanov, and Y. Panchin. 2004. The mammalian pannexin family is homologous to the invertebrate innexin gap junction proteins. Genomics.
19. Wakimoto, B.T., F.R. Turner, and T.C. Kaufman. 1984. Defects in embryogenesis in mutants associated with the antennapedia gene complex of Drosophila melanogaster. Dev. Biol.
20. Panchina, Y., I. Kelmanson, M. Matz, K. Lukyanov, N. Usman, and S. Lukyanov. 2000. A ubiquitous family of putative gap junction molecules [2]. Curr. Biol. 10(13): 473-474.
21. Alexopoulos, H., A. Böttger, S. Fischer, A. Levin, A. Wolf, T. Fujisawa, S. Hayakawa, T. Gojobori, J.A. Davies, C.N. David, and J.P. Bacon. 2004. Evolution of gap junctions: The missing link? [1]. Curr. Biol. .
22. D'hondt, C., R. Ponsaerts, H. De Smedt, G. Bultynck, and B. Himpens. 2009. Pannexins, distant relatives of the connexin family with specific cellular functions? BioEssays.
23. Goodenough, D.A., and D.L. Paul. 2009. Gap junctions. Cold Spring

Harb. Perspect. Biol.
24. Meşe, G., G. Richard, and T.W. White. 2007. Gap junctions: Basic structure and function. J. Invest. Dermatol.
25. Scemes, E., S.O. Suadicani, G. Dahl, and D.C. Spray. 2007. Connexin and pannexin mediated cell-cell communication. In: Neuron Glia Biology.
26. Phelan, P., and T.A. Starich. 2001. Innexins get into the gap. BioEssays. 23: 388–396.
27. Güiza, J., I. Barría, J.C. Sáez, and J.L. Vega. 2018. Innexins: Expression, regulation, and functions. Front. Physiol. 9: 1–9.
28. Hughes, A.L. 2014. Evolutionary Diversification of Insect Innexins. J. Insect Sci. 14: 1–5.
29. Wu, C.L., M.F.M. Shih, J.S.Y. Lai, H.T. Yang, G.C. Turner, L. Chen, and A.S. Chiang. 2011. Heterotypic gap junctions between two neurons in the drosophila brain are critical for memory. Curr. Biol. 21: 848–854.
30. Panfilio, K.A., G. Oberhofer, and S. Roth. 2013. High plasticity in epithelial morphogenesis during insect dorsal closure. Biol. Open. 2: 1108–1118.
31. Bucher, G., J. Scholten, and M. Klingler. 2002. Parental RNAi in tribolium (coleoptera). Curr. Biol. 12: 85–86.
32. Altschul, S.F., T.L. Madden, A.A. Schäffer, J. Zhang, Z. Zhang, W. Miller, and D.J. Lipman. 1997. Gapped BLAST and PSI-BLAST: A new generation of protein database search programs. Nucleic Acids Res. 25(17): 3389–3402.
33. Galtier, N., M. Gouy, and C. Gautier. 1996. Seaview and phylo_ win: Two graphic tools for sequence alignment and molecular phylogeny. Bioinformatics. 12: 543–548.
34. Abascal, F., R. Zardoya, and D. Posada. 2005. ProtTest: Selection of best-fit models of protein evolution. Bioinformatics. .
35. Guindon, S., and O. Gascuel. 2003. A Simple, Fast, and Accurate Algorithm to Estimate Large Phylogenies by Maximum Likelihood. Syst. Biol. 52: 696–704.
36. Kumar, S., K. Tamura, and M. Nei. 2004. MEGA3: Integrated software for Molecular Evolutionary Genetics Analysis and sequence alignment. Brief. Bioinform. 5: 150–163.
37. Van Der Zee, M., N. Berns, and S. Roth. 2005. Distinct functions of

the Tribolium zerkn??llt genes in serosa specification and dorsal closure. Curr. Biol. 15: 624–636.
38. Zee, M. v. d., O. Stockhammer, R.N. d. Fonseca, C. v. Levetzow, and S. Roth. 2006. Sog/Chordin is required for ventral-to-dorsal Dpp/BMP transport and head formation in a short germ insect. Proc. Natl. Acad. Sci. 103: 16307–16312.
39. Veneman, W.J., J. de Sonneville, K.J. van der Kolk, A. Ordas, Z. Al-Ars, A.H. Meijer, and H.P. Spaink. 2015. Analysis of RNAseq datasets from a comparative infectious disease zebrafish model using GeneTiles bioinformatics. Immunogenetics. 67: 135–147.
40. Da Wei Huang, Brad T Sherman, L.R. 2009. Systematic and integrative analysis of large gene lists using DAVID bioinformatics resources. Nat. Protoc. 4: 44–57.
41. Huang DW, Sherman BT, L.R. 2009. Bioinformatics enrichment tools: paths toward the comprehensive functional analysis of large gene lists. Nucleic Acids Res. 37: 1–13.
42. Martina Kutmon, Martijn P. van Iersel, Anwesha Bohler, Thomas Kelder, Nuno Nunes, Alexander R. Pico, C.T.E. 2015. PathVisio 3: An Extendable Pathway Analysis Toolbox. PLoS Comput ational Biol. 11.
43. Mavrakis, M., O. Pourquié, and T. Lecuit. 2010. Lighting up developmental mechanisms: how fluorescence imaging heralded a new era. Development. 137: 373–387.
44. Sarrazin, A.F., A.D.Peel, and M. Averof. 2012. A Segmentation Clock with Two-Segment periodicity in insects. Science (80-.). : 338–342.
45. van Drongelen, R., T. Vazquez-Faci, T.A.P.M. Huijben, M. van der Zee, and T. Idema. 2018. Mechanics of epithelial tissue formation. J. Theor. Biol. 454: 182–189.
46. Riedl, J., A.H. Crevenna, K. Kessenbrock, J.H. Yu, D. Neukirchen, M. Bista, F. Bradke, D. Jenne, T.A. Holak, Z. Werb, M. Sixt, and R. Wedlich-Soldner. 2008. Lifeact: a versatile marker to visualize F-actin. Nat. Methods. 5: 605–607.
47. van der Zee, M., M.A. Benton, T. Vazquez-Faci, G.E.M. Lamers, C.G.C. Jacobs, and C. Rabouille. 2015. Innexin7a forms junctions that stabilize the basal membrane during cellularization of the blastoderm in Tribolium castaneum. Development. 142: 2173–2183.
48. Recolin, B., S. van der Laan, N. Tsanov, and D. Maiorano. 2014.

Molecular mechanisms of DNA replication checkpoint activation. Genes (Basel). 5: 147–175.
49. Kopan, R., and M.X.G. Ilagan. 2009. The Canonical Notch Signaling Pathway: Unfolding the Activation Mechanism. Cell. 137: 216–233.
50. Bauer, R., C. Lehmann, J. Martini, F. Eckardt, and M. Hoch. 2004. Gap junction channel protein Innexin 2 is essential for epithelial morphogenesis in the Drosophila embryo. Mol. Biol. Cell. 15(6):2992-3004.
51. Zhang, C.X., M.P. Lee, A.D. Chen, S.D. Brown, and T.S. Hsieh. 1996. Isolation and characterization of a Drosophila gene essential for early embryonic development and formation of cortical cleavage furrows. J. Cell Biol. 134(4):923-34.
52. Shestopalov, V.I., and Y. Panchin. 2008. Pannexins and gap junction protein diversity. Cell. Mol. Life Sci. 65(3):376-94.
53. Handel, K., C.G. Grünfelder, S. Roth, and K. Sander. 2000. Tribolium Embryogenesis 2000. : 167–179.
54. Mazumdar, A., and M. Mazumdar. 2002. How one becomes many: blastoderm cellularization in Drosophila melanogaster. BioEssays. 24: 1012–1022.
55. Anderson, D.T. 1972. The development of holometabolous insects. In Developmental Systems: Insects. London: Academic Press.
56. Handel, K., A. Basal, X. Fan, and S. Roth. 2005. Tribolium castaneum twist: Gastrulation and mesoderm formation in a short-germ beetle. Dev. Genes Evol. 215: 13–31.
57. EDE, D.A. 1964. an Inherited Abnormality Affecting the Development of the Yolk. J. Embryol. Exp. Morphol. 12: 551–562.
58. Bullock, S.L., M. Stauber, A. Prell, J.R. Hughes, D. Ish-Horowicz, and U. Schmidt-Ott. 2004. Differential cytoplasmic mRNA localisation adjusts pair-rule transcription factor activity to cytoarchitecture in dipteran evolution. Development. 131: 4251–4261.
59. Berghammer, A.J., M. Weber, J. Trauner, and M. Klingler. 2009. Red flour beetle (Tribolium) germline transformation and insertional mutagenesis. Cold Spring Harb. Protoc. 4: 1–18.
60. Posnien, N., J. Schinko, D. Grossmann, T.D. Shippy, B. Konopova, and G. Bucher. 2009. RNAi in the red flour beetle (Tribolium). Cold Spring Harb. Protoc. 4.
61. Horn, C., and E. a. Wimmer. 2000. A versatile vector set for animal

transgenesis. Dev. Genes Evol. 210: 630–637.
62. S. Javad Rasouli & Didier Y.R. Stainier. 2017. Regulation of cardiomyocyte behavior in zebrafish trabeculation by Neuregulin 2a signaling. Nat. Commun. 8.
63. Hashimoto, Y., M. Takahashi, E. Sakota, and Y. Nakamura. 2017. Nonstop-mRNA decay machinery is involved in the clearance of mRNA 5'-fragments produced by RNAi and NMD in Drosophila melanogaster cells. Biochem. Biophys. Res. Commun. 484(1):1-7.
64. Rehwinkel, J., I. Behm-Ansmant, D. Gatfield, and E. Izaurralde. 2005. A crucial role for GW182 and the DCP1:DCP2 decapping complex in miRNA-mediated gene silencing. Rna. 11: 1640–1647.
65. White, B. 2007. Recombinant DNA: Genes and genomes—A short course (3rd ed.). Biochem. Mol. Biol. Educ.
66. Lechner, H., F. Josten, B. Fuss, R. Bauer, and M. Hoch. 2007. Cross regulation of intercellular gap junction communication and paracrine signaling pathways during organogenesis in Drosophila. Dev. Biol. 310: 23–34.
67. Scemes, E., D.C. Spray, and P. Meda. 2009. Connexins, pannexins, innexins: Novel roles of "hemi-channels." Pflugers Arch. Eur. J. Physiol. 457(6):1207-1226.
68. Largrée, V., K. Brunschwig, P. Lopez, N.B. Gilula, G. Richard, and M.M. Falk. 2003. Specific amino-acid residues in the N-terminus and TM3 implicated in channel function and oligomerization compatibility of connexin43. J. Cell Sci. 116: 3189–3201.
69. Giuliani, F., G. Giuliani, R. Bauer, and C. Rabouille. 2013. Innexin 3, a New Gene Required for Dorsal Closure in Drosophila Embryo. PLoS One. 8: 1–16.
70. Käll, L., A. Krogh, and E.L.L. Sonnhammer. 2005. An HMM posterior decoder for sequence feature prediction that includes homology information. Bioinformatics. 1:251-257 .
71. Richards, S., R. a Gibbs, G.M. Weinstock, S.J. Brown, R. Denell, R.W. Beeman, R. Gibbs, R.W. Beeman, S.J. Brown, G. Bucher, M. Friedrich, C.J.P. Grimmelikhuijzen, M. Klingler, M. Lorenzen, S. Richards, S. Roth, R. Schröder, D. Tautz, E.M. Zdobnov, D. Muzny, R. a Gibbs, G.M. Weinstock, T. Attaway, S. Bell, C.J. Buhay, M.N. Chandrabose, D. Chavez, K.P. Clerk-Blankenburg, A. Cree, M. Dao, C. Davis, J. Chacko, H. Dinh, S. Dugan-Rocha, G. Fowler, T.T. Garner, J. Garnes,

A. Gnirke, A. Hawes, J. Hernandez, S. Hines, M. Holder, J. Hume, S.N. Jhangiani, V. Joshi, Z.M. Khan, L. Jackson, C. Kovar, A. Kowis, S. Lee, L.R. Lewis, J. Margolis, M. Morgan, L. V Nazareth, N. Nguyen, G. Okwuonu, D. Parker, S. Richards, S.-J. Ruiz, J. Santibanez, J. Savard, S.E. Scherer, B. Schneider, E. Sodergren, D. Tautz, S. Vattahil, D. Villasana, C.S. White, R. Wright, Y. Park, R.W. Beeman, J. Lord, B. Oppert, M. Lorenzen, S. Brown, L. Wang, J. Savard, D. Tautz, S. Richards, G. Weinstock, R. a Gibbs, Y. Liu, K. Worley, G. Weinstock, C.G. Elsik, J.T. Reese, E. Elhaik, G. Landan, D. Graur, P. Arensburger, P. Atkinson, R.W. Beeman, J. Beidler, S.J. Brown, J.P. Demuth, D.W. Drury, Y.-Z. Du, H. Fujiwara, et al. 2008. The genome of the model beetle and pest Tribolium castaneum. Nature. 452: 949–955.

72. Bucher, G., J. Scholten, and M. Klingler. 2002. Parental RNAi in Tribolium (Coleoptera). Curr. Biol. 12: R85–R86.

Supplementary data

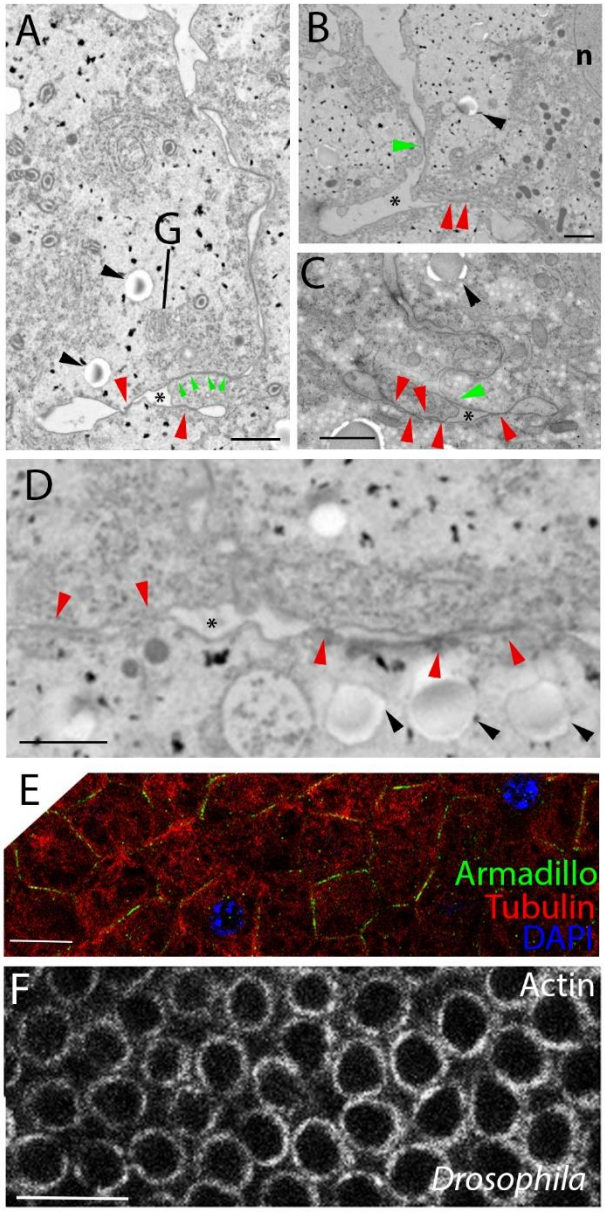

Figure S1. Novel junctions form along the basal membrane that are not adherens junctions (A-D) TEM visualization of both the lateral BAJ (green arrowheads) as well as novel junctions between the nascent basal cell membrane and the forming yolk plasmalemma (red arrowheads). Note that the number of junctions increases as the basal m embrane extends, until junctions are present along the whole basal membrane (D). Asterisks indicate the split furrow. Black arrowheads point at vesicles that could be lipid droplets. G denotes Golgi in (A). n denotes nucleus in (B) (E) Immunofluorescence (IF) visualization of Armadillo (green), Tubulin (red) and DAPI (blue) at the basal membrane towards the end of basal cell closure. Note that Armadillo is mainly detected between neighboring cells, not at the whole basal membrane. (F) IF visualization of actin at the bases of the cells in Drosophila.Note the conspicuous actin rings. Scale bars in (A-D): 1 µm. Scale bar in (E): and (F) 10 µm.

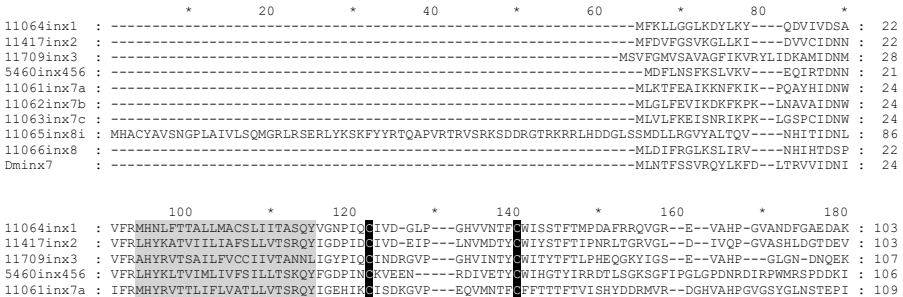

Figure S2 Alignment of the Tribolium Innexins with Drosophila Innexin 7 using Praline (http://www.ibi.vu.nl/programs/pralinewww). The four Transmembrane (TM) domains were predicted by Phobius (1) and are shaded in grey. The conserved YYQW motif in the first TM domain is indicated in white letters. The conserved C-residues in the extracellular loops are shaded in black. The peptide against which the Drosophila Innexin7 antibody was raised is underlined (2). A distinctive Trp residue at the beginning of TM3 is indicated in bold. 11065inx8i is an isoform of inx8 with alternative first exons.

Table S1 Results of the parental RNAi screen for cell adhesion genes

TCnumber	CGnumber	*Drosophila* name	general name	junction	phenotype of offspring after pupal injection	after adult injection
TC013706	CG1560	*myospheroid*	integrin-beta	focal	normal, 10% abnormal growth zones, 5% empty eggs	
TC013570	CG3722	*shotgun*	DE cadherin	adherens	mothers died	mothers died
TC014460	CG10624	*sinuous*	PMP-22/claudin	septate	sterile	sterile
TC014461	CG14779	*pickel*	PMP-22/claudin	septate	normal, 8% very inconsistent phenotypes	
TC014139	CG9326	*varicose*	PALS2	septate	sterile	sterile
TC014459	CG1298	*kune-kune*	PMP-22/claudin	septate	sterile	10% curved larvae
TC004424	CG6383	*crumbs*	crumbs	tight/apical	variety of strong phenotypes, strongly affected germband extension	
TC011064	CG3039	*ogre*	innexin1	gap	normal, 5% mild dorsal closure problems	
TC011417	CG4590	*kropf*	innexin2	gap	20% mild dorsal closure phenotypes, some curved larvae	
TC011709	CG1448	*inx3*	innexin3	gap	most eggs hatched, 6% strong impairment of morphogenetic movements	
TC005460	CG10125	*zero population growth*	innexin456	gap	10% mild dorsal closure phenotypes, some curved larvae	
TC011061	CG2977	*inx7*	innexin7a	gap	100% strong cellularization phenotype	
TC011062			innexin7b	gap	normal	
TC011063			innexin7c	gap	not cloned	
TC011065/6	CG34358	*shak-B*	innexin8	gap	normal	

Potential orthologs of *Drosophila* cell adhesion molecules were identified with BLAST (3) in the genome of *Tribolium castaneum (4).* A 500-600 bp fragment of these genes was cloned into pCRII-TOPO vector (Invitrogen) and sequenced for confirmation. PCR templates for dsRNA synthesis were generated with M13 primers, and dsRNA was synthesized using SP6 and T7 polymerases (Ambion). About 25 pupae were injected according to Bucher et al 2002 (5). If pupal RNAi was lethal or resulted in sterile adults, we injected adults directly according to van der zee 2006 (6), see last column. Eggs (usually around 60) were collected during a period of 3 days, fixed in a 4% formaldehyde/heptane mix and stained with DAPI. In addition to defects in cellularization, embryos were screened for general morphology and morphogenetic movements like gastrulation, germ band extension and dorsal closure. In addition, larvae or unhatched eggs were treated overnight with lactic acid and mounted for light microscopy. This screen is not exhaustive; for instance, another *myospheroid* (integrin-beta)

like gene (TC011707) is present in the *Tribolium* genome. Furthermore, actual knockdown (absence of the mRNA) was not verified, and phenotypes not visible by DAPI staining were obviously missed.

Table S3. ***Primers for inx7a RNAi fragments****. All primers are written 5'- 3'*

RNAi primer sets:		
inx7a fragment 1	CTGTCACGACTCTGGACGAA	CTCTTCGTCGCTCTCCAAAC
inx7a fragment 2	CGACGCTCCTAGTGACTTCC	ACCACCGAGACCAGGATTTA
inx7a fragment 3	CGACGCTCCTAGTGACTTCC	CTCTTCGTCGCTCTCCAAAC

Reference

1. Käll, L., A. Krogh, and E.L.L. Sonnhammer. 2005. An HMM posterior decoder for sequence feature prediction that includes homology information. Bioinformatics. 1:251-7.
2. Ostrowski, K., R. Bauer, and M. Hoch. 2008. The Drosophila Innexin7 gap junction protein is required for development of the embryonic nervous system. Cell Commun. Adhes. 15: 155–167.
3. Altschul, S.F., T.L. Madden, A.A. Schäffer, J. Zhang, Z. Zhang, W. Miller, and D.J. Lipman. 1997. Gapped BLAST and PSI-BLAST: A new generation of protein database search programs. Nucleic Acids Res. .
4. Richards, S., R. a Gibbs, G.M. Weinstock, S.J. Brown, R. Denell, R.W. Beeman, R. Gibbs, R.W. Beeman, S.J. Brown, G. Bucher, M. Friedrich, C.J.P. Grimmelikhuijzen, M. Klingler, M. Lorenzen, S. Richards, S. Roth, R. Schröder, D. Tautz, E.M. Zdobnov, D. Muzny, R. a Gibbs, G.M. Weinstock, T. Attaway, S. Bell, C.J. Buhay, M.N. Chandrabose, D. Chavez, K.P. Clerk-Blankenburg, A. Cree, M. Dao, C. Davis, J. Chacko, H. Dinh, S. Dugan-Rocha, G. Fowler, T.T. Garner, J. Garnes, A. Gnirke, A. Hawes, J. Hernandez, S. Hines, M. Holder, J. Hume, S.N. Jhangiani, V. Joshi, Z.M. Khan, L. Jackson, C. Kovar, A. Kowis, S. Lee, L.R. Lewis, J. Margolis, M. Morgan, L. V Nazareth, N. Nguyen, G. Okwuonu, D. Parker, S. Richards, S.-J. Ruiz, J. Santibanez, J. Savard,

S.E. Scherer, B. Schneider, E. Sodergren, D. Tautz, S. Vattahil, D. Villasana, C.S. White, R. Wright, Y. Park, R.W. Beeman, J. Lord, B. Oppert, M. Lorenzen, S. Brown, L. Wang, J. Savard, D. Tautz, S. Richards, G. Weinstock, R. a Gibbs, Y. Liu, K. Worley, G. Weinstock, C.G. Elsik, J.T. Reese, E. Elhaik, G. Landan, D. Graur, P. Arensburger, P. Atkinson, R.W. Beeman, J. Beidler, S.J. Brown, J.P. Demuth, D.W. Drury, Y.-Z. Du, H. Fujiwara, et al. 2008. The genome of the model beetle and pest Tribolium castaneum. Nature. 452: 949–955.

5. Bucher, G., J. Scholten, and M. Klingler. 2002. Parental RNAi in Tribolium (Coleoptera). Curr. Biol. 12: R85–R86.

6. Zee, M. v. d., O. Stockhammer, R.N. d. Fonseca, C. v. Levetzow, and S. Roth. 2006. Sog/Chordin is required for ventral-to-dorsal Dpp/BMP transport and head formation in a short germ insect. Proc. Natl. Acad. Sci. 103: 16307–16312.

CHAPTER 4

Tribolium laminin is involved in closure of the serosal window.

Tania Vazquez Faci, Niels Pijnaker and Maurijn van der Zee.

Abstract

The serosa is a crucial extraembryonic epithelium in insects that protects the egg against desiccation and pathogens. As this epithelium is absent in the highly derived main insect model *Drosophila*, knowledge on genes regulating morphogenesis of the serosa is limited. Some transcription factors such as zerknüllt and dorsocross have been identified, but no involved structural molecules are known.

To identify such structural genes, we rescreened 17 potential cell adhesion molecules from the genome-wide *Tribolium* iBeetle screen for involvement in development of the serosa. We find that *Tribolium* laminin α is involved in closure of the serosal window towards the end of gastrulation. Furthermore, we show expression of Laminin protein in the necklace cells around the serosal window during closure. Using live imaging movies, we demonstrate that simultaneous knock down of laminin β and γ results in aberrant and delayed closure of the serosal window towards the end of gastrulation.

Laminin is the first structural molecule now reported to be involved in morphogenesis of the serosa. This study suggests that a basal lamina is involved in closure of the serosal window. As the observed closure defects are similar to the phenotype reported after *dorsocross* knock-down, it is likely that laminins are a target of the Dorsocross transcription factor during serosal window closure in *Tribolium*.

Introduction

Insect eggs possess two extraembryonic epithelia: an inner amnion that covers the embryo at the ventral side, and an outer serosa that completely envelops embryo and yolk (1, 2). These epithelia are an innovation of the insects and are not present in other arthropod groups such as crustaceans or myriapods (3, 4). The serosa secretes a cuticle (5, 6) and has been suggested to play a role in desiccation resistance of the egg (7–9). Furthermore, an immune function has been proposed (10, 11). Both functions have been experimentally demonstrated using *zerknüllt* RNAi-mediated deletion of the serosa in the beetle *Tribolium castaneum* (12, 13). Serosa-less *Tribolium* eggs desiccate at low relative humidity and do not upregulate an immune response upon infection (12, 13). Thus, the extraembryonic epithelia are of crucial importance in insects.

In the main insect model *Drosophila melanogaster*, the two extraembryonic epithelia have been strongly reduced to a single small amnioserosa that covers the yolk dorsally (14). Its development has been extensively studied. The amnioserosa develops from a small rim of dorsal-most blastodermal cells that express the Hox gene *zerknüllt* (*zen*) (15–17). In *zen* null mutants, the amnioserosa is absent, and germband extension is severely compromised (18). To maintain amnioserosal cell fate, the U-shaped transcription factors are required (19). Loss of the U-shaped gene *hindsight* or all three copies of *dorsocross*, for instance, leads to failure of germ-band retraction (20, 21).Besides these transcription factors, the cell adhesion molecules Laminin and Integrin are required for germband retraction (22).

Finally, the amnioserosa is essential for dorsal closure in *Drosophila* (23). More than 140 genes have been described to be involved in this process (see Kiehart, Crawford, Aristotelous, Venakides, & Edwards, 2017). In the amnioserosa, a contractile actomyosin network (25, 26) regulated by Crumbs (27), Rho GTPases (28) and genes from the PAR complex (29) seems to be a main driving force. In addition, cell adhesion molecules such as DE-cadherin, integrins and Innexin3 have been shown to be required for dorsal closure (30–33).

Despite this massive amount of work on the amnioserosa in *Drosophila*, surprisingly little attention has been paid to the development of the serosa in other insects (2, 34). The serosa differentiates from the germ anlage at the blastoderm stage (35). In most hemimetabolous insects, the embryo then invaginates into the yolk leaving the serosa to fully cover the yolk (anatrepsis, see Panfilio, 2008 for review). During later katatrepsis, the amnion and serosa fuse, then the serosa retracts, and finally the embryo emerges from the yolk (36). Final dorsal closure follows and is mainly driven by the amnion (37). In many holometabolous insects, such as the beetle *Tribolium castaneum*, the serosa folds over the germ rudiment during gastrulation. The folds progress to form a serosal window which eventually closes, resulting in an amnion that covers the embryo ventrally and a serosa that completely covers the yolk (38). To achieve dorsal closure, the amnion and serosa attach to each other under the head and rupture. The serosa then retracts together with the amnion to the dorsal side of the egg (39).

A limited number of studies have addressed genes involved in these morphogenetic movements. Zerknüllt (zen) is known to specify serosal cell fate in the flies *Megaselia abdita* and *Episyrphus balteatus* and in the beetle *Tribolium castaneum* (40–42). Furthermore, zen is required to open the amniotic cavity for dorsal closure in *Tribolium* and in the milkweed bug *Oncopeltus fasciatus.* RNAi leads to a completely everted (inside-out) topology of the embryo (42, 43). The U-shaped genes *dorsocross* and *hindsight* are involved in closure of the serosal window in *Tribolium* (44), and depletion of *Folded gastrulation* (Fog) signaling completely blocks all morphogenetic movements (45). Besides these important signaling pathways and transcription factors, no structural molecules have been identified in gastrulation. One exception is Integrin that was recently shown to anchor the anterior-ventral of the germ anlage to the surrounding vitelline membrane to counteract the contractile forces needed for morphogenetic movement of the serosa (46).

Here, we aim to expand our knowledge on structural molecules involved in the morphogenesis of the serosa. From a genome-wide RNAi screen in *Tribolium*, we rescreened 17 genes that were reported to show wing blisters in pupae or adults upon RNAi (47, 48). Wing blisters are indicative of cell adhesion defects, and this phenotype maps to mutations in morphogenetically relevant cell adhesion molecules such as Laminin or

Integrin in *Drosophila* (49–51). We rescreened these 17 wing blister-producing dsRNAs for defects in the early morphogenesis of the amnion and serosa in *Tribolium*. We find that Laminin is involved in closure of the serosal window towards the end of gastrulation.

Laminins are key components of the extracellular matrix in the basement membrane of all animal epithelia (52, 53). They function as trimeric glycoproteins, consisting of one α, one β and one γ subunit, and form networks that connect to the membrane receptors of epithelial cells (54, 55). Although the human genome contains 5 different α, 4 different β and 3 different γ subunits, practically all invertebrates possess 4 Laminin genes: 2 distinct α subunits, called α1,2 (orthologous to human laminin α1 and α2) and α3,4 (orthologous to human α3 and α4), one β subunit, and one γ subunit (56, 57).

Mutations in *Drosophila* Laminin α1,2 (called *wing blister, wb*) cause wing blisters and defects in and defects in the dorsal vessel, trachea, muscles and rhabdomeres (50). Null mutations of *Drosophila* Laminin α3,5 (called *LamininA, LanA*) produce embryonic lethality with defects in somatic muscles, dorsal vessel and endoderm (58, 59). The α3,5 chain is also required for localization of anterio-posterior markers in the oocyte and for pathfinding of axons in the brain (60, 61). Absence of *Drosophila* laminin β (*called Laminin B1, LanB1*) prevents the normal morphogenesis of most organs and tissues, including the gut, trachea, muscles and nervous system (62). Finally, null mutants of Drosophila Laminin γ (called *Laminin B2, LanB2*) produce a phenotype with reduced midgut regions where gaps appear in the endodermal layer. Laminin γ is essential for the proper organization and arrangement of visceral tissue (63). Importantly, laminins are involved in morphogenetic cell movements, such as germ band retraction (64, 65).

In our screen, we identify *Tribolium* laminin α1,2 to be involved in proper morphogenesis of the serosa. In addition, we show presence of Laminin γ protein in the necklace cells around the serosal window. Using live imaging movies, we demonstrate that simultaneous knock down of laminin β and γ results in aberrant and delayed closure of the serosal window towards the end of gastrulation.

Materials and methods

Parental RNAi

Seventeen dsRNAs causing wing blisters (Table 1), and dsRNAs against laminin β (iB_08660) and laminin γ (iB_01705) were ordered from the company Eupheria, Germany. pRNAi in 40 female adults per gene was performed as described in M. v. d. Zee, Stockhammer, Fonseca, Levetzow, & Roth, 2006.

*Table 1**. Genes included in the parental RNAi screen**. Their TC-number, the corresponding dsRNA ordered from Eupheria (iB number), and closest* Drosophila melanogaster *ortholog identified by protein blast are given in the columns, as well as the gene name and possible function as indicated on the NCNI web site https://www.ncbi.nlm.nih.gov/gene/*

TC number	iB number	Fly ortholog	Gene Name	Protein function/prediction
TC012762	iB_02017	CG32138	formin-like protein	actin binding; Rho GTPase binding
TC012571	iB_05272	CG3403	MOB kinase activator-like 4	protein kinase binding
TC014797	iB_05697	CG11940	pico-pico (Drosophila)	protein phosphatase 1 binding
TC003474	iB_00573	CG9984	negative elongation factor D	mRNA binding
TC007565	iB_01221	CG7392	striatin-3	protein binding
TC001525	iB_00257	CG7183	protein coding gene	Unknown
TC001765	iB_00300	CG11081	plexin A	14-3-3 protein binding; GTPase activator activity; heparin binding; protein binding
TC010914	iB_01762	CG10295	serine/threonine-protein kinase PAK 3	protein serine/threonine kinase activity; Rac GTPase binding; Rho GTPase binding; SH3 domain binding
TC016062	iB_02548	CG5734	uncharacterized LOC103314950	phosphatidylinositol binding
TC013912	iB_05522	CG8787	polycomb protein Asx	chromatin binding; deubiquitinase activator activity
TC014773	iB_05688	CG42677	laminin subunit alpha-1	EGF-like domain; Laminin G domain; Laminin EGF domain;
TC000185	iB_00037	CG17838	heterogeneous nuclear ribonucleoprotein Q	mRNA binding; nucleotide binding
TC003007	iB_00499	CG8174	SRSF protein kinase 1	ATP binding; protein kinase activity; protein serine/threonine kinase activity, positive regulation of cell cycle
TC003342	iB_00557	CG10443	Lar Leukocyte antigen related like (Drosophila)	protein tyrosine phosphatase activity; SAM domain binding, regulation of cell projection organization
TC004140	iB_00666	CG4931	cytoplasmic FMR1-interacting protein	Rho GTPase binding
TC005546	iB_00881	CG5092	serine/threonine-protein kinase mTOR	macromolecular complex binding; protein kinase activity; protein serine/threonine kinase activity
TC013882	iB_02218	CG7266	LIM domain-containing protein jub	peptide methionine sulphoxide reductase MsrA; Peptide methionine sulfoxide reductase

Egg fixation

Eggs were dechorionized in undiluted commercial bleach (4% NaClO) for 4 minutes, and fixed for 20 minutes in 5 ml heptane, 4 ml PBS and 1ml 36% formaldehyde. Eggs were devitellinized using a methanol shock, and stored at -20 °C.

Immunohistochemistry and DAPI staining

The standard buffer used in all steps was PBS with 1% Triton, supplemented with 0.05% acetylated BSA. Blocking was done with BSA and NGS. The primary anti-Laminin γ1(Abcam, ab47651) antibody was incubated overnight at 4 °C in a dilution of 1:500. The secondary antibody was goat anti-rabbit 488nm Alexa from Boehringer, Mannheim in a dilution of 1:100. DAPI was added 1:1000 to one of the last washes in PBST. DAPI stained embryos of the RNAi screen were imaged using an upright microscope equipped with epifluorescence (Zeiss Axioplan 2 imaging) with a 20X objective. Immunohistochemically stained embryos were imaged on an inverted Zeiss confocal (Zeiss 710). We took 85-200 focal planes with a 40X or 20X objective, and all the focal planes were summed to make one picture.

Western blot

From eight to fifty six hours old eggs that were laid in a period 3-7 days after dsRNA injection into the adults, and 8-72 h old eggs that were laid in a period 7-10 days after injection were homogenized in five times the egg volume of Laemmli buffer (ChemCruz), and were stored at -20 °C. 30 µl of these samples was loaded on a 30% SDS-PAGE gel for western blotting next to comparable samples of wild type eggs, and 30 µl of a 1 mg/ml alpha-tubulin solution as control. Primary antibodies used are anti-Laminin γ1(Abcam, ab47651) in a concentration of 1:500 and anti-α-tubulin (Sigma, T5168) in a concentration of 1:5000. Secondary antibodies were anti-rabbit IgG (Boehringer Mannheim) in a dilution of 1:1000 and anti-mouse (NA931, GE Healthcare) in a concentration of 1:2000. Visualization was done with ECL Western blotting detection reagents (Clarity Western, Biorad).

Live imaging movies

From zero to two hours old eggs from the LAN-GFP transgenic line (chapter 2) were incubated for 6h at 30 °C. A 40 second incubation in bleach(4% NaClO) followed by a 1 minute wash in water was repeated twice to dechorionated the eggs. Eggs were then aligned on a microscope cover slip and covered with Voltalef 10S Halocarbon oil to avoid desiccation. The embryos were imaged on an inverted Zeiss confocal microscope (Zeiss 710) at 30^{o} C. We took eleven focal planes with a 20X or 40X objective in a time interval of 3 minutes. We summed all the focal planes. The total observation time was 14 hours.

Statistical analysis of time for serosal window closure

We measured the time between the frame just before the onset of the differentiated blastoderm stage (i.e. after completion of cellularization) and the completion of serosal window closure in 7 wildtype embryos and in 16 embryos in which laminin β and γ were simultaneously silenced. The results of the two groups of embryos were compared applying a 1-tailed ANOVA.

Results

RNAi against TC014773 disturbs closure of the serosal window

To identify structural genes involved in the morphogenesis, we performed a small-scale parental RNAi screen against 17 genes that showed wing blisters in pupae or adults upon knockdown in the iBeetle screen (47, 48), Table 1. In several cases, RNAi caused a severe reduction in fecundity (<1.0 egg per female per day), indicated with red squares in Figure 1. Analysis of phenotypes in DAPI stained embryos revealed 15 categories of developmental defects, ranging from the undifferentiated blastoderm stage, to dorsal closure (see legend of Figure 1, and illustrated in supplementary Figures 1 – 14). Knockdown of TC007565, TC010914 and TC012571 caused a high percentage of embryos with irregularly spaced nuclei in the syncytial blastoderm (see supplementary Figure 1), possibly indicative of cellularization defects (chapter 3). Notably, knockdown of TC014773 disturbed closure of the serosal window in a considerable

percentage of eggs (Figure 2). Although the beginning of morphogenetic movements seems relatively normal (Figure 2 A, F), the serosal window seems larger during further development (Figure 2 B, G), and sometimes has irregular borders (Fig. 2 C, H). Importantly, closure of the serosal window seems delayed (Figure 2 C, H). Although the serosal window does finally proceed in most eggs (Figure 2 D, I, E, J), the germband is incorrectly positioned (more towards posterior), similar to what has been reported for affected serosal window closure in *dorsocross* RNAi (44). In conclusion, TC014773 RNAi disturbs serosal window closure.

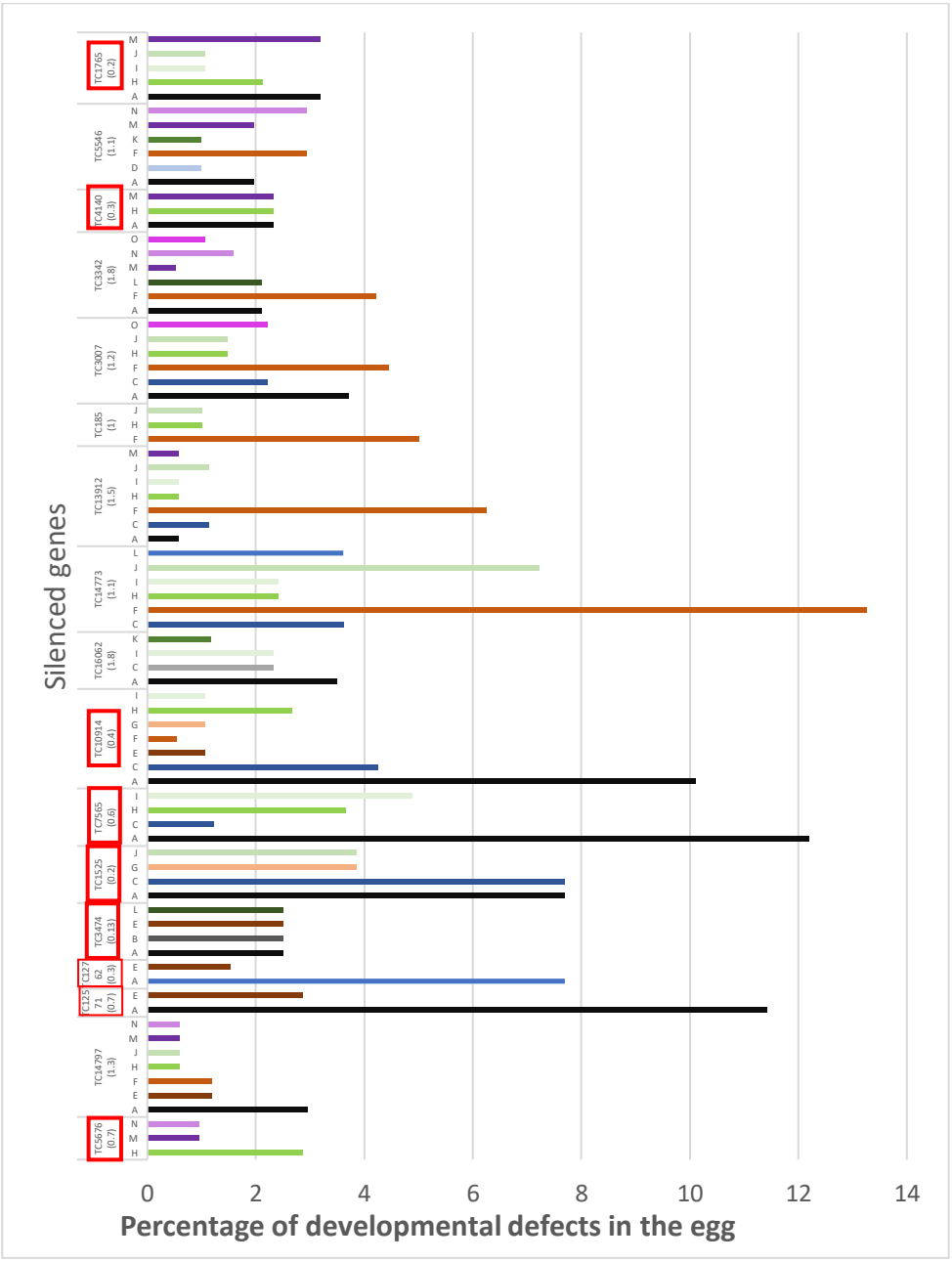

Figure 1. Results of the RNAi screen. *TC numbers of the genes against which RNAi was performed are indicated below the bars. Each bar represents the percentage of eggs showing the phenotype of a certain category indicated by the capital letter, see legend on next page. Under every TC-number, the fecundity is indicated as eggs per female per day. The red squares are around TC numbers whose knockdown lead to a fecundity below 1.0 eggs per female per day.*

Undifferentiated blastoderm:	
-nuclei irregularly spaced	A
-holes in the blastoderm	B
Differentiated blastoderm:	
-condensation of the germ rudiment disturbed	C
-irregularly positioned germ rudiment	D
Gastrulation:	
-gastrulation disturbed	E
-delayed serosal window formation	F
-irregularly positioned germ rudiment	G
Germ band stage	
-(irregularly) curved germband	H
-irregularly positioned germ band	I
-head lobe defects	J
-border of the embryo irregular	K
-flat/broad germ band	L
Late	
-germ band retraction defects	M
-dorsal closure defects	N
-Serosa nuclei irregular spaced	O

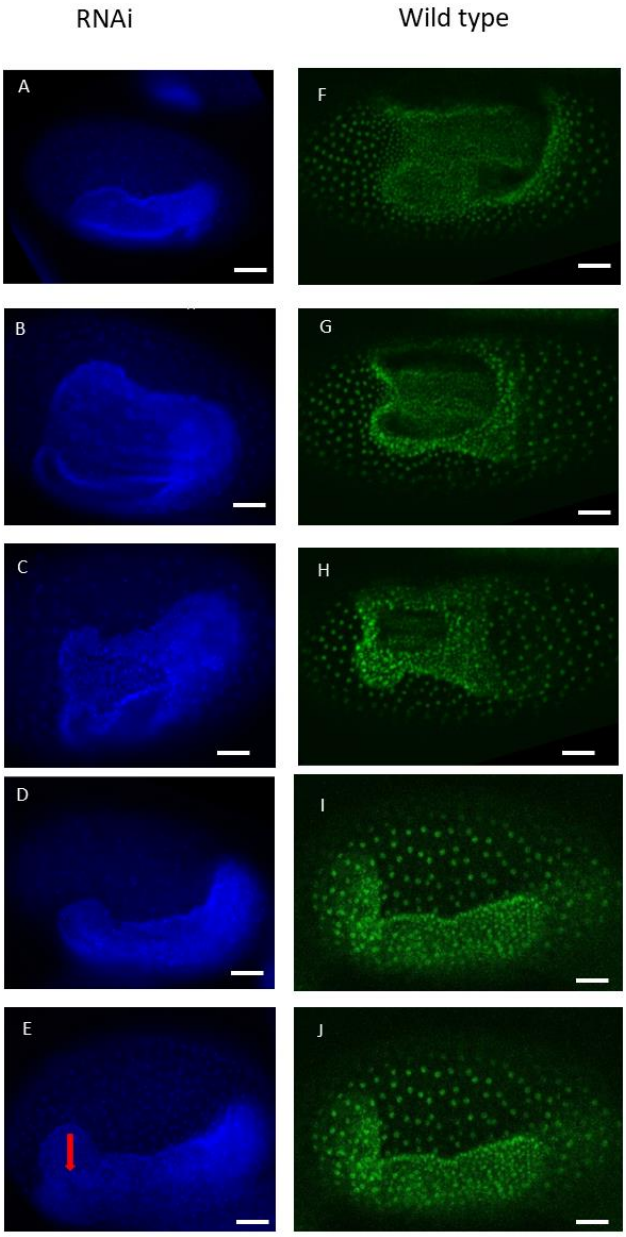

Figure 2. RNAi against TC014773 disturbs closure of the serosal window*. (A-E) DAPI stainings after RNAi against TC014773. (F-J) Stills from a live imaging movie using LAN-GFP (chapter 2) showing the comparable wild type. (B) The serosal window seems larger than in wildtype. (C) Serosal window closure seems delayed, and the borders of the window are irregular. (D, E) Serosal window closure proceeds, but the position of the germ band is more toward posterior than in the wild type.*

TC014773 is the laminin α1,2 subunit

In NCBI and iBeetle databases, TC014773 is annotated as *laminin subunit α1,2*. Analysis of the protein domains using Prosite (67, 68) confirmed this annotation and unambiguously identified TC014773 as the *Tribolium* Laminin α1,2 ortholog (Figure 3). Like in practically all invertebrates (57), we identified three other Laminin subunits in the *Tribolium* genome. All of them showed the highly conserved protein domains typical of the respective subunits. LOC661583, a fusion of the former gene models TC003460 and TC032383, is Laminin α3,5; TC005184 is Laminin β, and TC010540 is Laminin γ (Figure 3).

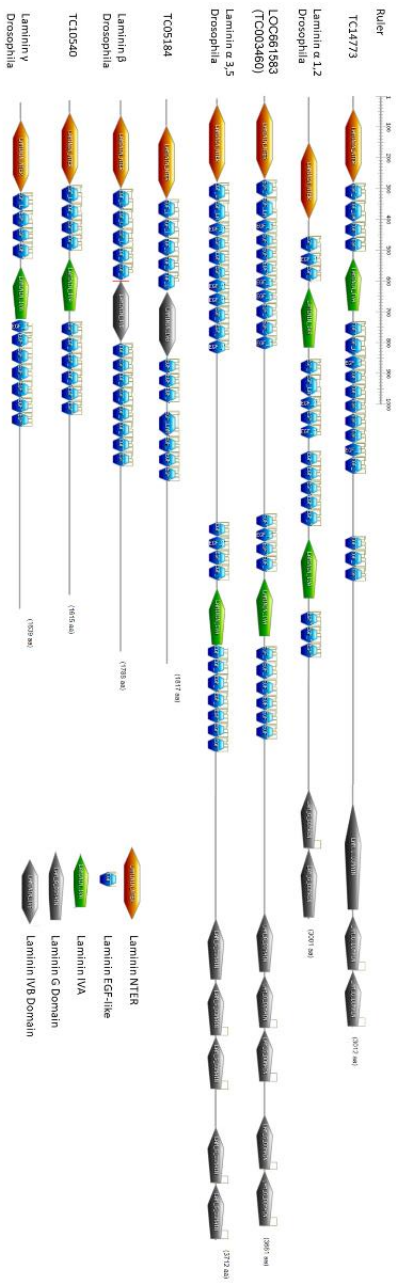

Figure 7. Comparison of domains in Laminin subunits of* Tribolium *and* Drosophila. Domains were identified using Prosite (67, 68). High conservation in protein architecture shows that TC014773 is Laminin α1,2; LOC661583, a fusion of the former gene models TC003460 and TC032383, is Laminin α3,5; TC005184 is Laminin β, and TC010540 is Laminin γ.*

As laminin α1,2 is a subunit of the Laminin trimer, we wondered if knockdowns the other members of the trimer give the same phenotype. We therefore performed RNAi against laminin β, laminin γ, and a combination of the two, and analyzed the phenotypic effect during closure of the serosal window. Similar to laminin α1,2 RNAi, these knockdowns all generated high percentages of defects in closure of the serosal window (Table 2). This suggests that the phenotype we observe is indeed caused by the absence of functional Laminin trimers. Simultaneous RNAi against the β and γ subunits gives the highest percentage of defects in serosal window closure (Table 2).

Table 2. percentage of embryos showing defects in serosal window closure upon RNAi against Laminin subunits

TC NUMBER	**Laminin subunit**	**% Serosal window closure defect**
TC14773	Laminin α 1,2	58%
TC05184	Laminin β	44%
TC10540	Laminin γ	30%
TC05184, TC10540	Laminin β and γ	60%

Laminin γ is enriched around necklace cells during closure of the serosal window

Although several antibodies are present against vertebrate Laminins, the only currently available antibody recognizing a *Drosophila* Laminin subunit is anti-Laminin γ1 (Abcam, ab47651). To obtain an indication whether this antibody also recognizes the very similar *Tribolium* Laminin γ, we performed a Western blot (Figure 4). In wildtype samples, we observe a band around 180 kDa, the expected size of Laminin γ (Figure 4, 3rd and 6th lane). Importantly, this band was not present after laminin γ RNAi (4th and 5th lane). These data indicate that ab7651 recognizes *Tribolium* laminin γ, silencing the protein.

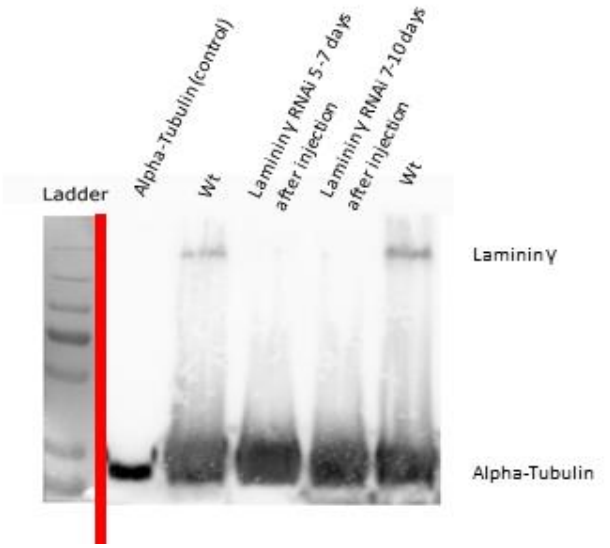

Figure 4. The ab7651 Drosophila laminin γ antibody recognizes Tribolium Laminin γ*. The first lane shows a 10-180 kDa ladder; the second lane a blotting control of alpha-Tubulin. In the wildtype lanes (lane 3 and 6), a 180 kDa band is visible, whereas this band is absent after the RNAi samples in lane 4 and 5. Alpha tubulin was used as loading control.*

We used this antibody to investigate expression pattern of laminin γ during closure of the serosal window. In wildtype embryos, we observe an enrichment of Laminin γ in the so-called "necklace cells", the cells at the border of the amnion and the serosa (69). A possibly extracellular enrichment of the protein is visible at the inner rim of the serosal window (Figure 5 A, arrowhead). This suggests that a basal lamina is present during closure of the serosal window. This expression pattern is absent after laminin γ knockdown (Figure 5 B), confirming that RNAi against laminin γ effectively prevents expression of the protein.

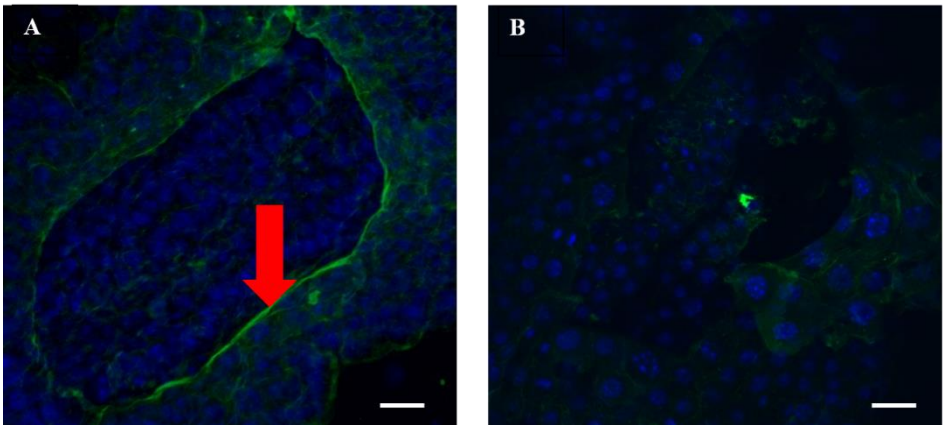

Figure 5. Laminin γ is enriched in necklace cells around the serosal window. *Embryos of around 10 hours after cellularization at 30oC. In green is Laminin stained with 488nm of Alexa and blue are the nuclei stained with DAPI. A) Wild type embryo; Laminin is expressed mainly at the edge of the serosal window (arrowhead) B) Laminin γ knock down embryo; Laminin is only detected at low levels all over the egg. Scale bar 50 µm.*

Absence of Laminin delays closure of the serosal window

To investigate the laminin knockdown phenotype in more detail, we analyzed development in live imaging movies of the LAN-GFP transgenic *Tribolium* line (chapter 2). We applied double RNAi against laminin β and γ, as this simultaneous knockdown generated the highest percentage of defects in closure of the serosal window (Table). Strikingly, these movies reveal an irregularly formed serosal window, with some necklace cells staying behind (red arrows in Figure 6 A, B and C), instead of a regularly formed serosal window. Importantly, serosal closure is delayed (Figure 6 C, D), and the germband irregularly curved and positioned more towards the posterior (Figure 6 D), as reported for dorsocross knockdown (44).

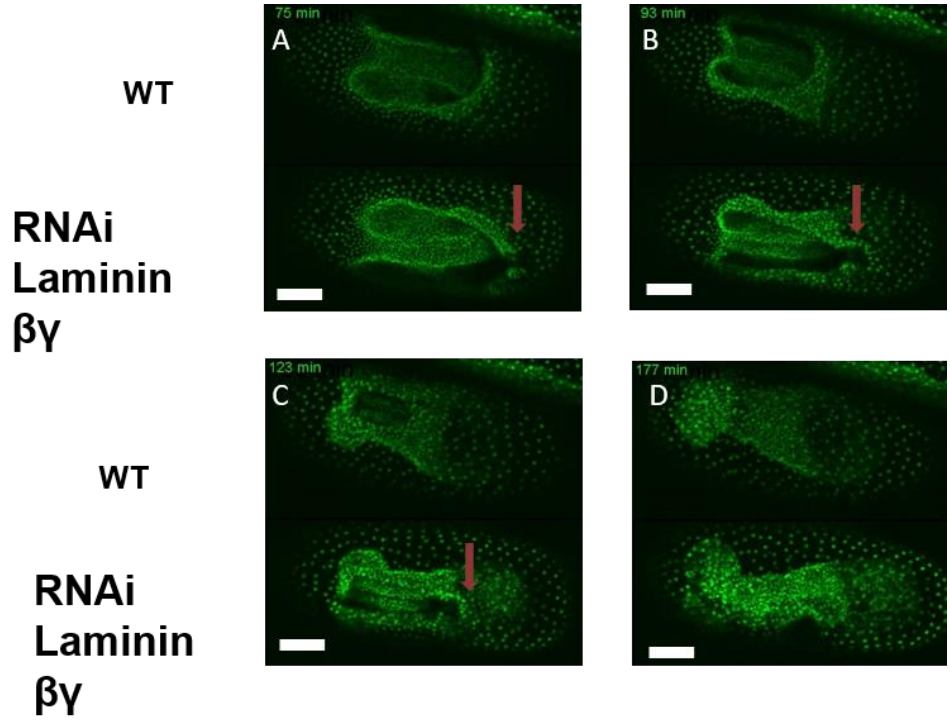

Figure 6. Serosal window closure is delayed in laminin β and γ double knock down embryos. *Stills of temporary aligned time lapse movies of a wild type embryo (Top) and an embryo with Laminin beta-gamma silenced (Bottom) of the LAN-GFP transgenic Tribolium line. Red arrows indicate necklace cells that stay behind at the irregular borders of the serosal window. Serosal window closure is delayed (C, D), and the germband is folded and positioned more towards posterior after RNAi (D). Scale bar 100 µm.*

To quantify the delay in closure of the serosal window upon simultaneous laminin β and γ RNAi, we measured the time between the onset of the differentiated blastoderm stage (i.e. the end of cellularization) and the completion of the serosal window closure in 16 knockdown embryos and 7 wildtype embryos. This revealed a conspicuous difference in closing time of the serosal window between wild type embryos (3.67 hours) and Laminin β and γ knock down embryos (3.92 hours) (Figure 7). Given the small number of movies in which this time could be measured, the p-value of this difference (0.07 in an ANOVA) might well drop when a higher number of embryos will be analyzed.

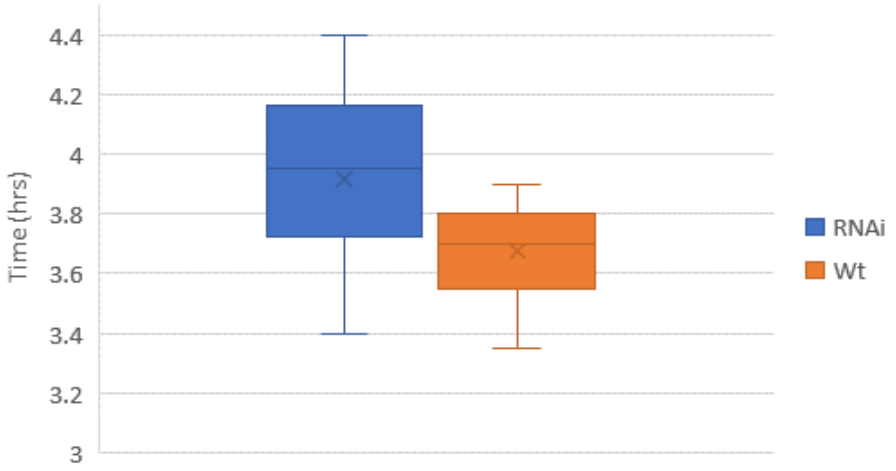

Figure 7. Comparison of the average of the time of serosal window closure between wild type and Laminin β and γ silenced. Using a t-test, we found that the difference of the serosal window closure time is different with a p-value of 0.07.

Taken together, we have identified laminin α 1,2 to be involved in closure of the serosal window in *Tribolium.* We have shown enrichment of Laminin γ in necklace cells of the serosa, and reveal that serosal window closure is delayed in laminin β and γ knockdown embryos. This demonstrates that the Laminin trimer is a key structural molecule for proper closure of the serosal window.

Discussion

We identify Laminin as key structural molecule involved in closure of the serosal window in Tribolium. Furthermore, we show the enrichment and potentially extracellular localization of Laminin γ protein around the necklace cells of the serosal window. As laminin is a component of the basal lamina in all animals (52, 53), it is likely that a basal lamina is present around the serosal window, and required for proper closure. It would be interesting to investigate this hypothesis by electron microscopy. In addition, disturbance of the basement membrane upon laminin RNAi could

be studied using antibody stainings for other components of the basal lamina, such as Collagen IV or Perlecan (62).

We have identified four laminin subunits in the *Tribolium* genome, like in all invertebrates. These subunits all show high conservation in protein domains with their respective orthologs. However, in a frequency below 10%, we observed a splice variant of laminin γ that lacks the N-terminal domain. Interestingly, one of te three human laminin γ genes (laminin γ2) also lacks the N-terminal domain, suggesting that this *Tribolium* splice variant might well have a biological function (70). Knock down of subunit α1,2, subunit β or subunit γ all give the same phenotype in serosal window closure. This strongly suggests that it is the laminin trimer composed of these three subunits that is required for proper closure of the window.

Finally, we show that closure of the serosal window is delayed in laminin deficient embryos. As the duration of serosal window closure can only be measured in particularly oriented embryos, and only during this particular period in development, we could only analyze 16 movies of the RNAi treatment. In addition, RNAi effects vary in strength per embryo. It is therefore not surprising that the p-value we found for the difference in serosal window closure time between wildtypes and knockdowns is slightly higher than 0.05 ($p=0.07$). Considering same striking movies like the one in Figure 6, and conspicuous pictures of fixed material, we feel confident that analysis of a larger number of eggs will decrease this p-value.

The phenotype we observe after laminin RNAi is comparable to the one reported for dorsocross RNAi (44). Not only the delay of closure of the serosal window is similar, but also the curved germ band that is positioned more towards the posterior (44). In absence of proper separation of the amnion and the serosa, the amnion connects the germ band to the serosa which is anchored to the outer vitelline membrane, preventing anterior movement of the germ band (44, 46). This probably happens I both *dorsocross* and laminin RNAi. In addition, the expression pattern of laminin γ resembles the reported expression pattern of *dorsocross* (44). This makes it highly likely that laminins are important target genes of the Dorsocross transcription factor during closure of the serosal window in *Tribolium*.

In conclusion, we have shown that Laminin is required for closure of the serosal window, a crucial step in the development of the serosa. As more genetic tools such as RNAi and CRISPR-Cas are now available for non-

model organisms, more genes will probably soon be described to be involved in morphogenesis of this crucial extraembryonic epithelium in insects.

Acknowledgments

We thank Rianne Grond from the group of Catherine Rabouille at the Hubrecht Institute for help with the Western blot.

References

1. Panfilio, K.A. 2008. Extraembryonic development in insects and the acrobatics of blastokinesis. Dev. Biol. .
2. Schmidt-Ott, U., and C.W. Kwan. 2016. Morphogenetic functions of extraembryonic membranes in insects. Curr. Opin. Insect Sci. 13: 86–92.
3. Jacobs, C.G.C., and M. Van Der Zee. 2013. Immune competence in insect eggs depends on the extraembryonic serosa. Dev. Comp. Immunol. .
4. Zeh, D.W., J.A. Zeh, and R.L. Smith. 1989. Ovipositors, amnions and eggshell architecture in the diversification of terrestrial arthropods. Q. Rev. Biol. .
5. Hinton, H.E. 2013. Biology of Insect Eggs. .
6. Lamer, A., and A. Dorn. 2001. The serosa of Manduca sexta (insecta, lepidoptera): Ontogeny, secretory activity, structural changes, and functional considerations. Tissue Cell. .
7. Goltsev, Y., G.L. Rezende, K. Vranizan, G. Lanzaro, D. Valle, and M. Levine. 2009. Developmental and evolutionary basis for drought tolerance of the Anopheles gambiae embryo. Dev. Biol. .
8. Rezende, G.L., A.J. Martins, C. Gentile, L.C. Farnesi, M. Pelajo-Machado, A.A. Peixoto, and D. Valle. 2008. Embryonic desiccation resistance in Aedes aegypti: Presumptive role of the chitinized Serosal Cuticle. BMC Dev. Biol. .
9. Vargas, H.C.M., L.C. Farnesi, A.J. Martins, D. Valle, and G.L. Rezende. 2014. Serosal cuticle formation and distinct degrees of desiccation resistance in embryos of the mosquito vectors Aedes aegypti, Anopheles aquasalis and Culex quinquefasciatus. J. Insect Physiol. .
10. Chen, G., K. Handel, and S. Roth. 2000. The maternal NF-κB/Dorsal gradient of Tribolium castaneum: Dynamics of early dorsoventral patterning in a short-germ beetle. Development. .
11. Gorman, M.J., P. Kankanala, and M.R. Kanost. 2004. Bacterial challenge stimulates innate immune responses in extra-embryonic tissues of tobacco hornworm eggs. Insect Mol. Biol. .
12. Jacobs, C.G.C., G.L. Rezende, G.E.M. Lamers, and M. van der Zee. 2013. The extraembryonic serosa protects the insect egg against desiccation. Proc. R. Soc. B Biol. Sci. 280.

13. Jacobs, C.G.C., H.P. Spaink, and M. van der Zee. 2014. The extraembryonic serosa is a frontier epithelium providing the insect egg with a full-range innate immune response. Elife. 3: 1–21.
14. Schmidt-Ott, U. 2000. The amnioserosa is an apomorphic character of cyclorrhaphan flies. Dev. Genes Evol. .
15. Doyle, H.J., K. Harding, T. Hoey, and M. Levine. 1986. Transcripts encoded by a homoeo box gene are restricted to dorsal tissues of Drosophila embryos. Nature. .
16. Rushlow, C., H. Doyle, T. Hoey, and M. Levine. 1987. Molecular characterization of the zerknüllt region of the Antennapedia gene complex in Drosophila. Genes Dev. .
17. Rushlow, C., and M. Levine. 1990. Role Of The zerknüllt Gene In Dorsal-Ventral Pattern Formation In Drosophila. Adv. Genet. .
18. Wakimoto, B.T., F.R. Turner, and T.C. Kaufman. 1984. Defects in embryogenesis in mutants associated with the antennapedia gene complex of Drosophila melanogaster. Dev. Biol. .
19. Frank, L.H., and C. Rushlow. 1996. A group of genes required for maintenance of the amnioserosa tissue in Drosophila. Development. 122: 1343–52.
20. Reim, I., H.H. Lee, and M. Frasch. 2003. The T-box-encoding Dorsocross genes function in amnioserosa development and the patterning of the dorsolateral germ band downstream of Dpp. Development. .
21. Yip, M.L., M.L. Lamka, and H.D. Lipshitz. 1997. Control of germ-band retraction in Drosophila by the zinc-finger protein HINDSIGHT. Development. 124: 2129–2141.
22. Schöck, F., and N. Perrimon. 2003. Retraction of the Drosophila germ band requires cell-matrix interaction. Genes Dev. 17: 597–602.
23. Scuderi, A., and A. Letsou. 2005. Amnioserosa is required for dorsal closure in Drosophila. Dev. Dyn. 232: 791–800.
24. Kiehart, D.P., J.M. Crawford, A. Aristotelous, S. Venakides, and G.S. Edwards. 2017. Cell sheet morphogenesis: Dorsal closure in drosophila melanogaster as a model system. Annu. Rev. Cell Dev. Biol. .
25. Pasakarnis, L., E. Frei, E. Caussinus, M. Affolter, and D. Brunner. 2016. Amnioserosa cell constriction but not epidermal actin cable tension autonomously drives dorsal closure. Nat. Cell Biol. .

26. Young, P.E., A.M. Richman, A.S. Ketchum, and D.P. Kiehart. 1993. Morphogenesis in Drosophila requires nonmuscle myosin heavy chain function. Genes Dev. .
27. Flores-Benitez, D., and E. Knust. 2015. Crumbs is an essential regulator of cytoskeletal dynamics and cell-cell adhesion during dorsal closure in Drosophila. Elife. .
28. Harden, N., M. Ricos, Y.M. Ong, W. Chia, and L. Lim. 1999. Participation of small GTPases in dorsal closure of the Drosophila embryo: Distinct roles for Rho subfamily proteins in epithelial morphogenesis. J. Cell Sci. .
29. David, D.J.V., A. Tishkina, and T.J.C. Harris. 2010. The PAR complex regulates pulsed actomyosin contractions during amnioserosa apical constriction in Drosophila. Development. .
30. Brown, N.H. 1994. Null mutations in the α(PS2) and β(PS) integrin subunit genes have distinct phenotypes. Development. .
31. Giuliani, F., G. Giuliani, R. Bauer, and C. Rabouille. 2013. Innexin 3, a New Gene Required for Dorsal Closure in Drosophila Embryo. PLoS One. 8: 1–16.
32. Tepass, U., E. Gruszynski-DeFeo, T.A. Haag, L. Omatyar, T. Török, and V. Hartenstein. 1996. shotgun encodes Drosophila E-cadherin and is preferentially required during cell rearrangement in the neurectoderm and other morphogenetically active epithelia. Genes Dev. .
33. Uemura, T., H. Oda, R. Kraut, S. Hayashi, Y. Kataoka, and M. Takeichi. 1996. Zygotic Drosophilia E-cadherin expression is required for processes of dynamic epithelial cell rearrangement in the Drosophila embryo. Genes Dev. .
34. Horn, T., M. Hilbrant, and K.A. Panfilio. 2015. Evolution of epithelial morphogenesis: Phenotypic integration across multiple levels of biological organization. Front. Genet. 6: 1–7.
35. Roth, S. 2004. Gastrulation in other insects. In: Gastrulations: from cells to embryo. .
36. Panfilio, K.A. 2009. Late extraembryonic morphogenesis and its zenRNAi-induced failure in the milkweed bug Oncopeltus fasciatus. Dev. Biol. .
37. Panfilio, K.A., and S. Roth. 2010. Epithelial reorganization events during late extraembryonic development in a hemimetabolous

insect. Dev. Biol. .
38. Handel, K., C.G. Grünfelder, S. Roth, and K. Sander. 2000. Tribolium embryogenesis: a SEM study of cell shapes and movements from blastoderm to serosal closure. Dev. Genes Evol. 210: 167–179.
39. Hilbrant, M., T. Horn, S. Koelzer, and K.A. Panfilio. 2016. The beetle amnion and serosa functionally interact as apposed epithelia. Elife. 5: 1–17.
40. Rafiqi, A.M., S. Lemke, S. Ferguson, M. Stauber, and U. Schmidt-Ott. 2008. Evolutionary origin of the amnioserosa in cyclorrhaphan flies correlates with spatial and temporal expression changes of zen. Proc. Natl. Acad. Sci. U. S. A. .
41. Schmidt-Ott, U., Rafiqi, A. M. and Lemke, S. 2010. Hox3/zen and the Evolution of Extraembryonic Epithelia in Insects. In Hox Genes: Studies from the 20th to the 21st Century. J. S. Deut. New York, NY: Springer New York.
42. Van Der Zee, M., N. Berns, and S. Roth. 2005. Distinct functions of the Tribolium zerkn??llt genes in serosa specification and dorsal closure. Curr. Biol. 15: 624–636.
43. Panfilio, K.A., P.Z. Liu, M. Akam, and T.C. Kaufman. 2006. Oncopeltus fasciatus zen is essential for serosal tissue function in katatrepsis. Dev. Biol. .
44. Horn, T., and K.A. Panfilio. 2016. Novel functions for Dorsocross in epithelial morphogenesis in the beetle Tribolium castaneum. Dev. .
45. Benton, M.A., N. Frey, R.N. da Fonseca, C. von Levetzow, D. Stappert, M.S. Hakeemi, K.H. Conrads, M. Pechmann, K.A. Panfilio, J.A. Lynch, and S. Roth. 2019. Fog signaling has diverse roles in epithelial morphogenesis in insects. Elife. .
46. Münster, S., A. Jain, A. Mietke, A. Pavlopoulos, S.W. Grill, and P. Tomancak. 2019. Attachment of the blastoderm to the vitelline envelope affects gastrulation of insects. Nature. .
47. Dönitz, J., C. Schmitt-Engel, D. Grossmann, L. Gerischer, M. Tech, M. Schoppmeier, M. Klingler, and G. Bucher. 2015. iBeetle-Base: A database for RNAi phenotypes in the red flour beetle Tribolium castaneum. Nucleic Acids Res. .
48. Schmitt-Engel, C., D. Schultheis, J. Schwirz, N. Ströhlein, N. Troelenberg, U. Majumdar, V.A. Dao, D. Grossmann, T. Richter, M. Tech, J. Dönitz, L. Gerischer, M. Theis, I. Schild, J. Trauner, N.D.B.

Koniszewski, E. Küster, S. Kittelmann, Y. Hu, S. Lehmann, J. Siemanowski, J. Ulrich, K.A. Panfilio, R. Schröder, B. Morgenstern, M. Stanke, F. Buchhholz, M. Frasch, S. Roth, E.A. Wimmer, M. Schoppmeier, M. Klingler, and G. Bucher. 2015. The iBeetle large-scale RNAi screen reveals gene functions for insect development and physiology. Nat. Commun. 6.

49. Brower, D.L., and S.M. Jaffe. 1989. Requirement for integrins during Drosophila wing development. Nature. .
50. Martin, D., S. Zusman, X. Li, E.L. Williams, N. Khare, S. DaRocha, R. Chiquet-Ehrismann, and S. Baumgartner. 1999. wing blister, A new Drosophila laminin chain required for cell adhesion and migration during embryonic and imaginal development. J. Cell Biol. 145: 191–201.
51. Wilcox, M., A. DiAntonio, and M. Leptin. 1989. The function of PS integrins in Drosophila wing morphogenesis. Development. .
52. Hohenester, E., and P.D. Yurchenco. 2013. Laminins in basement membrane assembly. Cell Adhes. Migr. .
53. Pozzi, A., P.D. Yurchenco, and R. V. Iozzo. 2017. The nature and biology of basement membranes. Matrix Biol. .
54. Aumailley, M. 2013. The laminin family. Cell Adhes. Migr. .
55. Hohenester, E. 2019. Structural biology of laminins. Essays Biochem. .
56. Aumailley, M., L. Bruckner-Tuderman, W.G. Carter, R. Deutzmann, D. Edgar, P. Ekblom, J. Engel, E. Engvall, E. Hohenester, J.C.R. Jones, H.K. Kleinman, M.P. Marinkovich, G.R. Martin, U. Mayer, G. Meneguzzi, J.H. Miner, K. Miyazaki, M. Patarroyo, M. Paulsson, V. Quaranta, J.R. Sanes, T. Sasaki, K. Sekiguchi, L.M. Sorokin, J.F. Talts, K. Tryggvason, J. Uitto, I. Virtanen, K. Von Der Mark, U.M. Wewer, Y. Yamada, and P.D. Yurchenco. 2005. A simplified laminin nomenclature. Matrix Biol. 24: 326–332.
57. Fahey, B., and B.M. Degnan. 2012. Origin and evolution of laminin gene family diversity. Mol. Biol. Evol. 29: 1823–1836.
58. Henchcliffe, C., L. Garcia-Alonso, J. Tang, and C.S. Goodman. 1993. Genetic analysis of laminin A reveals diverse functions during morphogenesis in Drosophila. Development. .
59. Yarnitzky, T., and T. Volk. 1995. Laminin is required for heart, somatic muscles, and gut development in the Drosophila embryo. Dev. Biol.

.
60. Deng, W.M., and H. Ruohola-Baker. 2000. Laminin A is required for follicle cell-oocyte signaling that leads to establishment of the anterior-posterior axis in Drosophila. Curr. Biol. .
61. García-Alonso, L., R.D. Fetter, and C.S. Goodman. 1996. Genetic analysis of Laminin A in Drosophila: Extracellular matrix containing laminin A is required for ocellar axon pathfinding. Development. .
62. Urbano, J.M., C.N. Torgler, C. Molnar, U. Tepass, A. López-Varea, N.H. Brown, J.F. de Celis, and M.D. Martín-Bermudo. 2009. Drosophila laminins act as key regulators of basement membrane assembly and morphogenesis. Development. .
63. Wolfstetter, G., and A. Holz. 2012. The role of LamininB2 (LanB2) during mesoderm differentiation in Drosophila. 2: 267–282.
64. Schöck, F., and N. Perrimon. 2003. Retraction of the Drosophila germ band requires cell-matrix interaction. Genes Dev. 17: 597–602.
65. Urbano, J.M., P. Domínguez-Giménez, B. Estrada, and M.D. Martín-Bermudo. 2011. PS integrins and laminins: Key regulators of cell migration during drosophila embryogenesis. PLoS One. .
66. Zee, M. v. d., O. Stockhammer, R.N. d. Fonseca, C. v. Levetzow, and S. Roth. 2006. Sog/Chordin is required for ventral-to-dorsal Dpp/BMP transport and head formation in a short germ insect. Proc. Natl. Acad. Sci. 103: 16307–16312.
67. Sigrist, C.J.A., L. Cerutti, N. Hulo, A. Gattiker, L. Falquet, M. Pagni, A. Bairoch, and P. Bucher. 2002. PROSITE: a documented database using patterns and profiles as motif descriptors. Brief. Bioinform. .
68. Sigrist, C.J.A., E. De Castro, L. Cerutti, B.A. Cuche, N. Hulo, A. Bridge, L. Bougueleret, and I. Xenarios. 2013. New and continuing developments at PROSITE. Nucleic Acids Res. .
69. Dearden, P., M. Grbic, F. Falciani, and M. Akam. 2000. Maternal expression and early zygotic regulation of the Hox3/zen gene in the grasshopper Schistocerca gregaria. Evol. Dev. 2: 261–270.
70. Tzu, J., and M.P. Marinkovich. 2008. Bridging structure with function: Structural, regulatory, and developmental role of laminins. Int. J. Biochem. Cell Biol. 40: 199–214.

Supplementary

Examples of the defects found in the embryos

All the embryos are stained with DAPI as mentioned in the method.

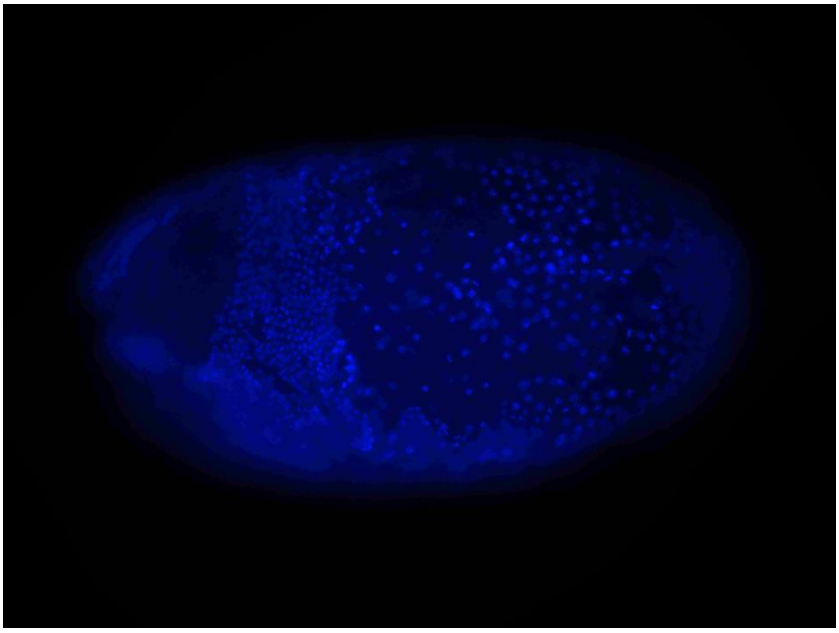

Figure 1. Embryo during the nuclei division with TC10914 gene silenced showing nuclei irregular spaced.

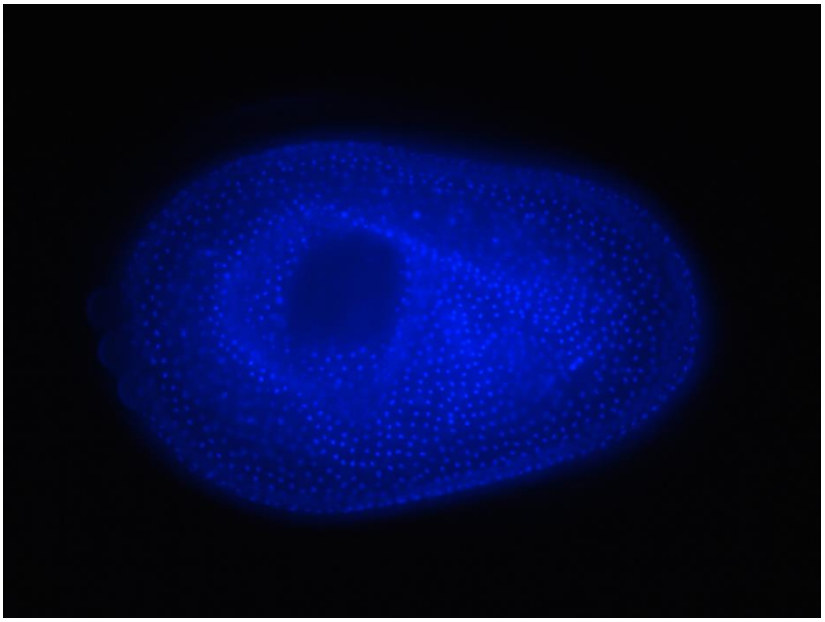

Figure 2. Embryo during the nuclei division with TC3474 gene silenced showing a hole in the blastoderm.

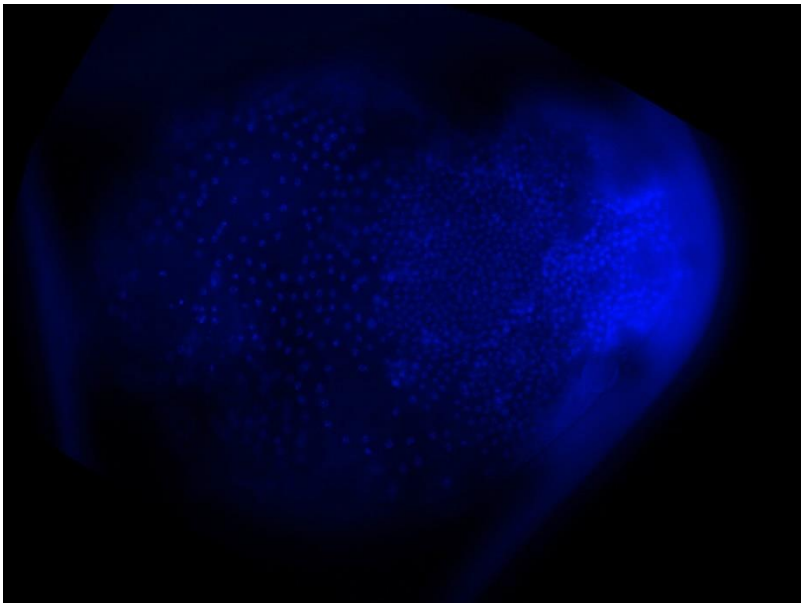

Figure 3. Embryo after cellularization with TC7565 gene silenced showing a wrong condensation of the germ rudiment.

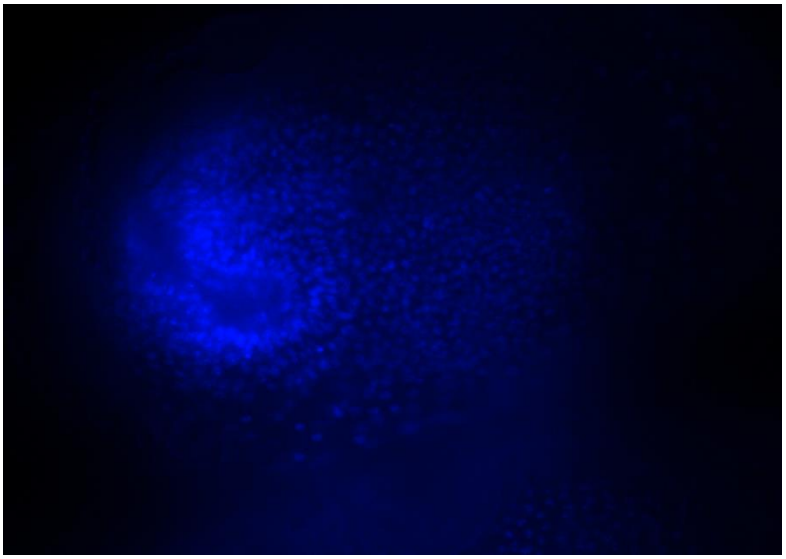

Figure 4. Embryo after gastrulation with TC1525 gene silenced showing a gastrulation disturbed.

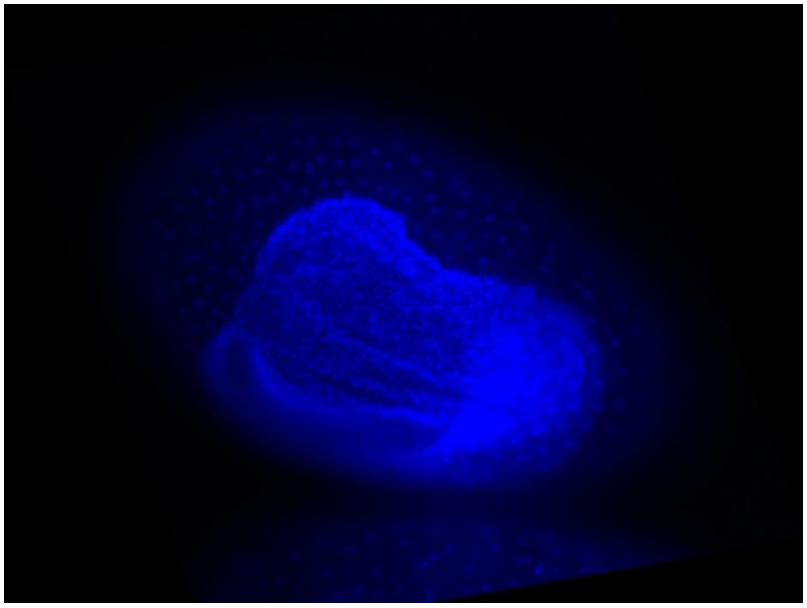

Figure 5. Embryo after cellularization with TC14773 (Laminin α) gene silenced showing a delay serosa closure.

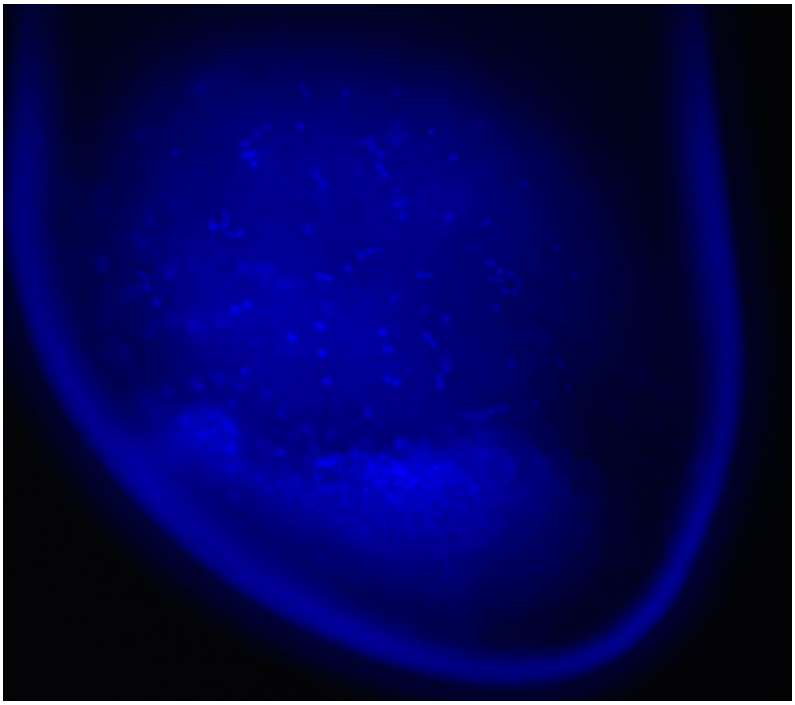

Figure 6. Embryo after gastrulation with TC3007 gene silenced showing irregular positioned germ rudiment.

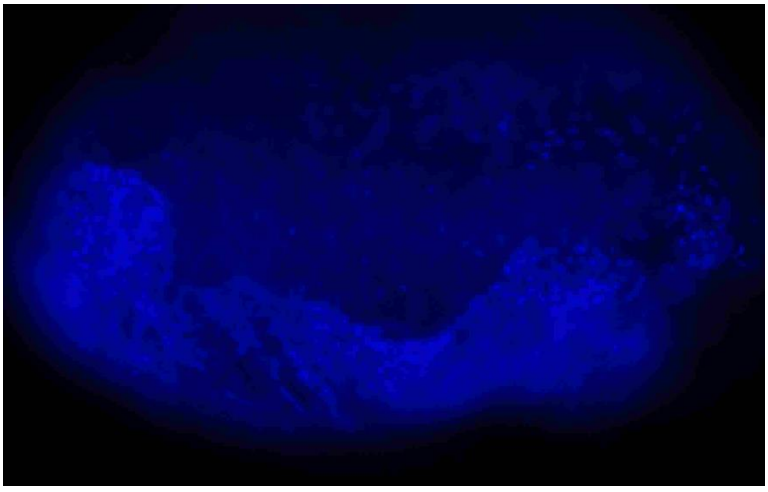

Figure 7. Embryo in the germband stage with TC10914 gene silenced showing irregular curved germband.

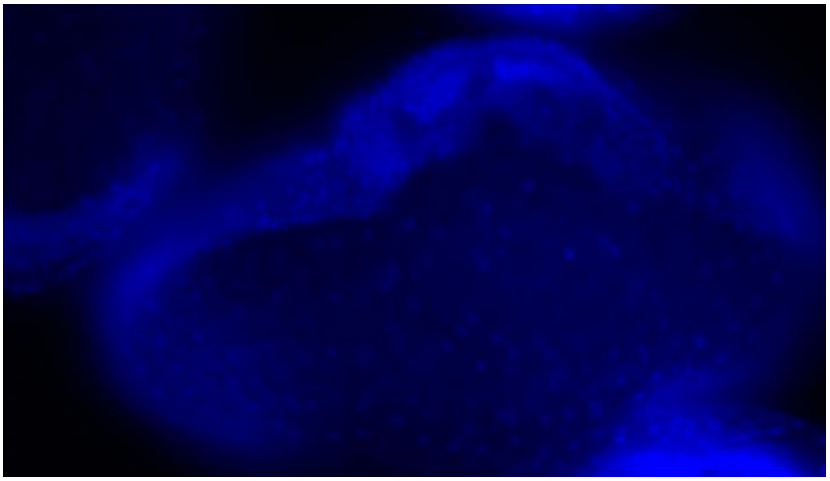

Figure 8. Embryo in the germband stage with TC14773 gene silenced showing irregular positioned germband.

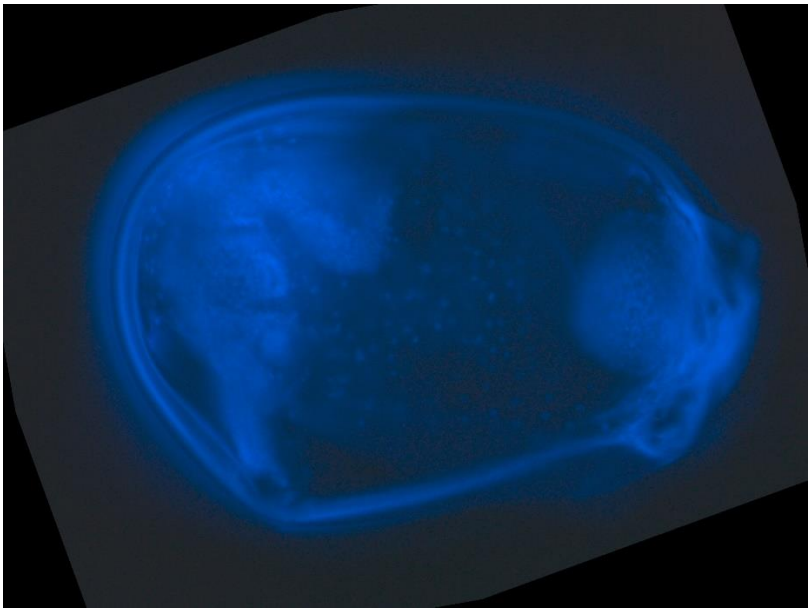

Figure 9. Embryo in the germband stage with TC5546 gene silenced showing head lobes defects.

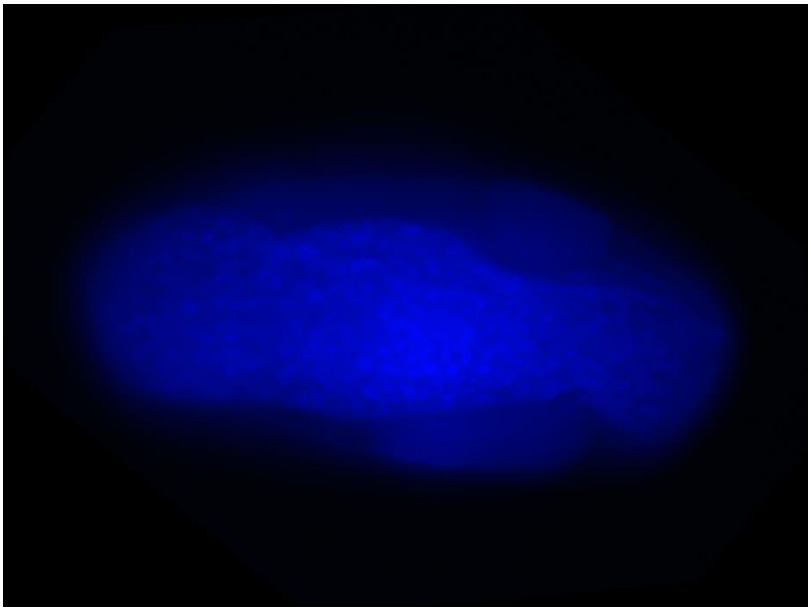

Figure 10. Embryo in the germband stage with TC16062 gene silenced showing an irregular border of the embryo.

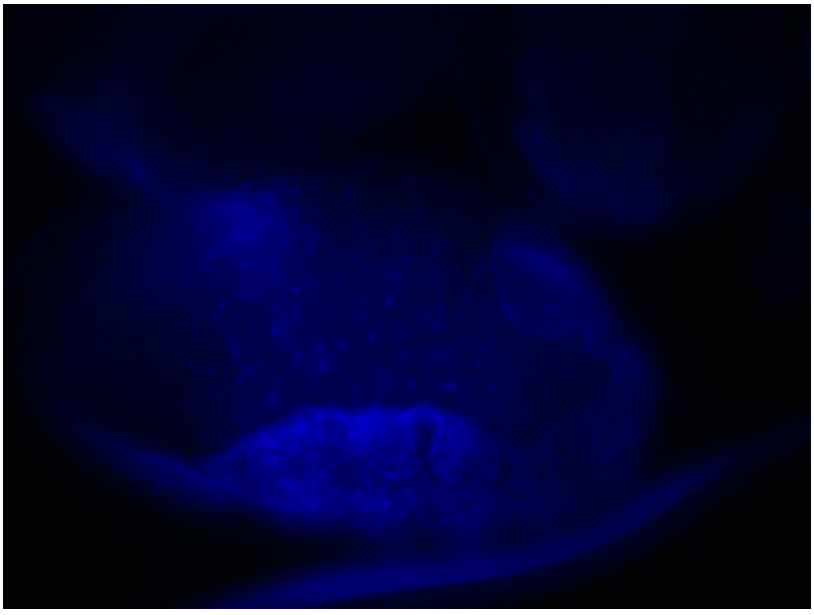

Figure 11. Embryo in the germband stage with TC3342 gene silenced showing a flat germband.

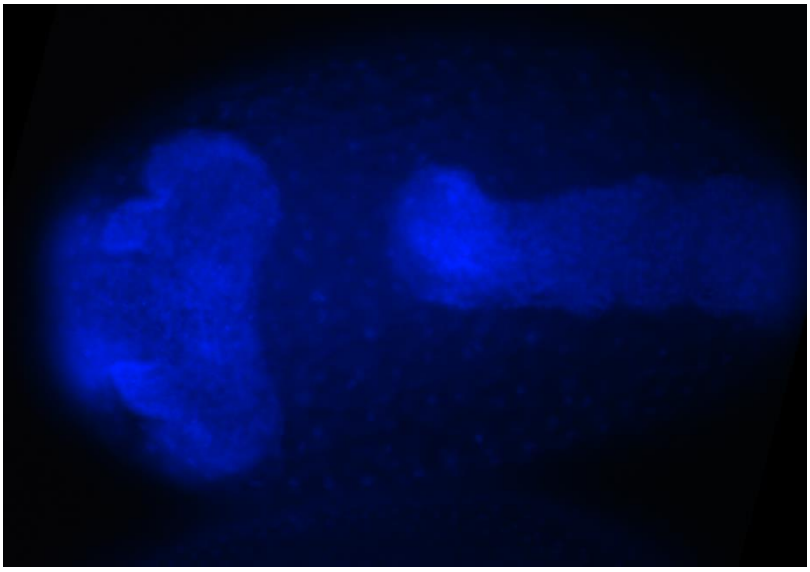

Figure 12. Embryo in the in a late germband stage with TC5676 gene silenced showing a germband retraction defect.

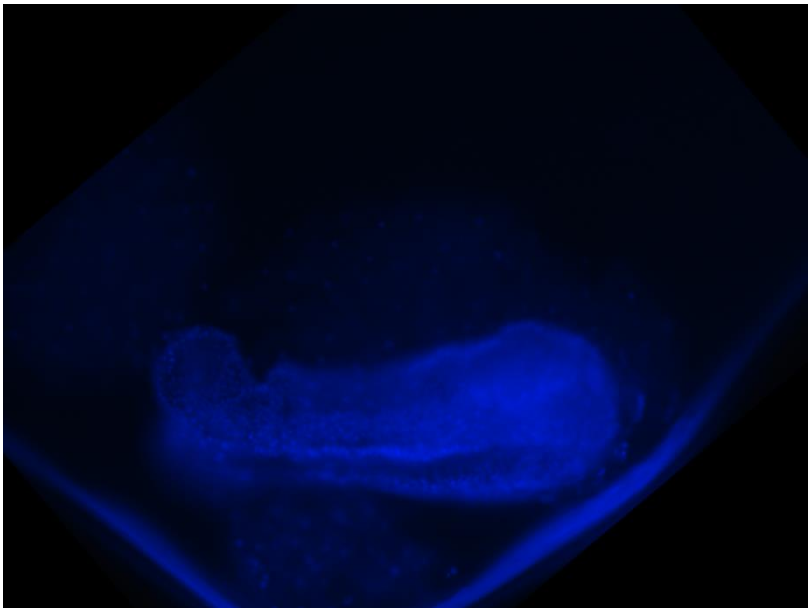

Figure 13. Embryo in the in a late germband stage with TC5546 gene silenced showing dorsal closure defects.

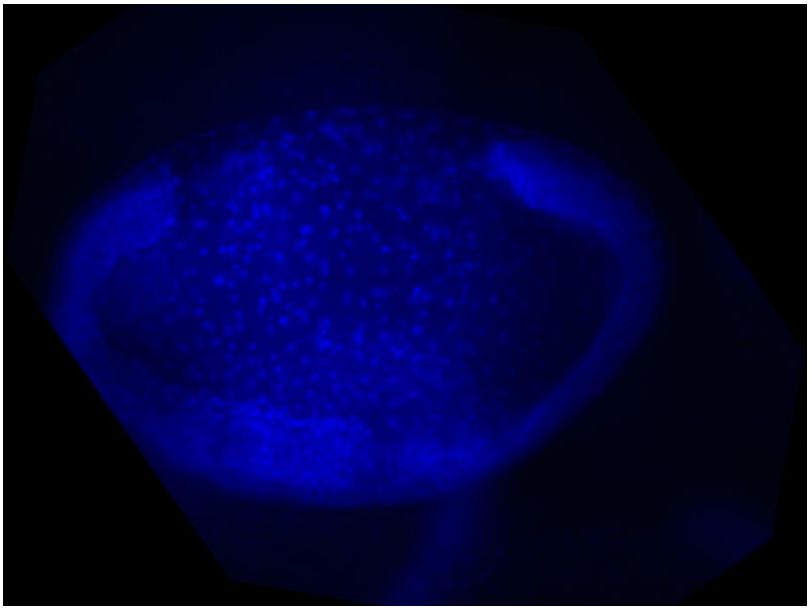

Figure 14. Embryo in the in a late germband stage with TC3007 gene silenced showing the serosal nuclei irregular spaced.

CHAPTER 5

General conclusions and discussion

In this chapter I present the conclusions of the work of this thesis, discuss possible applications and future prospects for follow-up work. First, I will give a small introduction of the processes that we studied. Then I will give a summary of the conclusions of each chapter.

In humans after fertilization the cells start to divide. In *Tribolium castaneum*, like all insects and some other invertebrates, the nuclei and not the cells divide. The nuclei are enclosed in a single membrane, and this whole single cell is called a syncytium. Until the 8th nuclear division, the nuclei are inside of the egg. After the 8th nuclear division, they migrate to the surface of the egg and form a single layer of nuclei, called the syncytial blastoderm. Once the nuclei are at the periphery of the egg, after the 12th nuclear division, the plasma membrane surrounding the entire egg moves in between the nuclei (invagination) to separate them. Finally, the plasma membrane closes around the protocells forming a ring (1). To close the membrane to form a cell, a clamping protein creates junctions between the developing basal membrane at the bottom of the furrows and the yolk plasmalemma underneath the protocells. These junctions act as patch-clamps, allowing the basal membrane to spread until it closes off the protocell (2), creating actual cells. This process, known as cellularization, turns the syncytial blastoderm into a proper epithelium tissue, known as the cellular blastoderm.

During gastrulation the embryo starts to form more epithelia. *T. castaneum* has two extraembryonic epithelia, the amnion and the serosa. Most of the insects have these two epithelia. The blastoderm differentiates into serosa cells and the embryo (the germ anlage) (3). In most hemimetabolous and holometabolous insects, the embryo invaginates into the yolk leaving the serosa to fully cover the yolk (anatrepsis) (4). After anatrepsis serosal window closure occurs. Finally, the amnion and serosa fuse during katatrepsis. (5).

In this thesis we study these processes of cellularization and serosa window closure using different approaches. In chapter 2, we study the cellularization from a mechanical point of view. In contrast, in chapter 3, we also study the cellularization using molecular biology and genetics. Finally, in chapter 4, we study serosal window closure, which is the next major change process after gastrulation in the insect development. In general, the results of this study are important to start to understand the

developmental processes of *T. castaneum*. The availability of this data is relevant as a new biological model besides *Drosophila melanogaster* because *T. castaneum* has a more similar development compared to the majority of the insects than *D. melanogaster*. The two processes studied in this thesis are complex and we had to use different approaches from physics and biology to understand them.

Mechanics of cellular blastoderm arrangement and cell shape in insect embryos

In chapter 2, we observed that a Voronoi tessellation using the nuclei as points is similar to the arrangement of the actual protocells. In Figure 1 A, a Voronoi tessellation is shown, the plane is divided in regions such that the points in each region are closest to a given center (red dots). The boundaries between two regions (black lines) are equidistant from the corresponding centers, and perpendicular to the line connecting these centers. Although Voronoi tessellations have occasionally been used to describe cellular patterns in epithelial tissues (6–11), to the best of our knowledge, the fact that the nuclei are located at the centers of the corresponding Voronoi cells has not been shown previously. The Voronoi tessellation and the actual assembly of the cells have the same area, form and their arrangement is such that the resulting tissue is just on the liquid side of the jamming transition (12) (Figure 1 B). The jamming transition is a type of phase transition between liquid and solid state by increasing the density of the material (13). We can understand the formation of a Voronoi tessellation pattern from mechanical interactions between the cells. When the protocells grow and duplicate, they have contact with their neighbors increasing the density of protocells in the egg resulting in a mechanical reaction that causes them to stop growing towards the neighbors. These contacts translate back to a mechanical force on the nuclei of the cells, which causes them to re-position and eventually form the observed Voronoi tessellation. Therefore, mechanical interactions are a factor which determine cell arrangement and shape in the blastodermal epithelium.

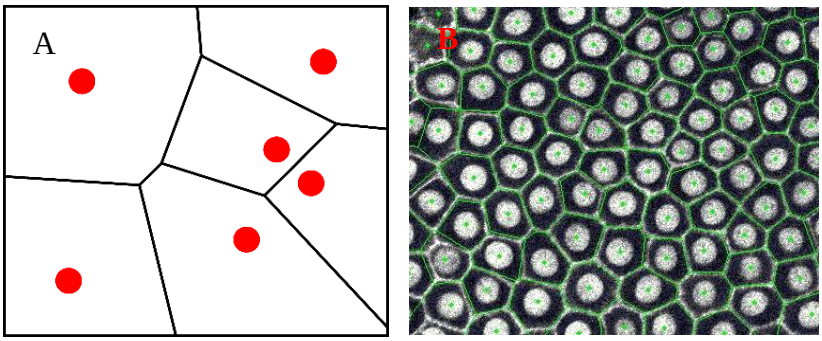

Figure 1. *A) Voronoi tessellation. Red dots are the seeds to create the tiling in the space (centers). The boundaries (black lines) between two centers are equidistant from the corresponding centers, and perpendicular to the line connecting these centers. B) In white, Image of the epithelium of the egg after cellularization with inserted Green Fluorescent Protein (GFP) in the membrane (life-actin) and the nuclei* (14, 15)*. In green, Voronoi tessellation using as centers the nuclei of the cells. The shape of the cells is similar to the shape of the Voronoi tessellation. Figure adapted from Van Drongelen et al 2017* (14)*.*

Role of Innexin 7 during cellularization in T. castaneum

In chapter 3, we also study the cellularization but using a molecular biology and genetics approach. First, we performed a screen for functions of junction proteins, then we performed an RNA sequencing experiment to study the effect on the transcriptome after parental RNAi (pRNAi) silencing of innexin 7a. Innexin 7a is a paralog of a set of 3 highly similar genes which we call further on the innexin 7 group because probably RNAi targeting cannot distinguish their function.

When we performed the screen for functions of junction proteins, we discovered that the Innexin 7 group has an important role in cellularization. When innexin 7a is silenced, the basal cell membranes are not formed and the ingressed plasma membrane retracts to the apical surface when the basal cell closure starts. Therefore, the Innexin7 group is a component of the newly identified junctions that stabilize the ingressed membrane. Furthermore, using immunolocalization, we showed that Innexin 7a forms junctions between the starting basal membrane and the yolk membrane in two ways. First, these junctions split the furrow canals immediately after the 12th division. In absence of proper splitting, membrane of a protocell can become skewed towards neighboring nuclei, as happens during

protocell delamination. Second, these junctions stabilize the furrow canals during the phase of actual basal cell closure. Absence of this stabilization leads to the retraction of the ingressed membrane to the apical surface, causing a complete reversal of the cellularization process.

We performed RNAseq of RNA isolated from eggs of which the parents were injected with dsRNA targeting innexin 7a (pRNAi) to study the effect of the silencing on the transcription of all genes. The results from the differential expression of genes after pRNAi as compared to the control show a large set of genes that are different expressed. It is important to mention that based on the close homology of the three identified innexin 7 paralogs we assume that the effects of the pRNAi approach could be the result of silencing of all three paralogs and therefore we use the generic name innexin 7 to indicate the entire gene group. Additionally, we performed gene enrichment analysis to describe the effects of the pRNAi on the transcriptome. Functional annotation charts obtained from DAVID (Data base for Annotation, Visualization and Integrated Discovery) showed a strong enrichment with very low P-values of many genes that are linked to development, particularly linked to insect cuticle development. Considering that the RNAi targeting inx7a resulted in severe developmental differences, it is very likely that many effects at the RNA level are indirectly caused by differences in developmental timing. In addition, our RNAseq results indicate a possible connection of inx7 with DNA replication. In this context, the publication of Doble et al (2004) that shows that phosphorylation of serine 262 in the gap junction protein connexin-43 regulates DNA synthesis in human cardiomyocytes supports our findings. It is therefore interesting to further investigate the role of gap junction regulation in the DNA replication process.

It might seem surprising that the sole depletion of Inx7a shows a strong cellularization phenotype, while the other innexins Tc-inx1, inx2, inx3, inx456 are also expressed during cellularization. However, specific protein properties might distinguish the Innexin7 paralogs from the other expressed Innexins. Since in other organisms, paralogs often develop to have a specialized function in heteromeric complexes (16) it wouldn't be surprising if the paralogs of the innexin 7 group are forming heteromeric gap junctions and therefore have an equally important function.

The proposed mechanism of basal cell closure involving Inx7 could be unique to *Tribolium*. However, since the *Drosophila* mode of

cellularization involving columnar cells is evolutionary derived, it seems more likely that the Inx7-mediated process is ancestral.

Role of the trimer Laminin α1,2, β and γ during serosal window closure in T. castaneum

In chapter 4, we studied the role of Laminin during serosal window closure. The protein of Laminin is in the basement membrane of animals (17–20). It is made by three subunits: Laminin α, β and γ. Depending on the organism there are different heterotrimers which they are made by different chains of α, β or γ. *T. castaneum* has four laminin chains: two α chains (α1,2 and α3,5), one β chain and one γ chain. We noted that the trimer Laminin α1,2, β and γ (Laminin 1) is one of the key cell adhesion molecules and the first cellular component involved in serosal window closure in *Tribolium castaneum*. Furthermore, we show the enrichment and potentially extracellular localization of Laminin γ protein around the necklace cells of the serosal window. Finally, we show that closure of the serosal window is delayed in laminin deficient embryos.

The phenotype we observe after laminin RNAi is comparable to the one reported for dorsocross RNAi (21). Not only the delay of closure of the serosal window is similar, but also the curved germ band that is positioned more towards the posterior (21). In absence of proper separation of the amnion and the serosa, the amnion connects the germ band to the serosa which is anchored to the outer vitelline membrane, preventing anterior movement of the germ band (21, 22). This probably happens in both *dorsocross* and laminin RNAi. In addition, the expression pattern of laminin γ resembles the reported expression pattern of *dorsocross* (21). This makes it highly likely that laminins are important target genes of the Dorsocross transcription factor during closure of the serosal window in *Tribolium*.

In conclusion, we have shown that Laminin is required for closure of the serosal window, a crucial step in the development of the serosa. As more genetic tools such as RNAi and CRISPR-Cas are now available for non-model organisms, more genes will probably soon be described to be involved in morphogenesis of this crucial extraembryonic epithelium in insects.

Applications

The applications of studying the early development of insects range from agriculture to material science. In agriculture, the study of the early development of insects can be applied to create new kinds of pesticides, less harmful to human health. For example, carbofuran is an insecticide that stops pests by disturbing the reproduction and development of insects. But, this insecticide does not just kill insects, it also has toxic effects in humans and other mammals (23). Understanding the early development of insects, can help in identifying a hormone or gene that has the same effect in insect development as carbofuran (El-Sheikh, Kamita, & Hammock, 2016; "Handbook of Hormones" 2016). In this way, insect pests can be eliminated with less environmental contamination. This kind of pesticides are called third-generation pesticides (26). There are already hormones on the market which can be used instead of pesticides (https://www.koppert.nl/). One example is Vidi Terrum, that is used to stimulate the defense and stress resistance of crops.

There are also applications for studies of the serosa that are not directly obvious, like the process of cryopreservation. Cryopreservation is a freezing process used to preserve the eggs of the insects for a long period and to hatch them after years of been fertilized (27–29). The possible use of this process is to make a bank of fertilized embryos similar to the seed bank in Norway (30). Unfortunately, not all insects are easily cryopreserved, such as the bee (31). The bee is a very important insect for human survival since it is the main pollinator on the planet (32). In the University of Humboldt in Germany, Dr. Jakob Wegener aims to preserve bee eggs by cryopreservation (33). He found that the permeability of the bee egg to the cryopreservation chemicals is the limiting factor. The serosa is one of the epithelia that is responsible of the permeability of the egg (34). Therefore, knowledge of the composition and formation of serosa is important to be able to cryopreserve bee and other insect eggs.

Other interesting applications could be in material science, by creating new materials that avoid desiccation. According to Jacobs et al 2013, the serosa protects the eggs from desiccation. The study of serosa components can help us to understand the biological principles of protection against desiccation. This can lead to the creation of new

biomimetic materials which are resistant to dry environments. These new materials can be used in deserts, in the Antarctic, by astronauts or for food preservation.

In conclusion the study of the development of *T. castaneum* has a lot of possible applications. Some of the applications are already on the market and some of them need more study and comprehension. Therefore, it is important to keep studying the development of *T. castaneum* specially from a multidisciplinary perspective.

Future work

In chapter 3, the next step for future investigations is to further study the role of innexins in signaling pathways. One of the reasons for this are the results of the study by Lechner, et al. 2007 (34) They observed that innexin 2 is part of the hedgehog pathway. The hedgehog signaling pathway is essential for the expression of wingless and Delta/Notch. Hedgehog and wingless regulate gap junction communication by transcriptionally activating the innexin 2 gene. In a feedback loop, innexin 2 is needed for the transcriptional activation of hedgehog, wingless and Delta/Notch (34). Our transcriptome study of chapter 3 also indicates a link of innexin 7 function with Notch signaling. To further study this in *Tribolium* is relevant because to the best of our knowledge there is not a link between innexin function and signaling pathways known in any species.

Following up from chapter 2, future work could address the physical properties of the egg. The egg can be seen as a liquid, and we can study properties such as the viscosity or diffusion constant. They can be measured by observing how a particle moves inside of the egg. To reach the aim we could study the movement of fluorescent beads through the egg of *D. melanogaster* and *T. castaneum* obtaining the diffusion constant by tracking the beads. The viscosity can be calculated by using the Stroke-Einstein equation (35):

$$\eta = \frac{kT}{6\pi Dr} \qquad \text{Eq 1}$$

Where D is the diffusion constant, η is the viscosity, k is the Boltzmann constant, T is the temperature of the medium and r is the radio of a spherical particle.

In chapter 4, the role of the second trimer of Laminin (α3,5, β and γ) could be studied. Although, it is possible that Laminin 2 has not any role in serosal window closure because in *D. melanogaster* null mutations of α3,5 produces embryonic lethality with defects in somatic muscles, dorsal vessel and endoderm (36, 37). It is known that the α3,5 chain is also required for localization of anterio-posterior markers in the oocyte and to bind pioneer axons in the brain (38, 39). Therefore, it is highly possible that in the case of *T. castaneum* the silencing of Laminin α3,5, β and γ can produce different effects than Laminin α1,2, β and γ. Using electron microscopy or observing Collagen IV or Perlecan proteins we could know if the basal membrane of the serosal epithelium is disturbed by knocking down Laminin α3,5, β and γ.

References

1. Handel, K., C.G. Grünfelder, S. Roth, and K. Sander. 2000. Tribolium embryogenesis: a SEM study of cell shapes and movements from blastoderm to serosal closure. Dev. Genes Evol. 210: 167–179.
2. van der Zee, M., M.A. Benton, T. Vazquez-Faci, G.E.M. Lamers, C.G.C. Jacobs, and C. Rabouille. 2015. Innexin7a forms junctions that stabilize the basal membrane during cellularization of the blastoderm in Tribolium castaneum. Development. 142: 2173–2183.
3. Roth, S. 2004. Gastrulation in other insects. In: Gastrulations: from cells to embryo. .
4. Panfilio, K.A. 2008. Extraembryonic development in insects and the acrobatics of blastokinesis. Dev. Biol. 313: 471–491.
5. Panfilio, K.A. 2009. Late extraembryonic morphogenesis and its zenRNAi-induced failure in the milkweed bug Oncopeltus fasciatus. Dev. Biol. .
6. Honda, H. 1978. Description of cellular patterns by Dirichlet domains: the two-dimensional case. J. Theor. Biol. 72: 523–543.

7. Sulsky, D., S. Childress, and J.K. Percus. 1984. A model of cell sorting. J. Theor. Biol. 106: 275–301.
8. Weliky, M., and G. Oster. 1990. The mechanical basis of cell rearrangement. I. Epithelial morphogenesis during Fundulus epiboly. Development. 109: 373–386.
9. Sharma, V., M. Crne, J.O. Park, and M. Srinivasarao. 2009. Structural origin of circularly polarized iridescence in jeweled beetles. Science (80-.). 325: 449–451.
10. Bock, M., A.K. Tyagi, J.-U. Kreft, and W. Alt. 2010. Generalized Voronoi tessellation as a model of two-dimensional cell tissue dynamics. Bull. Math. Biol. 72: 1696–1731.
11. Yu, W., H.K. Lee, S. Hariharan, W. Bu, and S. Ahmed. 2010. Evolving generalized voronoi diagrams for accurate cellular image segmentation. Cytom. Part A. 77: 379–386.
12. Bi, D., X. Yang, M.C. Marchetti, and M.L. Manning. 2016. Motility-driven glass and jamming transitions in biological tissues. Phys. Rev. X. 6: 021011.
13. Biroli, G., C.E.A. Saclay, and O. Merisiers. 2007. JAMMING A new kind of phase transition ? 3: 222–223.
14. Drongelen, R. Van, T. Vazquez-Faci, M. Van Der Zee, and T. Idema. 2017. Mechanics of epithelial tissue formation. : 1–11.
15. Sarrazin, a. F., a. D. Peel, and M. Averof. 2012. A Segmentation Clock with Two-Segment Periodicity in Insects. Science (80-.). 336: 338–341.
16. Kramer, J.M. 2005. Basement membranes. WormBook. 27: 1–15.
17. Engel, J., E. Odermatt, A. Engel, J.A. Madri, H. Furthmayr, H. Rohde, and R. Timpl. 1981. Shapes, domain organizations and flexibility of laminin and fibronectin, two multifunctional proteins of the extracellular matrix. J. Mol. Biol. 150: 97–120.
18. Kusche-Gullberg, M., K. Garrison, A.J. MacKrell, L.I. Fessler, and J.H. Fessler. 1992. Laminin A chain: expression during Drosophila development and genomic sequence. EMBO J. 11: 4519–27.
19. Fessler, J.H., and L.I. Fessler. 1989. DROSOPHILA EXTRACELLULAR MATRIX. Annu. Rev. Cell Biol. 5: 309–39.
20. Horn, T., and K.A. Panfilio. 2016. Novel functions for Dorsocross in epithelial morphogenesis in the beetle Tribolium castaneum. Dev. .

21. Münster, S., A. Jain, A. Mietke, A. Pavlopoulos, S.W. Grill, and P. Tomancak. 2019. Attachment of the blastoderm to the vitelline envelope affects gastrulation of insects. Nature. .
22. Gupta, R.C. 1994. Carbofuran toxicity. J. Toxicol. Environ. Health. .
23. El-Sheikh, E.S.A., S.G. Kamita, and B.D. Hammock. 2016. Effects of juvenile hormone (JH) analog insecticides on larval development and JH esterase activity in two spodopterans. Pestic. Biochem. Physiol. 128: 30–36.
24. 2016. Handbook of Hormones. Edited by: Yoshio Takei, Hironori Ando and Kazuyoshi Tsutsui. Second edition. Elsevier Inc.
25. Omkar. 2016. Ecofriendly Pest Management for Food Security. .
26. Leopold, R.A. 2012. Cryopreservation of Insect Germplasm: Cells, Tissues and Organisms. In: Insects at Low Temperature. .
27. Štětina, T., P. Hůla, M. Moos, P. Šimek, P. Šmilauer, and V. Koštál. 2018. Recovery from supercooling, freezing, and cryopreservation stress in larvae of the drosophilid fly, Chymomyza costata. Sci. Rep. 8: 1–13.
28. Vyletova, L., L.V.P. Rennalls, K.J.L. Wood, and V.M. Good. 2016. Long-term, large scale cryopreservation of insect cells at −80 °C. Cytotechnology. 68: 303–311.
29. Charles, D. 2006. SPECIES CONSERVATION: A “Forever” Seed Bank Takes Root in the Arctic. Science (80-.). .
30. Collins, A.M. 2002. Collection of honey bee eggs for cryopreservation. J. Apic. Res. 41: 89–95.
31. Klein, A.M., B.E. Vaissière, J.H. Cane, I. Steffan-Dewenter, S.A. Cunningham, C. Kremen, and T. Tscharntke. 2007. Importance of pollinators in changing landscapes for world crops. Proc. R. Soc. B Biol. Sci. 274: 303–313.
32. Jakob Wegener, S.A.-K.& K.B. 2009. Collection of viable honey bee (Apis mellifera) larvae after hatching in vitro. J. Apic. Res. 48.
33. Jacobs, C.G.C., G.L. Rezende, G.E.M. Lamers, and M. van der Zee. 2013. The extraembryonic serosa protects the insect egg against desiccation. Proc. R. Soc. B Biol. Sci. 280.
34. Lechner, H., F. Josten, B. Fuss, R. Bauer, and M. Hoch. 2007. Cross regulation of intercellular gap junction communication and paracrine signaling pathways during organogenesis in Drosophila. Dev. Biol. 310: 23–34.

35. Hoffmann, M.M., M.D. Too, M. Vogel, T. Gutmann, and G. Buntkowsky. 2020. Breakdown of the Stokes-Einstein Equation for Solutions of Water in Oil Reverse Micelles. J. Phys. Chem. B. 124(41):9115-9125.
36. Henchcliffe, C., L. Garcia-Alonso, J. Tang, and C.S. Goodman. 1993. Genetic analysis of laminin A reveals diverse functions during morphogenesis in Drosophila. Development. 18(2):325-37.
37. Yarnitzky, T., and T. Volk. 1995. Laminin is required for heart, somatic muscles, and gut development in the Drosophila embryo. Dev. Biol. 169(2):609-18.
38. Deng, W.M., and H. Ruohola-Baker. 2000. Laminin A is required for follicle cell-oocyte signaling that leads to establishment of the anterior-posterior axis in Drosophila. Curr. Biol. 10(11):683-6.
39. García-Alonso, L., R.D. Fetter, and C.S. Goodman. 1996. Genetic analysis of Laminin A in Drosophila: Extracellular matrix containing laminin A is required for ocellar axon pathfinding. Development. 122(9):2611-21.

Summary

After *Drosophila melanogaster*, *Tribolium castaneum* has started to be the most used insect in evolutionary Biology. The main reason is because *T. castaneum* has a short germ development. In this kind of development just the head and the thorax are present in the blastoderm after gastrulation. Later the rest of the segments develop. This kind of development is closer to most of the insects than the kind of development of *D. melanogaster.* The development of *D. melanogaster* is long germ development which means that after gastrulation all the segments develop at the same time. Therefore, if we want to study general aspects of the development of insects, it is better to study it in *T. castaneum*. The study of the development of *Tribolium castaneum* has a lot of possible applications. Some of the applications are already in the market such as new ways of control to insect pests and some of them need more study and understanding. Therefore, it is important to study the development of *Tribolium castaneum* specially from a multidisciplinary perspective.

In this thesis we study the early development of *T. castaneum* which covers from after fertilization until serosal window closure. In mammals, after fertilization the cells start to divide, in the case of the insects the nuclei start to divide. After fertilization all the nuclei are embedded in a single membrane without separation between them. Therefore, if we are strict with the definition of a cell, shortly after fertilization, there is just one cell with a lot of nuclei called syncytium. In *T. castaneum* the nuclei divide 12 times before they separate to form cells with one nucleus. During the first nuclear divisions the nuclei are inside of the egg. After the 8^{th} nuclear division, they migrate to the surface of the egg and form a single layer of nuclei. Once the nuclei are at the periphery of the egg, the plasma membrane surrounding the entire egg moves in between the nuclei (invagination) and separates them. Finally, after the 12^{th} nuclear division the plasma membrane closes around the protocells, creating actual cells creating the blastoderm epithelium. This process is known as cellularization. At the blastoderm stage, the serosa starts to differentiate from the germ anlage. In most holometabolous insects, the serosa folds over the germ rudiment, forming a serosal window that finally closes so that the serosa completely covers the yolk and embryo.

In this thesis we studied the development period from a multidisciplinary perspective. In the chapter 2 we studied the mechanical interaction between cells which is important to form the cell shape during cellularization. To understand this pattern-forming process, we simulate the growth of the cells using a mechanical model comprising the nuclei, radial microtubules and actin cortex of the cells. We found that the mechanical interaction between cells lead to the formation of a Voronoi tessellation. The geometric and topological properties of the tessellations we find in our experiments quantitatively match with our simulations. Moreover, comparison with recent jamming models suggests that the tissues spontaneously organize at the highest possible density that is still on the liquid side of the jamming transition. In chapter 3, we studied the genetics of cellularization. Performing RNA sequencing, we found that the Innexin 7 gene group is central to finish the process. In Chapter 4, we made a gene screening of the genes involved in serosal window closure. We found that Laminin α1,2 produces a delay in the start of serosal window closure. As Laminin α1,2 is a subunit of the functional Laminin trimer, we also studied the other two subunits Laminin β and γ. We found that the trimer Laminin α1,2, β and γ is a key cell component in the process of serosal window closure.

In conclusion, *T. castaneum* has a lot of potential to become an important biological model. In this thesis we used this small beetle to perform a multidisciplinary study about the early development. But not just *T. castaneum* is useful to study the early development, but also it can be used in different studies with different applications, ranging from agriculture to material science.

Curriculum Vitae

Tania Vazquez Faci was born in Mexico City on August 9th 1983. She was born in a scientific family of biologist, physicist and engineers. One of the events that marked her career path was the cloning of Dolly, the sheep. She was amazed when saw how the ovum was injected with the cloned information, then she wanted to do the same. During her PhD, Tania introduced a gene from a jellyfish into the egg of *Tribolium castaneum* to make the cells fluorescent to study the cellularization. At that moment, she was so happy because she could fulfill her dream.

To get to that point, Tania followed an unconventional career path. First of all, she studied Biology at the National University of Mexico (UNAM). She worked extensively in two projects. In the first one, she studied *Drosophila melanogaster*'s neurons using biological and physical methods to understand the ion channels during the neural connection. In the second project, she studied the genetoxicity of Nitrosodimethylamine (NDMA, a strong human carcinogenic compound) using *D. melanogaster* as biological model. After her bachelor, Tania moved to France to do her master in applied physics with a specialization in Biophysics. During this period, she was involved in a project at the Institute d'Optique. There, she studied the protein translation from a single molecule perspective. Later, in collaboration with the bionanoscience department of TUDelft, Tania studied the bacterial antibiotic resistance using microchips and she modeled the *D. melanogaster* early development. After this experience she decided to pursue a PhD. Tania obtained a personal grant to perform her PhD project from the National Council of Science and Technology of Mexico. The PhD was done at Leiden University in the Netherlands under the direction of Prof. Dr. Herman Spaink as promotor and Dr. Maurijn van der Zee as supervisor. She studied the mechanics and genes involved in the early development of *T. castaneum*.

Publications

Van Der Zee, M., Benton, M. A., **Vazquez-Faci, T.**, Lamers, G. E. M., Jacobs, C. G. C., & Rabouille, C. (2015). Innexin7a forms junctions that stabilize the basal membrane during cellularization of the blastoderm in Tribolium castaneum. *Development (Cambridge)*, *142*(12), 2173–2183. https://doi.org/10.1242/dev.097113

van Drongelen, R., **Vazquez-Faci, T.**, Huijben, T. A. P. M., van der Zee, M., & Idema, T. (2018). Mechanics of epithelial tissue formation. *Journal of Theoretical Biology*, *454*, 182–189. https://doi.org/10.1016/j.jtbi.2018.06.002